

## STATUS OF THESIS

Title of thesis

**The Study of Adhesion Bonding Between Steel Substrate and  
Intumescent Coating**

I **WIDYA CHRYSANTI PUSPITASARI** hereby allow my thesis to be placed at the Information Resource Center (IRC) of Universiti Teknologi PETRONAS (UTP) with the following conditions:

1. The thesis becomes the property of UTP.
2. The IRC of UTP may make copies of the thesis for academic purposes only.
3. This thesis is classified as

☐

Confidential

☒

Non-confidential

If this thesis is confidential, please state the reason:

\_\_\_\_\_

The contents of the thesis will remain confidential for \_\_\_\_\_ years.

Remarks on disclosure:

\_\_\_\_\_

Endorsed by

**WIDYA CHRYSANTI PUSPITASARI**

Pondok Bambu Asri Timur 4/11  
Jakarta Timur, Indonesia

**ASSOC. PROF. DR. PATTHI HUSSAIN**

Department of Mechanical Engineering  
Universiti Teknologi PETRONAS  
Bandar Seri Iskandar, 31750 Tronoh  
Perak Darul Ridzuan, Malaysia

Date: \_\_\_\_\_

Date: \_\_\_\_\_

## APPROVAL PAGE

UNIVERSITI TEKNOLOGI PETRONAS

Approval by Supervisor (s)

The undersigned certify that they have read, and recommend to The Postgraduate Studies Program for acceptance, a thesis entitled **“The Study of Adhesion Bonding Between Steel Substrate and Intumescent Coating”** submitted by (**Widya Chrysanti Puspitasari**) for the fulfillment of the requirements for the degree of Master of Science in Mechanical Engineering.

\_\_\_\_\_  
Date

Signature : \_\_\_\_\_  
Main supervisor : AP. Dr. Patthi Hussain  
Date : \_\_\_\_\_

Signature : \_\_\_\_\_  
Co-Supervisor : AP. Dr. Puteri Sri Melor Megat Yusoff  
Date : \_\_\_\_\_

Signature : \_\_\_\_\_  
Co-Supervisor : AP. Dr. Faiz Ahmad  
Date : \_\_\_\_\_

UNIVERSITI TEKNOLOGI PETRONAS

The Study of Adhesion Bonding Between Steel Substrate and Intumescent Coating

By

Widya Chrysanti Puspitasari

A THESIS

SUBMITTED TO THE POSTGRADUATE STUDIES PROGRAMME  
AS A REQUIREMENT FOR THE DEGREE OF MASTER OF SCIENCE  
IN MECHANICAL ENGINEERING

BANDAR SERI ISKANDAR

PERAK

FEBRUARY 2010

## DECLARATION

I hereby declare that the thesis is based on my original work except for quotations and citations which have been duly acknowledged. I also declare that it has not been previously or concurrently submitted for any other degree at Universiti Teknologi PETRONAS (UTP) or other institutions.

Signature : \_\_\_\_\_

Name : WIDYA CHRYSANTI PUSPITASARI \_\_\_\_\_

Date : \_\_\_\_\_

## **ACKNOWLEDGEMENT**

First of all, praises and thanks are due to Allah SWT, the almighty God, the creator, the source of life and grace: for giving the strength and wisdom I needed to succeed in life.

I would like to thank all the people who helped and inspired me during my study; my gratitude is due to my supervisor, AP. Dr. Patthi Hussain, for his guidance during my research at Universiti Teknologi PETRONAS. I gratefully acknowledge AP. Dr. Puteri Sri Melor and AP. Dr. Faiz, my co-supervisors, for their suggestions, criticism and assistance during the construction of my thesis. Their involvement became a source of encouragement for my research aside from the fact that they are always there when I needed help and as a result, research life became efficient and rewarding for me.

I would also like to acknowledge all UTP technologists especially to the Material Laboratory Technologist namely: En Anuar, En. Faisal, En. Omar, En. Shairul, En. Irwan, and En. Jani for the assistance and support they offered when I was conducting my experiments. My sincere gratitude is also due to the Postgraduate office staffs for their assistance during my study.

It is a pleasure to pay tribute also to all my friends in UTP for the past two years, especially to my friends who were always there to support me when I needed some advice and comfort. I am grateful for the friendship that we made through tough times and I wish you all the best. I hope that we will all meet again sometime in the future outside the four corners of UTP.

This work could not be completed without the love and support of my whole family. Words fail to express my appreciation to my mom who's never ending support and prayer has taken the load of my shoulder. I would also like to thank my two beautiful sisters for their encouragement and taking care of our mom and for always sending me pictures of our cats. Lastly, I express my thanks to my beloved, for his support, patience, advices and for understanding me since we have been together.

Finally, I would like to thank everybody who was important to the successful realization of this thesis, as well as expressing my apology that I could not mention personally one by one.

This thesis is dedicated with love to my father. I believe you are now at peace joining Allah SWT in heaven. You will always be your daughter's inspiration.

Thank you.. Papa. *I Love You.*

## ABSTRACT

The aim of the current study is to characterize the adhesion bonding of intumescent coating on steel substrate with respect to its mechanical, physical and chemical properties, before and after a fire test. Carbon steel was used as the substrate material and its surface was sand blasted to ensure strong bonding between the steel substrate and the intumescent coating. A primer coating was applied on the steel substrate prior to applying the intumescent to further strengthen the bonding. The coated steel substrates were subjected to fire in a furnace at 1000°C for various durations ranging from 30, 45, and 90 to 120 min. All coated steel substrates were also subjected to corrosion test by immersing them in 2% sodium chloride (NaCl) both for 15 min and three months duration using Electrochemistry Impedance Spectroscopy. For mechanical property, the shear strength of the intumescent coating was measured for various coating thicknesses ranging from 1, 2, 3, 4, 10 to 22 mm through lap shear test. The changes in microstructure of the adhesion bonding were monitored using the Scanning Electron Microscope (SEM).

The microstructure observation indicated a profound mechanical interlocking mechanism between the primer coating and the steel substrate. However, separation between the resultant char and steel was observed for all the fired specimens. The specimen's impedance before fire test and before immersion was  $437 \times 10^6 \Omega \cdot \text{cm}^2$ . After 15 min exposure to NaCl, this value was reduced by 26, 53, 60 and 65% for specimens fired for 30, 45, 90 and 120 min, respectively. Further reduction in the impedance by 97.6, 97.8, 97.9 and 98.9% for samples fired for 30, 45, 90 and 120 min, respectively, were measured after three months of NaCl immersion. The results showed that the corrosion resistance of the substrates worsened with the duration of firing and immersion in NaCl. A marked decrease in shear strength of the intumescent coating from 1.95 MPa to 0.23 MPa was also measured as the thickness increased from 1 mm to 22 mm, respectively. Despite the two hours of firing, the temperature of the steel substrate was kept below 100°C and no re-crystallization was observed. Hence, the strength of the steel was maintained.

*Keywords: intumescent coating, adhesion bonding, lap shear, interface, fire test*

## ABSTRAK

Objektif kajian semasa adalah untuk mencari sifat-sifat mekanikal, fizikal dan kimia bagi ikatan lekatan (adhesion bonding) antara salutan intumescent dan substrat keluli sebelum dan selepas ujian kebakaran dijalankan. Kesemua permukaan substrat keluli melalui proses pembagasan pasir untuk memastikan ikatan salutan yang kuat. Malah, salutan primer juga diguna sebelum salutan intumescent disapu di atas permukaan substrat bagi tujuan yang sama. Substrat bersalut intumescent dibakar di dalam ketuhar pada suhu 1000°C selama 30, 45, 90 dan 120 min secara berasingan. Sampel substrat juga diuji ketahannya terhadap kakisan di dalam rendaman larutan 2% natrium klorida (NaCl) untuk kedua-dua tempoh selama 15 min dan tiga bulan. Ujian ricih bertindih juga dijalankan untuk mengukur kesan perubahan ketebalan salutan terhadap kekuatan ricih salutan. Bagi melengkapkan siasatan, perubahan mikrostruktur ikatan lekatan sebelum dan selepas ujian pembakaran turut diperhatikan.

Pemerhatian mikrostruktur menunjukkan ikatan lekatan mekanikal yang saling berpautan antara salutan primer dan substrat keluli. Di samping itu, pemisahan antara debu arang yang terhasil dan permukaan keluli turut dicerap bagi kesemua spesimen yang dibakar. Impedan spesimen sebelum dibakar dan tanpa rendaman NaCl ialah  $437 \times 10^6 \Omega \cdot \text{cm}^2$ . Ujian kakisan menunjukkan penurunan nilai impedan sebanyak 26, 53, 60 dan 65% masing-masing bagi sampel yang dibakar selama 30, 45, 90 dan 120 min. Peratusan penurunan meningkat kepada 97.6, 97.8, 97.9 dan 98.9% bagi sampel yang dibakar selama 30, 45, 90 dan 120 min akibat direndam di dalam NaCl selama 3 bulan. Keputusan ini menunjukkan ketahanan kakisan substrat menurun dengan meningkatnya tempoh pembakaran dan pendedahan kepada NaCl. Penurunan ketara kekuatan ricih salutan intumescent daripada 1.95 MPa kepada 0.23 MPa disukat apabila ketebalan salutan bertambah masing-masing daripada 1 kepada 22 mm. Sepanjang ujian kebakaran, suhu substrat keluli direkod di bawah paras 100°C dan tiada tanda-tanda pengkristalan semula berlaku. Ini menunjukkan kekuatan keluli masih dipertahankan.

*Kata kunci: salutan intumescent, ikatan lekatan, tindih ricih, ujian kebakaran*



## TABLE OF CONTENTS

<b>STATUS OF THESIS .....</b>	<b>i</b>
<b>APPROVAL PAGE .....</b>	<b>ii</b>
<b>DECLARATION.....</b>	<b>iv</b>
<b>ACKNOWLEDGEMENT .....</b>	<b>v</b>
<b>ABSTRACT.....</b>	<b>vii</b>
<b>ABSTRAK .....</b>	<b>viii</b>
<b>TABLE OF CONTENTS.....</b>	<b>ix</b>
<b>LIST OF TABLES .....</b>	<b>xii</b>
<b>LIST OF FIGURES .....</b>	<b>xiii</b>
<b>CHAPTER 1 INTRODUCTION .....</b>	<b>1</b>
<b>1.1 Background.....</b>	<b>1</b>
<b>1.2 Problem Statement.....</b>	<b>4</b>
<b>1.3 Research Objectives .....</b>	<b>5</b>
<b>1.4 Scope of Work .....</b>	<b>5</b>
<b>1.5 Organization of the Thesis .....</b>	<b>6</b>
<b>CHAPTER 2 THEORY AND LITERATURE REVIEW .....</b>	<b>7</b>
<b>2.1 Categories of Flame Retardant.....</b>	<b>9</b>
<b>2.2 Intumescent Coating .....</b>	<b>10</b>
2.2.1 Type of Intumescent Coatings .....	10
2.2.2 Properties of Intumescent Coatings .....	12
2.2.3 Intumescent Coating Application.....	13
2.2.4 Intumescent Coating Reaction Mechanism.....	14
<b>2.3 Carbon Fiber .....</b>	<b>20</b>
<b>2.4 Steel Substrate .....</b>	<b>21</b>
2.4.1 Thermal Properties of Steel.....	21
2.4.2 Mechanical Properties of Steel.....	22
2.4.3 Chemical Properties of Steel .....	23
<b>2.5 Adhesion.....</b>	<b>23</b>
2.5.1 Adhesion Theory .....	24
2.5.2 Adhesion Bonding Between Coating and Steel Substrate .....	26
<b>2.6 Electrochemical Description of an Organic Coating on a Metal Substrate...</b>	<b>27</b>
<b>2.7 Literature Review.....</b>	<b>30</b>
2.7.1 Effect Thermo Oxidation to Adhesion.....	30
2.7.2 Effect of Coating Thickness to Adhesion .....	31
2.7.3 Effect of Water Uptake to Adhesion.....	32
<b>CHAPTER 3 MATERIALS AND METHODOLOGY .....</b>	<b>34</b>
<b>3.1 Materials .....</b>	<b>34</b>

3.1.1	Intumescent Coating.....	34
3.1.2	Primer Coating .....	35
3.1.3	Steel Substrate.....	35
<b>3.2</b>	<b>Material Preparation .....</b>	<b>36</b>
3.2.1	Steel Substrate Preparation .....	36
3.2.2	Intumescent Coating Preparation .....	36
<b>3.3</b>	<b>Physical Properties Characterization.....</b>	<b>37</b>
3.3.1	Microstructure Examination.....	37
<b>3.4</b>	<b>Chemical Properties Measurement .....</b>	<b>38</b>
3.4.1	Salt Spray Test .....	38
3.4.2	Electrochemistry Impedance Spectroscopy (EIS) Test.....	38
<b>3.5</b>	<b>Lap Shear Test .....</b>	<b>38</b>
<b>3.6</b>	<b>Coating Characterization .....</b>	<b>39</b>
3.6.1	Thermal Properties Characterization.....	39
3.6.1.1	<i>Thermo Gravimetric Analysis (TGA)</i> .....	39
3.6.1.2	<i>Differential Scanning Calorimetry (DSC)</i> .....	39
3.6.1.3	<i>Fourier Transform Infrared Spectroscopy (FTIR)</i> .....	39
3.6.2	Coating Composition Measurement.....	40
3.6.2.1	<i>Energy Dispersive X-Ray (EDX) and X-Ray Fluorescence (XRF)</i> .....	40
<b>3.7</b>	<b>Mechanical Properties Characterization .....</b>	<b>40</b>
3.7.1	Hardness Test.....	40
<b>3.8</b>	<b>Fire Test .....</b>	<b>41</b>
<b>CHAPTER 4</b>	<b>RESULTS AND DISCUSSION.....</b>	<b>43</b>
<b>4.1</b>	<b>Physical Properties Characterization.....</b>	<b>43</b>
4.1.1	Optical Micrographs Analysis Before Fire Test .....	43
4.1.2	Optical Micrographs Analysis After Fire Test.....	44
4.1.3	Electron Micrographs Analysis Before Fire Test.....	46
4.1.4	Electron Micrographs Analysis After Fire Test.....	48
4.1.5	Energy Dispersive X-Ray Analysis .....	54
<b>4.2</b>	<b>Chemical Properties Measurement .....</b>	<b>61</b>
4.2.1	Salt Spray .....	61
4.2.1.1	<i>Bare Steel Substrate</i> .....	61
4.2.1.2	<i>Primer Coating Coated Steel Substrate</i> .....	62
4.2.2	Steel Substrate Coated with Intumescent Coating .....	62
4.2.3	Electrochemistry Impedance Spectroscopy (EIS).....	63
4.2.3.1	<i>After fire test</i> .....	63
4.2.3.2	<i>After three months immersion in sodium chloride</i> .....	64
4.2.4	Electron micrographs of EIS sample.....	66
<b>4.3</b>	<b>Lap Shear Test .....</b>	<b>66</b>
<b>4.4</b>	<b>Coating Characterization .....</b>	<b>69</b>
4.4.1	Thermal Properties Measurement .....	69
4.4.1.1	<i>Thermo Gravimetric Analysis (TGA)</i> .....	69
4.4.1.2	<i>Differential Scanning Calorimetry (DSC)</i> .....	72
4.4.1.3	<i>Fourier Transform Infrared Spectroscopy (FTIR)</i> .....	73
4.4.2	Coating Composition Measurement.....	75
4.4.2.1	<i>X-Ray Fluorescent (XRF) : Intumescent Coating</i> .....	75
4.4.2.2	<i>X-Ray Fluorescent (XRF) : Primer Coating</i> .....	77
4.4.3	Mechanical Properties .....	78
<b>4.5</b>	<b>Steel Substrate Characterization .....</b>	<b>79</b>

4.5.1	Hardness of Steel Substrate.....	79
4.5.2	Chemical Properties Measurement of Steel Substrate .....	81
4.5.2.1	<i>Energy Dispersive X-Ray (EDX)</i> .....	81
4.5.2.2	<i>X-Ray Diffraction (XRD)</i> .....	82
4.5.2.3	<i>X-Ray Fluorescent (XRF)</i> .....	82
4.6	Fire Test .....	83
<b>CHAPTER 5 CONCLUSION AND RECOMMENDATIONS .....</b>		<b>88</b>
5.1	Conclusions .....	88
5.2	Recommendations .....	89
<b>REFERENCES .....</b>		<b>90</b>

## LIST OF TABLES

Table 2-1 Compares of the coefficient of thermal expansion, melting temperature, thermal conductivity and specific heat of the different materials .....	23
Table 3-1 Intumescent coating Chartek 7 resin and hardener composition .....	34
Table 3-2 Technical data of intumescent coating Chartek 7 .....	34
Table 3-3 Primer coating Intergard 251 composition .....	35
Table 4-1 Energy Dispersive X-Ray results for sample before fire test. ....	57
Table 4-2 Energy Dispersive X-Ray result for sample after fire test. The element weight is in wt. %.....	60
Table 4-3 Coating degradation observation through Rp and Rest Potential .....	65
Table 4-4 The FTIR analysis of intumescent coating and char .....	74
Table 4-5 Intumescent coating composition by using XRF .....	76
Table 4-6 Zinc phosphate primer coating composition by using XRF .....	78
Table 4-7 Hardness of intumescent coating (Shore D) .....	79
Table 4-8 Hardness of Steel Substrate before and after Fire Test.....	80
Table 4-9 XRF chemical composition analysis of steel substrate.....	82
Table 4-10 Fire test of uncoated steel for 60 minutes duration.....	83
Table 4-11 The temperature of flame from fire, back of steel substrate and environment during fire test .....	85

## LIST OF FIGURES

Figure 1-1 Condensed phase during combustion .....	3
Figure 2-1 Specific strength versus specific stiffness for a range of engineering materials. ....	8
Figure 2-2 Strength per volume cost versus stiffness per volume cost for a range of engineering materials. ....	8
Figure 2-3 The different time temperature curves for this kind of hydrocarbon fire and cellulosic fires (as used for most building regulations standards on fire protection) .....	15
Figure 2-4 The burning cycle.....	16
Figure 2-5 Pyrolysis reaction during fire test.....	17
Figure 2-6 Schematic of frontal model. ....	18
Figure 2-7 Model prediction of substrate thermal response.....	19
Figure 2-8 Iron Carbon phase diagram. ....	22
Figure 2-9 Van der Waals interaction. ....	24
Figure 2-10 A liquid drop on a solid substrate with three different phases. ....	25
Figure 2-11 Equivalent circuit of an organic coating on a metal substrate overlaid on a schematic of a painted metal surface. ....	28
Figure 2-12 Purely Capacitive Coating.....	29
Figure 2-13 Nyquist plot for excellent coating. ....	30
Figure 2-14 Nyquist plot for damage coating. ....	30
Figure 2-15 Schematic drawing of tri-layer models. ....	32
Figure 2-16 Effect of moisture (wet and dry) on mechanical properties of adhesive joints.....	33
Figure 2-17 Effect of water uptake on joint strength .....	33
Figure 3-1 Surface roughness of steel substrate using profilometer. ....	36
Figure 3-2 Schematic of intumescent coated steel sample (all dimensions are in mm). ....	37
Figure 3-3 The schematic of lap shear test sample dimension (all dimensions are in mm).....	39
Figure 3-4 The hardness indentation on steel substrate of the sample using Vickers hardness tester, Leco LM 247AT.....	41
Figure 3-5 a) The experimental set up the fire test, b) The center of the sample (arrow) taken for further examination.....	41
Figure 4-1 Optical micrographs. a) steel substrate, b) cross section of intumescent coated steel. Magnification : 100x.....	43
Figure 4-2 Microstructure of steel substrate conditioned with different fire test duration of a) 30 min, b) 45 min, c) 90 min and d) 120 min of fire test duration. Magnification: 100x. ....	45
Figure 4-3 Effect of annealing cold-worked carbon steel.....	46
Figure 4-4 Electron micrographs for sample before fire test. a) Overall sample structures, b) interface of intumescent coating and primer coating, c) interface of primer coating and steel substrate, d) carbon fiber in intumescent coating. ....	47
Figure 4-5 Electron micrographs for sample after fire test for 30 minutes. a) Overall sample structures, b) interface of intumescent coating and primer coating, c)	

interface of primer coating and steel substrate, d) carbon fiber in intumescent coating. ....	49
Figure 4-6 Electron micrographs for sample after fire test for 45 minutes. a) Overall sample structures, b) interface of intumescent coating and primer coating, c) interface of primer coating and steel substrate, d) charring layer. ....	50
Figure 4-7 Electron micrographs for sample after fire test for 90 minutes. a) Overall sample structures, b) interface of intumescent coating and primer coating, c) interface of primer coating and steel substrate, d) carbon fiber and charring layer in intumescent coating.....	51
Figure 4-8 Electron micrographs for sample after fire test for 120 minutes. a) Overall sample structures, b) interface of intumescent coating and primer coating, c) interface of primer coating and steel substrate, d) carbon fiber and charring layer in intumescent coating.....	53
Figure 4-9 Electron micrographs on interface of intumescent coating and primer coating before fire test. Points 1-4 refer to the EDX analysis. ....	54
Figure 4-10 Energy Dispersive X-Ray analysis, 1) primer coating and 2) at the interface between primer coating and intumescent coating before fire test.....	55
Figure 4-11 Energy Dispersive X-Ray analysis of intumescent coating before fire test at point no 3 and 4.....	56
Figure 4-12 Electron micrographs on interface of intumescent coating and primer coating after fire test.....	57
Figure 4-13 Energy Dispersive X-Ray analysis, 1) primer coating and 2) interface of intumescent coating and primer coating after fire test. ....	58
Figure 4-14 Energy Dispersive X-Ray analysis of intumescent coating after fire test...	59
Figure 4-15 Steel substrate was sprayed with 2% NaCl, a) before salt spray test, b) after salt spray. ....	61
Figure 4-16 Steel substrate coated with zinc phosphate primer coating, a) before salt spray test, b) after salt spray.....	62
Figure 4-17 Steel substrate coated with intumescent coating, ....	63
Figure 4-18 Nyquist plot of intumescent coated steel sample before and after exposure for 30 to 120 minutes of fire test.....	64
Figure 4-19 Nyquist plot of intumescent coating resistance of before and after fired samples for three months immersion in 2% NaCl. ....	65
Figure 4-20 Electron micrographs of intumescent coated sample, a) before immersion and b) after 3 months immersion in 2% NaCl. ....	66
Figure 4-21 Lap shear test sample, a) 1 mm thickness and b) 10 mm thickness. ....	67
Figure 4-22 Primer coating respond as adhesion promoter to intumescent coating. ....	67
Figure 4-23 Lap shear test result of six different intumescent coating thickness. ....	68
Figure 4-24 The adhesion interaction pulls the epoxy coating into complete contact with the rough steel substrate surface. ....	68
Figure 4-25 The thermal degradation of intumescent coating, primer coating and carbon fiber by using Thermo Gravimetric Analyzer with range temperature 30°C to 850°C.....	70
Figure 4-26 Thermal decomposition of Intumescent coating analysis using DSC.....	72
Figure 4-27 FTIR results of functional group structural changes of intumescent coating and char. ....	74
Figure 4-28 Graph of hardness measurement of steel substrate for 0, 30, 45, 90 and 120 min of fire test. ....	80
Figure 4-29 Energy Dispersive X-Ray analysis of steel substrate.....	81
Figure 4-30 X-Ray Diffraction (XRD) graph of steel substrate. ....	82

Figure 4-31 The fire test result of uncoated and intumescent coating coated steel after one hour fire test.....	84
Figure 4-32 The temperature of flame, back of steel substrate and environment during fire test.....	86
Figure 4-33 Intumescent coated steel fire test sample, a) before fire test and b) after fire test. ....	87

# CHAPTER 1

## INTRODUCTION

### 1.1 Background

Recently, adhesion phenomena become a very important field of study since they are relevant to many scientific and technological areas. Adhesion happens when solids are brought in contact such as in coatings, paints, and composite materials. The final performance of these materials are highly dependent on the quality of the interface that is formed between the coating and substrate.

The adhesion plays an important role especially for steel and intumescent coating in steel structures. The use of intumescent coating is for steel protection from fire and also for aesthetic value. Therefore, weak adhesion strength will result the separation of steel and intumescent coating which is one of the principal causes for deterioration or damage on the structural steel.

Steel is a material that is commonly used in construction of bridges, buildings, boats and cars. Steel also plays an important role in other fields like marine furniture and offshore platforms. The structural steelwork used in buildings usually requires fire protective materials to reduce the devastating cost of fire in terms of property damage and life hazard. Indeed, preventing structural collapse of a building during fire, which could occur if load bearing steel elements reach a temperature above 550°C, is paramount to ensure safe evacuation of people from the building, and is a prime requirement of building regulations (HMSO, 1992) in many countries such as United Kingdom, USA and Europe countries [1, 2].

Passive fireproofing materials are the materials commonly used to protect steel structures which are composed of insulating systems designed to decrease heat transfer from a fire to the structure being protected. These can be panels or blankets, however usually, coatings such as mineral-based or organic resin-based products, known as intumescent coatings, are preferred. Intumescent coatings are designed to perform under severe conditions to maintain



the steel integrity between 1 to 3 hours when the temperature of the surroundings in excess of 1100 °C [3,4,5,6].

Fire retardant coatings such as intumescent coatings are widely used to reduce flammability of various structures. The use of intumescent coating is one of the most cost-effective, convenient, and efficient way to protect materials against fire [7,8]. It has two main advantages: it can prevent the penetration of heat and the spreading of flames, and it does not modify the intrinsic properties such as mechanical properties of the intumescent coated material [9].

Intumescence is defined as the swelling of certain substances as they are heated. Upon heating, intumescent coatings will expand into multi cellular layer which acts as a thermal barrier. These layers effectively protect its substrate against rapid increase of temperature and thereby maintain the structural integrity of the structure. Intumescent coatings contain active ingredients which are bound together by a binder (such as epoxy). Generally, the active ingredients are composed of an acid source (normally ammonium polyphosphate or other mineral acid), a carbon source (such as char forming polymers or polyols) and a blowing agent (e.g. melamine). The composition of an intumescent coating has to be optimized in terms of physical and chemical properties in order to form an effective protective char [10].

Several researchers have studied about intumescent coating since past decades. Ammonium polyphosphate (APP) as acid source is one of the fire retardant active ingredients which have important effect to coating performance and durability. The APP act as acid source and it contains many phosphates. It has ideal II crystalline type with high polymerization degree ( $n > 1000$ ) which ensures low-water-solubility, preferable decentralization and excellent waterproof performance. However, APP possesses high heat stability and lack of transference performance. The flame-retardant coating with the addition of APP has good adhesive attraction, forms steady intumescent charring layer under flame, prevents the coating from falling off and ensures the flame-retardant performance [9, 10]. An investigation on the combination of different ingredients of fire retardant in a thermoset epoxy coating was reviewed by Jimenez *et.al* [11].

The combination between APP and boric acid gave the best protection results. The experiment showed that this combination leads to the smallest decrease of viscosity when the resin degrades while the highest mechanical resistance and the highest expansion were achieved. Furthermore, this additive interacts with the thermoset resin epoxy to increase its thermal stability. The reaction between boric acid and APP occurs during heating - permitting an adhesion between the coating and the steel substrate [11].

Figure 1-1 describes the condensed phase of intumescent coating during combustion. Anderson *et. al* have discussed further investigation of intumescent system [12,13]. The experimentation on intumescent reaction mechanism system with simplified mathematical model was performed. The development of frontal model provided considerable insight to intumescent reaction mechanisms. The frontal model assumed that the important physics of intumescent took place in a narrow zone which was relatively sensitive to temperature. With this assumption, the frontal model predicted and explained a fundamental property of intumescent system which was the formation of an isothermal front which moved from the free surface to the substrate. As long as the isothermal front persisted, the heat transfer to the substrate was limited by the temperature gradient between the front and the substrate. As an effect, the substrate was protected from higher temperatures of fire by an intervening front that was characterized by a temperature considerably lower than the fire temperature [13]. Though this model and simulation can predict the intumescent coating reaction mechanism, there was considerable interest in achieving better understanding of the mechanism in terms of the adhesion of intumescent coating on the steel substrate.

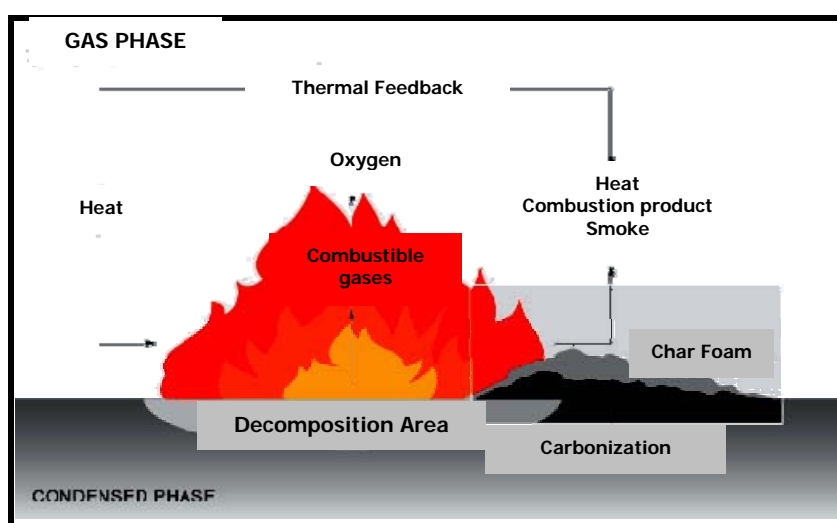


**Figure 1-1** Condensed phase during combustion [14].

## 1.2 Problem Statement

The interface mechanism and the phenomena at the bonding between steel substrate and intumescent coating are not fully understood yet. In coating of structural building, the adhesion and adhesion strength are important in assessing the performance of the coating which also determines its quality. The bonding strength depends on wetting ability, surface tension as well as surface roughness of the substrate.

The wetting between contacts of two surfaces is necessary to get good adhesion between coatings to coatings and coatings to steel substrate. The loss of solvent or wrong coating proportion may destroy the bonding. In addition, one material must absorb on the other to achieve good adhesion. In order to achieve, they must be highly compatible with each other [15]. Besides the properties of coating material, the interface interaction between the steel substrate and coating also became a fundamental aspect for coating durability. The reactions between the ingredients and additives play an important role in intumescent coating system, especially at the interface between the intumescent coating and the steel substrate.

It is also well known that the wet ability of the coating is significantly influenced with surface roughness of a steel surface. The thickness of the coating also influences the adhesive bonding strength. In order to achieve good adhesion, the bonding should have consistent strength and long durability. The suitable surface roughness and thickness are necessary to get optimum adhesion strength.

The use of a primer coating to promote adhesion and fill in the voids in the steel substrate can help to improve part appearance and quality. Generally, the inhibitive pigments are added into organic coatings as the main substance for corrosion inhibition. For this purpose, zinc phosphate is commonly used as additives because it is known as a green pigment in contrary to toxic pigments like chromate pigments [16]. Zubielewicz and Bastos [17, 18] considered that zinc phosphate neither acted in compliance with electrochemical mechanism nor improved the barrier function of the binder, and they further believed that the addition of zinc phosphate did not exhibit any positive effect on the corrosion performance of the coatings.

The reactions of the intumescent coating during combustion at high temperature can in either or both of the vapor phase and the condensed phase occur. The combustion of the intumescent coating is a complex process where there may be different mechanisms occurring as the combustion increases. The formation of charring layer during the combustion will give effect to the bonding strength of the steel substrate. However, from the literature reviews there are not many works and revelation regarding the adhesion bonding between steel substrate and intumescent coating especially after combustion and also primer coating resistance to aggressive environment. Therefore, the study of adhesion on contact area becomes an interesting subject to be discussed.

### **1.3 Research Objectives**

As the adhesion bonding of steel substrate and intumescent coating is influenced by coating thickness and aggressive environment, it is the objective of the current study to investigate and characterize the effect of adhesion bonding of intumescent coating to steel substrate with respect to the mechanical, physical and chemical properties. The properties of the bonding, coatings and steel substrate were also investigated after the fire test.

### **1.4 Scope of Work**

The study is focused on the adhesion bonding between intumescent coating/primer coating and primer coating/steel substrate. It involves the characterization of the intumescent coating, primer coating, carbon fiber and steel substrate, specifically on the mechanical, physical, chemical, and thermal properties.

Six different commercial intumescent coating thicknesses were evaluated to investigate the adhesion strength to steel substrate. The variable thicknesses are 1, 2, 3, 4, 10 and 22 mm according to the actual condition. The effect of combustion on adhesion was also studied with four variable fire test duration of 30 min, 45 min, 90 min and 120 min with temperature maintain above 1000°C. The adhesion after combustion and three months immersion in salt water were also investigated using electrochemical impedance spectroscopy (EIS). EIS is a well-known electrochemical analysis to evaluate the performance of organic coatings to corrosion. The morphology of the interface of steel

substrate and intumescent coating were also examined to study the effect of the combustion and EIS test on the adhesion characteristics.

## **1.5 Organization of the Thesis**

The thesis is presented in five chapters. Chapter 1 describes the research background related to steel substrate and intumescent coating, their limitations and fire protection system that can overcome their limitations. The motivation of the study and followed by the research objectives and scope of study were presented.

Chapter 2 contains an extensive review on the mechanism of intumescent coating at room and elevated temperatures. It also describes the effect of additives on the intumescent coating, coating strength as well as the surface roughness of the substrate. The properties of intumescent coating, primer coating, and steel substrate as well as the preparation methods are also presented. Literature review on the properties of intumescent coating and steel related to the current study are also presented to gauge the development of intumescent coating research.

In Chapter 3, details of the materials used, equipment required and sample preparation of the coating samples are described. Here, the mechanical properties, thermal, chemical testing and morphological study involved are reported in detail.

Chapter 4 analyzes the obtained results. The study of surface roughness on steel surface, as well as on the mechanical properties of the intumescent coating and steel substrate are presented. The coating resistance to corrosion attack after fire test is also discussed as qualitative method to assess the intumescent coating bonding quality on steel substrate. The fire test and lap shear test of the intumescent coating sample on steel substrate, as well as the thermal characteristics of the intumescent coating are discussed.

In Chapter 5, conclusions on the mechanical properties, thermal properties and chemical properties of the intumescent coating on steel substrate are drawn. The effects of fire test duration to coating resistance are also summarized. Finally, suggestions for future research are also given.

## CHAPTER 2

### THEORY AND LITERATURE REVIEW

Coatings in the USA contain flame retardants less than 1% of paints in 2001, from SRI International reports it can be estimated that the value of the flame retardant market worldwide for paints and coatings was around \$200 million in 2001. Business Communications Company postulated that solutions to other environmental issues faced the paint and coating industry in the 1990's and these had more urgency than flame retardant [19]. Over the last decade, the paint and coating industry has made tremendous progress in developing of flame retardant coatings. The intumescent coating market in the UAE was estimated at around AED50 million in 2005. The rapid increase in construction has led to more steel structures which in turn have resulted in more than double the demand for protective coatings [20]. The importance of greater protection to fire for both life and property has made both developers and consumers more aware of the need of flame retardant.

Composite materials such as intumescent coating consist of resin matrix and glass fiber reinforcement. The use of this composite increased for application on offshore installations. This intumescent coating is a useful alternative to steel where corrosion resistance, low weight, low cost, long service life and reduced maintenance are desirable. Intumescent coating protects the metal by forming a char layer through thermo-chemical decomposition in actual flight. It is seen in Figure 2-1 and Figure 2-2 that nearly all composites are superior to metallic structures in their specific strength which is particularly advantageous for offshore use. Advantages of the polymer composites are [21]:

- High specific strength properties (20-40% weight savings)
- Ability to fabricate directional mechanical properties
- Outstanding corrosion resistance
- Excellent fatigue and fracture resistance
- Lower tooling cost alternatives
- Lower thermal expansion properties
- Simplification of manufacturing by parts integration
- Ability to meet stringent dimensional stability requirements

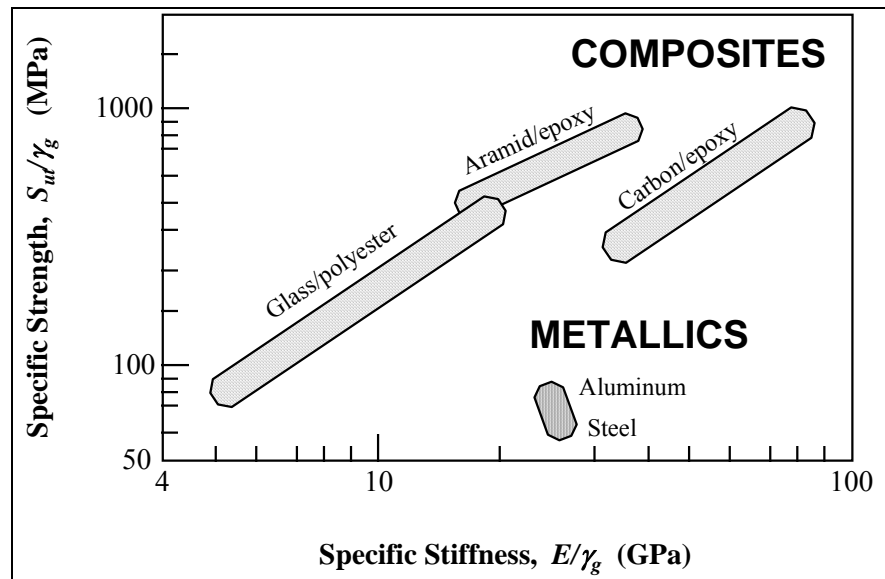


**Figure 2-1** Specific strength versus specific stiffness for a range of engineering materials.

Specific strength is defined as the ratio of the ultimate tensile strength ( $S_{ut}$ ) to specific gravity ( $\gamma_g$ ) and specific stiffness as the ratio of Young's modulus ( $E$ ) to specific gravity [22].

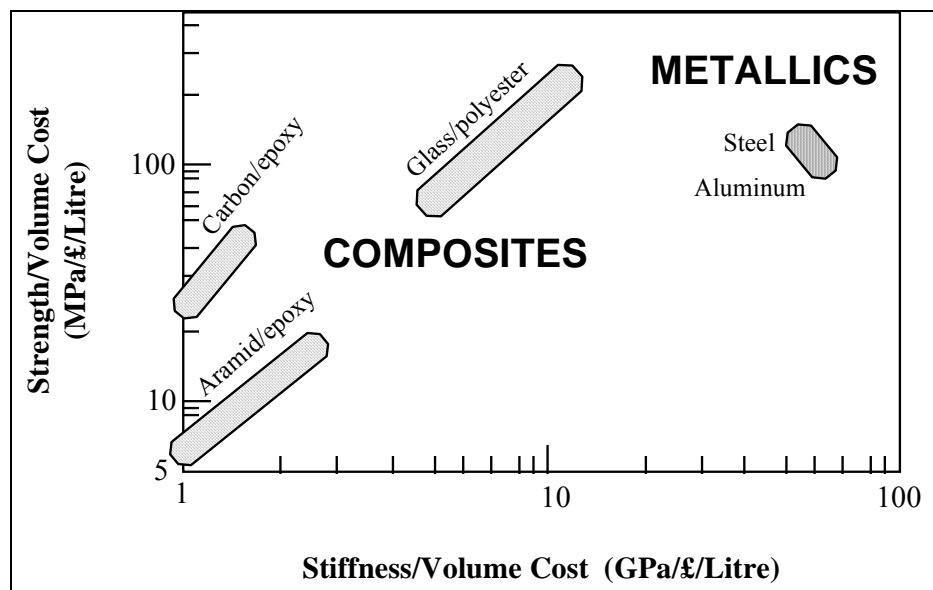


**Figure 2-2** Strength per volume cost versus stiffness per volume cost for a range of engineering materials [22].

Epoxy resin are used in load-bearing structures such as aircraft, military vehicles, ships, buildings and offshore structures due to their good mechanical, physical and chemical properties and high strength to light weight ratios. However, for flammable matrix resins -

attention must be paid to fire risks, hazards from smoke and fumes. In order to increase safety, some researches and improvements in flame retardancy have been given significant priority. In infrastructures, and in many other civil engineering applications of fiber reinforced plastic (FRP) structures, a fire situation may cause a very rapid rise of temperature, and consequently strength degradation and final collapse. Thus, a predictability of life under a rapidly rising temperature is extremely important for FRP structural designers [23].

## **2.1 Categories of Flame Retardant**

Flame retardants consist of some categories: inorganic, organophosphorus, nitrogen-based organic, halogenated and intumescent flame retardant. Inorganic flame retardant is a number of inorganic compounds which are used as flame retardant. The mechanism is interfering by various physical processes with the burning process such as release of water or non-flammable gases which dilute the gas feeding flames, absorption of heat energy thus cooling the fire, production of a non-flammable and resistant layer on the surface of material. These mechanisms of inorganic compounds are relatively low efficiency and the products having to often be used in relatively large concentrations, or more usually, in combination with other types of flame retardants. Specific application forms of these products can enable such high concentrations to be added to plastics without modifying their performance properties [24].

Organophosphorus flame retardants are primarily phosphate esters and represent around 20% by volume of the total global production. This category is widely used both in polymers and textile cellulose fibres. Organophosphorus flame retardants in particular, triaryl phosphates are used as alternatives to brominated flame retardants. Organophosphorus flame retardants may in some cases also contain bromine or chlorine [25].

Nitrogen-based organic flame retardants hinder the formation of flammable gases and are primarily used in polymers containing nitrogen such as polyurethane and polyamide. Melamines and melamine derivatives are the most important nitrogen-based flame retardants and these acts as intumescent swelling systems [26].



Phosphorus based flame retardants is often used to increase the effectiveness of nitrogen based flame retardants. They can be either simply added to plastics, or reacted into the plastic molecules. Melamine-based products are the most widely used type of nitrogen flame retardant today, and are used in furniture and building foams, nylons [27].

Halogenated flame retardant is flame retardant which is containing chlorine or bromine atoms. These act by effectively removing the  $H^+$  and  $OH^-$  radicals in the gas flame phase. This considerably slows or prevents the burning process, thus reducing heat generation and so the production of further gaseous flammable material [27].

Barrier technologies have a wide immediate commercial applicability and involve layers of materials that provide fire resistance. These include boric acid-treated cotton materials used in mattresses, blends of natural and synthetic fibers used in furniture and mattresses. In addition, the high performance synthetic materials are also used in fire fighter uniforms and space suits [28]. Intumescent coating is one of these technologies.

## **2.2 Intumescent Coating**

### **2.2.1 Type of Intumescent Coatings**

Additives are added to intumescent coating in order to optimize the performance at high temperature. Intumescent coating additives undergo a thermal degradation process on heating which produces a thermally stable, foamed, multi cellular residue called intumescent char. The additives are added to a polymeric material which is later involved in a fire, they produce an intumescent char which accumulates on the surface, while the polymer is consumed. The char layers will be providing insulation to the underlying materials and partially protecting it from the action of flame [29].

There are two different types of intumescent coatings: traditional chemical intumescent fire retardant coatings with chemical fire retardant mechanism and physical intumescent coatings containing expandable graphite with physical fire retardant mechanism. The development of these coatings is focused on improving the fire retardant efficiency, weather durability of the products, and reducing the emission of smoke and volatile organic

compounds (VOC) as well as toxic gases to provide safe and environmental-friendly products for end-users [30].

The types of traditional intumescent coatings consist of three basic components which are carbon source, acid source and gas source [31]. A carbon source can be a carbon-rich polyhydric compound, such as a starch, glucose, pentaerythritol. An acid source or a dehydrating agent is capable of promoting the formation of a carbonaceous char from the carbon source. This is usually a source of phosphoric acid, such as ammonium phosphate, diammonium phosphate, and the other phosphates. The last important substance is a gas source. An intumescent agent that would expand the film of coating upon heating depends with the gas content. Nitrogen or halogen releasing compound such as urea, melamine and melamine phosphates or chlorinated paraffin are usually used as gas source [32].

The ideal compatibility between these three basic components is important to producing an excellent fire retardancy at high temperature. The dehydration to char and release of gas in a transitional semi-liquid state sufficient to enable foaming and expansion to occur, followed by full carbonization without char collapse [33].

A water-based intumescent coating for various lignocellulosic materials, such as lumber, was formulated by expandable graphite, limestone, a polymeric binder such as phenol-formaldehyde resin, pentaerythritol and urea. Aluminum hydroxide is often used to increase absorption and neutralization of toxic gases and as an absorbent promoter [34].

Combining melamine phosphates and ammonium polyphosphate might give better products with synergism. Recent results illustrated that combining layered double hydroxides with ammonium polyphosphate in polyamid-6/polypropylene would give synergistic fire retardant effect [35]. Similar studies of aluminosilicates on intumescent flame retardancy of ammonium polyphosphate and pentaerythritol in polypropylene had been reported [36]. Results suggested that synergistic effect might give better products. Smaller amount of fire retardant additives can be used so that the mechanical properties would not be changed.

Expandable graphite intumescent coatings are the second type of intumescent coating. This type of intumescent coatings contains expandable graphite which is a new generation of fire retardant additives. Expandable graphite is formed by treating crystalline graphite, which is

composed of stacks of parallel planes of carbon atoms, with intercalates such as sulfuric acid and/or nitric acid. The chemical reaction in the case of  $\text{H}_2\text{SO}_4$  is expressed by the following equation [37]:



Since no covalent bonding exists between the planes of the carbon atoms, intercalates can be inserted into the gap and positioned within the graphite lattice. When the intercalated graphite is exposed to heat or flame, the inserted molecules would decompose and release gases. The gas forces the graphite layer planes apart and the graphite would expand. Expandable graphite coatings can expand to a greater degree than the traditional intumescent coatings, and thus provide better insulation to the underlying materials [38].

However, drawbacks with expandable graphite coatings are the popcorn effect and the blow off the graphite at high temperature. The popcorn effect can often be hindered, where the expansion of the grains of graphite would cause the grains to pop off the surface of the underlying material. Second, the expanded graphite might be blown off the underlying material by the air turbulence induced in a fire. A suitable choice of binder or carbon source can be used to prevent the popcorn effect and to hold the expanded coating together. Expandable graphite is often used with ammonium polyphosphate or polyurethane to produce a synergistic fire retardant effect [39,40].

### **2.2.2 Properties of Intumescent Coatings**

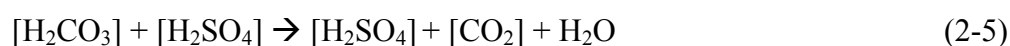
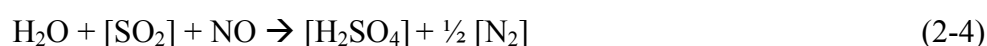
The development of intumescent coatings in the past few years are to increase the properties of this coating at high temperature. Intumescent coatings are supposed to have better fire retardancy, lower smoke emission, low hygroscopic property, high temperature resistance, resistance to mildew and rot, and other multi-functions.

Leach resistant and durable to weather are the basic properties of intumescent coatings. Some additives such as a microencapsulated ammonium polyphosphate with low water solubility were used in an intumescent coating formulation. A methylstyrene-acrylate copolymer with better leach resistance and weather durability, as well as adhesion under wet conditions was chosen as the binder. For this coating, no ammonium is given off at 75%

to 100% relative humidity conditions, and fire classification (DIN 4102) F 30 [41] is reached before and after accelerated tropical weathering [42]. As disclosed by some patents, amorphous silica, ammonium tri hydrate (ATH) and magnesium hydroxide can act as a filler and smoke suppressant or absorbent promoters apart from being water-resistant in the intumescent coatings [43, 44].

The addition of transition metal oxides are usually used to hold smoke and promote char formation via a reductive coupling mechanism in poly (vinyl chloride) [45,46]. Cerium oxide and/or molybdenum oxide can also be added into the intumescent coating formulation to inhibit smoke release [47] as disclosed in a patent.

Zinc borate and boric acid can be used not only as fire retardants, but also to reduce smoke release and after-glowing of the coating [48]. Toxic gas absorbent materials such as limestone (CaO), calcium carbonate (CaCO<sub>3</sub>), sodium bicarbonate (NaHCO<sub>3</sub>), or sodium carbonate (Na<sub>2</sub>CO<sub>3</sub>) can be added into the intumescent coating containing expandable graphite to remove and eliminate those toxic gases. Typical reaction mechanisms can be described by the following chemical equations [49]:



An intumescent coating should not only have fireproof and waterproof properties, but also anti-corrosion and resistance to mildew and rot.

### 2.2.3 Intumescent Coating Application

The Intumescent coatings can be applied to various substrates such as metal, plastics, textiles and wood. The intumescent coating application also might be applied in a wide range of places including hallways, stairwells, and furnace areas of public buildings such as hospitals, nursing homes and courthouses.

Intumescent coatings are also used to protect LPG Vessels. A significant delay in the operation of the safety valve can be made with the presence of the intumescent coating. These methods for the protection of LPG vessels are promising in regard to the prevention of explosions in these vessels under fire [50,51].

The protection of electric wire and cable also use intumescent coating. Some literatures discussed about the technology and testing methods of various intumescent coatings for electric wire and cable [52,53]. The intumescent coatings were found to be quite effective in reducing the burning behavior of power cables at high temperature.

The epoxy intumescent paint is also suitable for restoring the interiors of railway passenger cars. Based on the assessment of brushing properties, indicative fire tests, and realistic fire rig tests carried out in a modified railway car [54]. An intumescent coating consisting of polyurethane, APP and pentaerythritol, as well as acrylic polymer binder has no moisture-uptake problems. It has a limiting oxygen index of at least 25%. It can be applied to the surface of blinds or curtains. [55].

The application of intumescent coating on the surface of the wood, for interior and exterior applications such as roofing, walls, and floor sheathing are highly developed. This coating can also be applied to other substrates such as glass-fiber laminated composites, etc [56]. Lots of information on the researches and applications of the fire coatings for wood or timber are reported in patents [57,58] and literatures [59,60].

#### **2.2.4 Intumescent Coating Reaction Mechanism**

There are two commonly used hydrocarbon fire test curves. Firstly, it is defined by several standards, including ISO 834 for hydrocarbon curve [61], the Norwegian Petroleum Directorate (NPD), Underwriters Laboratory in their standard UL1709 [62] and BS 476 Appendix D [63]. The comparison of cellulosic fire and hydrocarbon fire are shown in Figure 2-3.

Fire test curves designed to replicate the time/temperature profile of a typical building fire fuelled by items such as wood and paper commonly called the cellulosic curve and defined in standards such as BS 476 Part 20 to 22 [63, 64] and ASTM E119 [65].

There are two types of hydrocarbon fuel. Hydrocarbon fuel burning under atmospheric pressure is classed as a pool fire, while fires that result from pressurized inventory streams are referred to as jet fires. Products tested to a hydrocarbon fire curve are required in both onshore and offshore oil and gas facilities, and may be required in other types of chemical plant depending on the hazardous nature of the process.

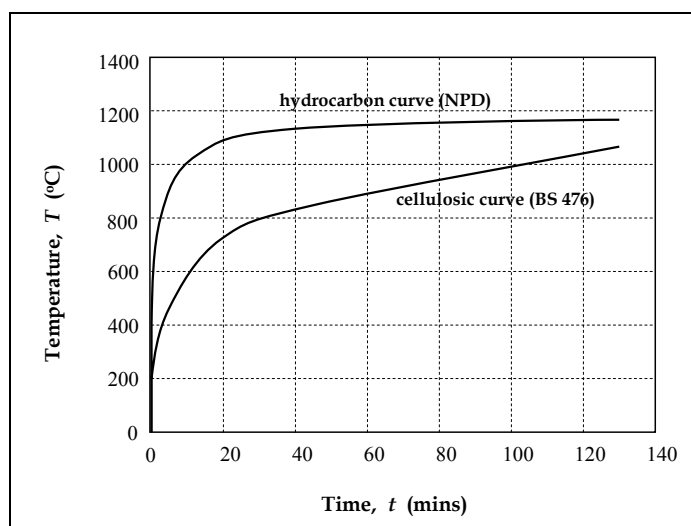


**Figure 2-3** The different time temperature curves for this kind of hydrocarbon fire and cellulosic fires (as used for most building regulations standards on fire protection) [14].

Hydrocarbon fires are characterized by a rapid and massive temperature increase as the fuel ignites. This also causes a high level of pressure that would seriously compromise traditional thin-film intumescent. Most other traditional structural steelwork fire protection systems would also find it difficult to cope with this level of force.

The intumescent coating mechanism at high temperature is almost similar with how materials burn. This intumescent coating does not burn directly but they must be first decomposed by heat (pyrolysis) to release flammable gases. Visible flames appear when these flammable gases burn with the oxygen ( $O_2$ ) in the air. If this coating does not break down into gases then they will only burn slowly. The formation of multi cellular chars forms a stable carbonaceous barrier which prevents access of the flame to the underlying material. However, even materials such as wood do in fact burn vigorously, because once ignited the heat generated breaks down long-chain solid molecules into smaller molecules which transpire as gases [66]. The intumescent coating charring layer performance is essentially known as physical barrier to heat and mass transfer between the flame and the

burning material. The pyrolysis reaction of the polymer produces combustible volatile products to feed flame. The combustion is reduced by the decrease in temperature, caused in turn by a lower heat supply from the flame. The diffusion of the volatile products towards the flame is hindered with further reduction of the flame feed. Furthermore, whatever may be the role of oxygen in the combustion process, its diffusion towards the polymer burning surface is also hindered. This series of events can lead to an interruption in the self-sustained combustion process because the flame is starved. As previously mentioned, flame retardants act by interfering with one or more steps of the burning cycle. A schematic diagram of this cycle is given Figure 2-4.

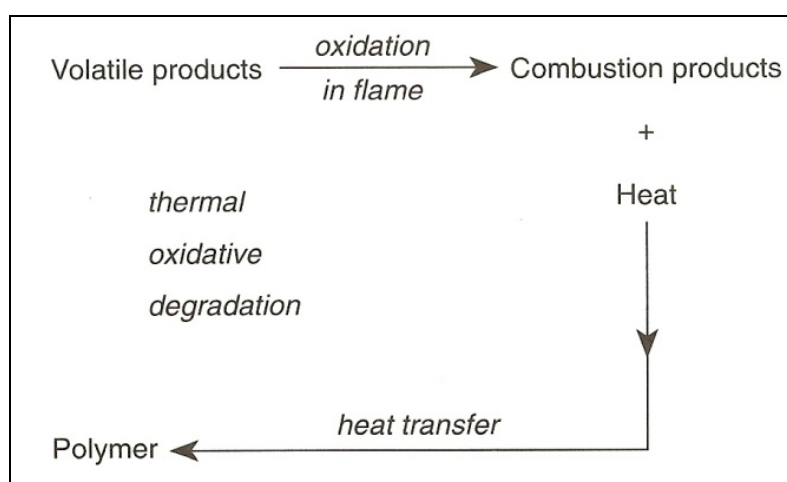
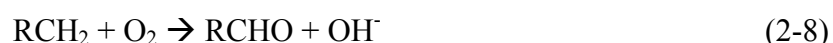


**Figure 2-4** The burning cycle [66].

As shown in burning cycle, a polymer burns via the vapor phase combustion of the volatile products produced during its thermal oxidation degradation. The vapors phase combustion is a free radical process which can be simplified and expressed as follows, where  $\text{RCH}_3$  is representative of the hydrocarbon undergoing combustion [66]:



Several flame retardants act by inhibiting this vapor phase combustion. They produce decomposition products at the same temperature as the polymer substrate decomposes. Less reactive radicals are formed, which inhibit the combustion process.

The combustion itself is maintained by the action of high energy radicals:  $H^+$  and  $OH^-$  at the gas phase. At this stage, molecules decompose to give free carbon which can react with oxygen in air to burn to  $CO$ , generating heat energy. The schematic of pyrolysis system is in Figure 2-5.

A simplified mathematical model has been developed [67] describing an intumescent system which complements the work done in the more detailed analytic model [68]. The model is constructed for intumescent systems in which it is assumed that the transition to the intumescent state occurs at an infinitesimally thin zone or front.

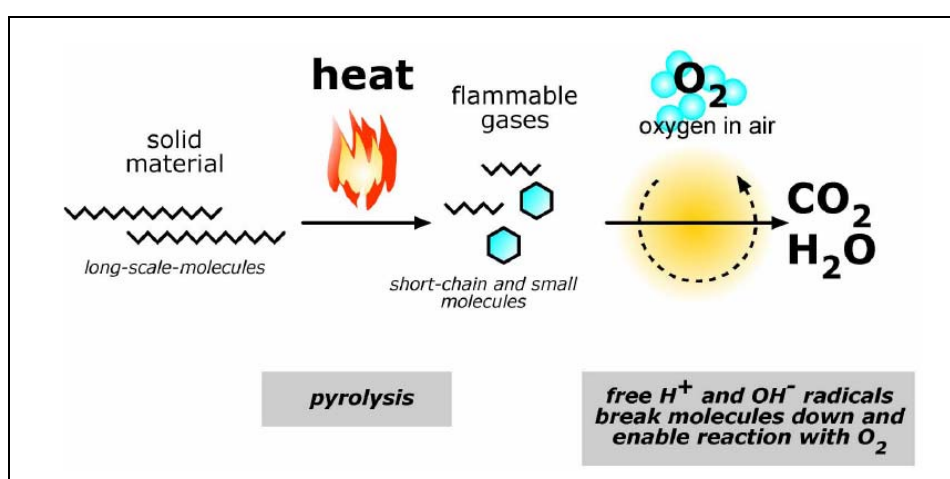


**Figure 2-5** Pyrolysis reaction during fire test.

In the analytic model developed by Anderson and Wauters [12], assumed the intumescence coating mechanism occur continuously as a function of mass loss. The frontal model that used is one dimensional. The coating can be divided into two regions separated by the front, as depicted in Figure 2-6. To the left of the front, the temperature is not sufficiently high to start Intumescence and the material velocity is zero. To the right of the front, intumescence has occurred and the char is moving with a uniform and nonzero velocity,  $u_f$ . It will be found, though, that  $u_f$  changes with time. The heat equation (2-12), applies to both regions, though the convective term is not present in the region to the left of the front since  $u = 0$ :



$$\rho C_p (\partial T / \partial t + u \partial T / \partial x) = \partial / \partial x (k \partial T / \partial x) \quad (2-12)$$

The symbol  $\rho$ ,  $C_p$ , and  $k$  are the density, specific heat and thermal conductivity, respectively. The material properties can be summarized for the two regions:

**Virgin State (Left Region)**

$$m = m_o$$

$$\rho = \rho_o$$

$$u = 0$$

$$k = k_o$$

**Char State (Right Region)**

$$m = m_f$$

$$\rho = \rho_f$$

$$u = u_f$$

$$k = k_f$$

Where  $m$  represents the total coating mass and the subscript zero refers to the initial or virgin state, and the subscript  $f$  refers to the final state after tumescence has occurred.

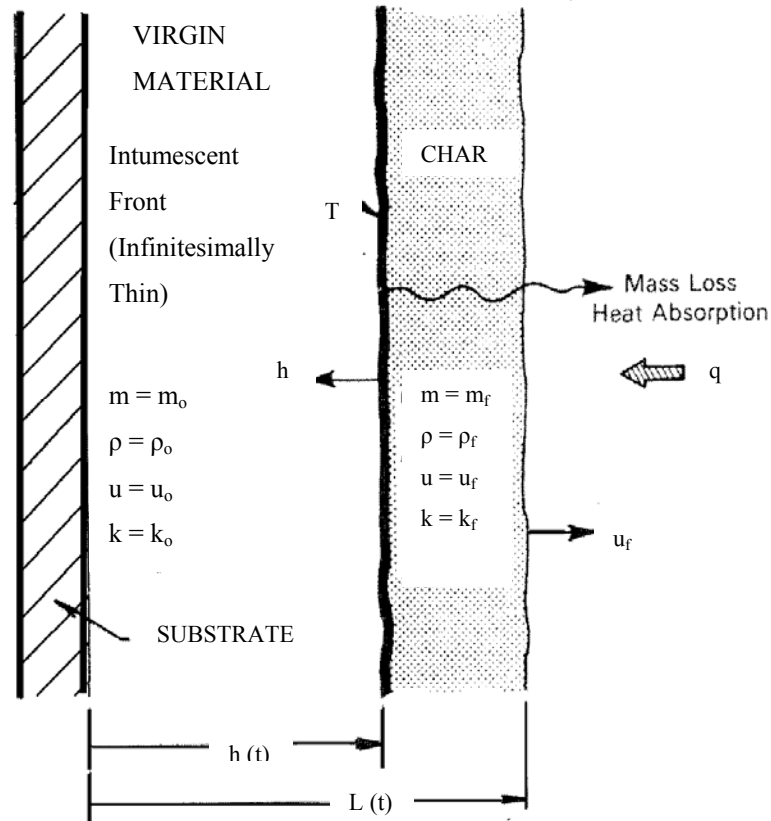


**Figure 2-6** Schematic of frontal model [12].

In order for intumescence to occur, several distinct reactions must occur nearly simultaneously in the proper sequence [13]. The development of a Frontal Model has

provided considerable insight into intumescent reaction mechanisms. The major assumption of the Frontal Model is that the important physics of Intumescence takes place in a narrow zone which is relatively sensitive to temperature. The Frontal Model then takes advantage of this assumption by approximating mathematically this pyrolyzation region, called the front, as infinitesimally thin and at a temperature  $T^*$  (intumescent coating critical temperature). The heat equation is applicable on both sides of the front (i.e., the virgin material side and the char side) and the two regions (virgin material and char regions) are connected by using jump conditions in the velocity, heat flux, and mass (such as mass loss). With these assumptions, the Frontal Model predicts and explains a fundamental property of an intumescent system-the formation of an isothermal front which moves from the free surface to the substrate. As long as the isothermal front persists, the heat transfer to the substrate is limited by the temperature gradient between the front and substrate. In effect, the substrate is protected from the higher temperatures of a fire by an intervening front that is characterized by a temperature considerably lower than the flame temperature.

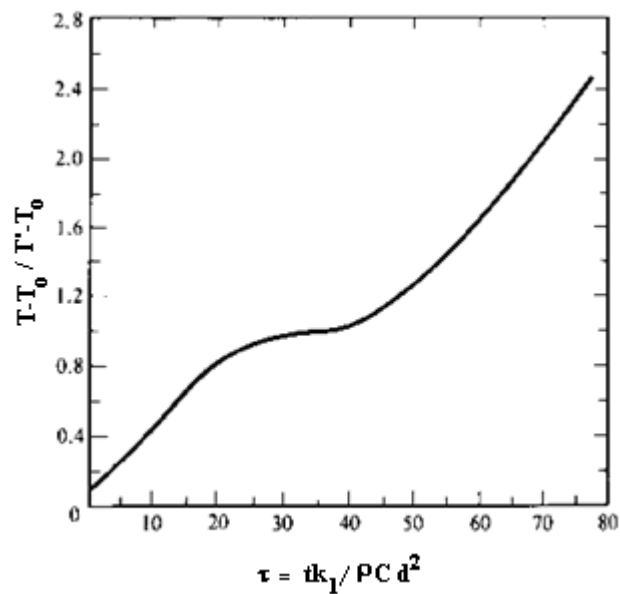


**Figure 2-7** Model prediction of substrate thermal response [13].

Figure 2-7 is representative of the temperature-time history of the substrate coating interface. Note the plateau or leveling off of the temperature in Figure 2-7. The interpretation of this interesting feature predicted by the frontal model is as follows: the substrate is heating with time. However, the heat conducted to the substrate is limited because the temperature of the front is clamped at  $T^*$ . The substrate is shielded effectively

from the high temperature of the external heat source which limits the heat flux until the front reaches the substrate. To be sure, the time it takes for the front to reach the substrate is dependent on the applied heat flux at the external surface and the effectiveness of the intervening char, but the substrate cannot rise in temperature past  $T^*$  until the front reaches the substrate. The time duration or length of the plateau is dependent on the external heat flux and the quantity of heat absorbed via endothermic process at the front. The time it takes for the front to reach the substrate depends upon the velocity of the front,  $h$ , which changes with position. The velocity has its largest value now the surface begins to intumesce and its smallest value the moment the front reaches the substrate. As char intervenes between the surface and the front, the velocity of the front can slow. Indeed, the slower the front moves toward the substrate, the more evident the plateau in Figure 2-7. If a char does not form between the surface and front that is the char ablates away, the front will see a larger heat flux than if there is an intervening char; the front would reach the substrate in a much shorter time, resulting in a short plateau [13].

### **2.3 Carbon Fiber**

Though the intumescent coatings adhere well to most substrate, it is known to embed carbon fiber in the coatings. The carbon fiber is mechanically attached to the substrate. The function of this carbon fiber is to reinforce the char once it forms in a fire. More specifically, this carbon fiber reduces the change that the coating will crack or fissure. Fissures reduce the protection provided by the coating because they allow heat to more easily reach the substrate. When fissure in the material do occur, they are not as deep when carbon fiber is used. As a result, the intumescent coating does not need to be applied as thickly. Glass cloth has also been used to reinforce intumescent coating. Glass, however, softens at temperature to which the coating might be exposed. Once the glass softens, it provides no benefits [69].

The carbon fiber also provides an additional advantage before there is a fire [69]. Intumescent coating are often applied to steel substrate and are often applied where the coating is exposed to harsh environmental condition including large temperature swings of as much as  $120^{\circ}\text{C}$ . Such temperatures swings can cause the intumescent coating debonding from the substrate. However, the carbon fiber will reduce debonding. Debonding occurs

because of temperature swings because of the difference in the coefficient of thermal expansion between the coating and the substrate. When the temperature changes, the coating and the substrate expand or contract by different amount. This difference in expansion or contraction stresses the bond between the coating and the substrate. Even though the intumescent coating is flexible, sufficient stress can break the bond between the coating and the substrate. However, carbon fiber embedded in the intumescent coating makes the coefficient of thermal expansion of the coating much closer to the coefficient of thermal expansion of the substrate. As a result, less stress occurs and debonding is much less likely to happen [70].

## **2.4 Steel Substrate**

Steel is non combustible material that is available in various product type: structural (hot rolled), reinforcing or cool formed. As with any other material, exposure to elevated temperature leads to temporary decrease in the strength and stiffness of steel. Such prolonged degradation adversely affect the resulting deformation and load carrying capabilities of steel during the fire exposure such as deformations are increased and strength and stiffness are reduced. Steel thermal properties are also affected, such as the coefficient of thermal expansion, specific heat and conductivity, which effect the heat transfer and temperature profile calculations [71].

### **2.4.1 Thermal Properties of Steel**

After exposure to temperatures in excess of about 600°C for more than 15 min or more, unprotected steel will quite visibly deform, twist and buckle. Starting from 600°C, the crystalline or metallurgical changes are inconsequential during the fire itself relative to the significant decrease in strength at these elevated temperatures. However, the significant heating effects of the fire could permanently alter the nature of the steel material. Usually steel that has experienced a hot and prolonged fire will have such extensive damage that replacement rather than its straightening and repair, will be prudent on cost consideration alone, so the long term metallurgical changes will be irrelevant [71]. According to iron carbon phase diagram in Figure 2-8, the maximum temperature of steel to maintain its metallurgical structure is below eutectoid temperature, 723°C. Steel that has not exposed to very significant temperature for a prolonged time will not be significantly deformed, its

metallurgy will not be affected after cooling and hence it will regain its original thermal properties.

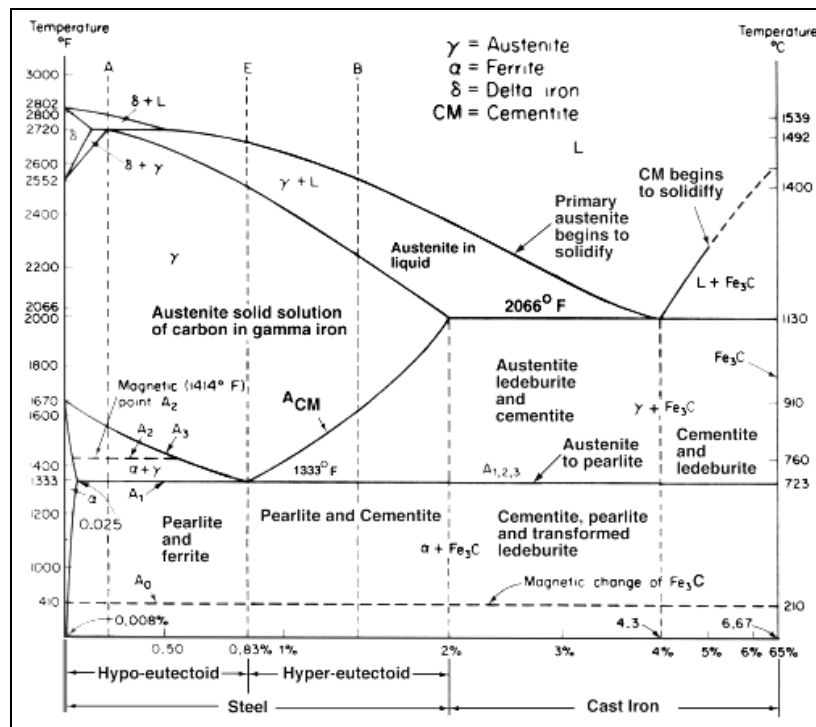


**Figure 2-8** Iron Carbon phase diagram [72].

The coefficient of thermal expansion, melting point, thermal conductivity, heat capacity and specific heat some materials are listed in the Table 2-1. When a metal is heated, it will expand. Some metals expand more rapidly than others as the temperature increases. The coefficient of thermal expansion describes how fast a material expands when subjected to heat. The greater the coefficient, the more a material expands. Melting point is another important thermal property. The material will change from a solid to liquid at this temperature. If heat can travel rapidly across the material, it has high thermal conductivity [73].

## 2.4.2 Mechanical Properties of Steel

Hardness, ductility and strength are the three properties which related to one and another. By measuring the hardness of a metal, the strength, brittleness and ductility of metal are indirectly measured. Factors to be considered include the nature of the applied load and its duration, as well as the environmental condition. Application time may be only a fraction of a second or it may extend over a period of many years. Service temperature may be an

important factor. Table 2-1 presents the comparison of each property for different materials. As temperature changes, mechanical properties also change. The strength, hardness, ductility and modulus of elasticity are normally affected. Generally, as the strength and hardness increase, ductility decreases and the material becomes brittle. A loss of ductility, tensile strength or impact strength as the temperature increases occur suddenly as the temperature reaches a thermal transition level [34].

**Table 2-1** Compares of the coefficient of thermal expansion, melting temperature, thermal conductivity and specific heat of the different materials [73].

Material	Coefficient of Thermal Expansion (per °F)	Melting Temperature (°F)	Thermal Conductivity (cal/cm <sup>2</sup> /°C/sec/cm)	Specific Heat (BTU/lb/°F)
Gray Iron	$6.0 \times 10^{-6}$	2400	0.11	0.130
Steel	$6.5 \times 10^{-6}$	2700	0.11	0.116
Nickel	$7.3 \times 10^{-6}$	2650	0.22	0.109
Copper	$9.2 \times 10^{-6}$	1980	0.94	0.093
Aluminum	$12.8 \times 10^{-6}$	1220	0.45	0.222
Magnesium	$14.4 \times 10^{-6}$	1200	0.37	0.095
Zinc	$17 \times 10^{-6}$	790	0.27	0.031
Nylon	$50 \times 10^{-6}$	300	0.0006	0.400
Polystyrene	$100 \times 10^{-6}$	250	0.001	0.320

### 2.4.3 Chemical Properties of Steel

Corrosion resistance is one of the most important chemical properties of a metal. A metal that has good corrosion resistance is able to protect itself against chemical attack by the environment. A corrosion resistance material can resist humidity without deteriorating. It can also resist sunlight, water and heat. The use of intumescent coating will protect steel from corrosion attack due to its high properties of chemical resistance.

## 2.5 Adhesion

The bonding of an adhesive to an object or a surface is the sum of a number of mechanical, physical, and chemical forces that overlap and influence one another. Mechanical interlocking is caused by the mechanical anchoring of the adhesive in the pores and the

uneven parts of the surface, electrostatic forces, as regard to the difference in electro negativities of adhering materials, and the other adhesion mechanisms dealing with intermolecular and chemical bonding forces that occur at the interfaces of heterogeneous systems [74].

### 2.5.1 Adhesion Theory

The adsorption theory states that adhesion results from intimate intermolecular contact between two materials, and involves surface forces that develop between the atoms in the two surfaces. The figure is presented in Figure 2-9.

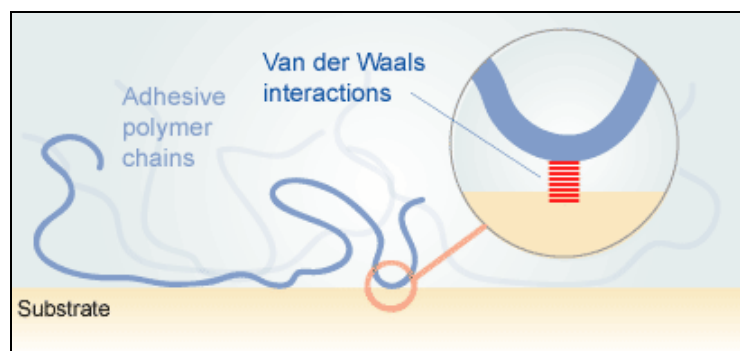


**Figure 2-9** Van der Waals interaction [75].

The adsorption theory is the most important mechanism to achieve good adhesion. The most common surface forces that form at the adhesive-adherent interface are Van der Waals forces. In addition, acid-base interactions and hydrogen bonds, generally considered a type of acid-base interaction, may also contribute to intrinsic adhesion forces. Research has experimentally demonstrated that the mechanism of adhesion in many adhesive joints only involves interfacial secondary forces. The calculated attractive forces between two surfaces are considerably higher than the experimentally measured strength of adhesive joints; this discrepancy between theoretical and experimental strength values has been attributed to voids, defects or other geometric irregularities which may cause stress concentrations during loading. To obtain good adsorption, intimate contact must be reached such that van der Waals interaction or the acid-base interaction or both take place; hence good wetting is essential [75, 74].

Consider a liquid drop on a solid substrate; there are three different phases present according to Figure 2-10. Therefore, there are three surface tensions that need to be considered: solid-liquid, liquid-gas and solid-gas. Young's equation [76] gives the relation between the equilibrium contact angle  $\theta$  the drop makes with the surface and the three surface tensions as:

$$\gamma_{SV} = \gamma_{SL} + \gamma \cos \theta_{\text{equilibrium}} \quad (2-13)$$

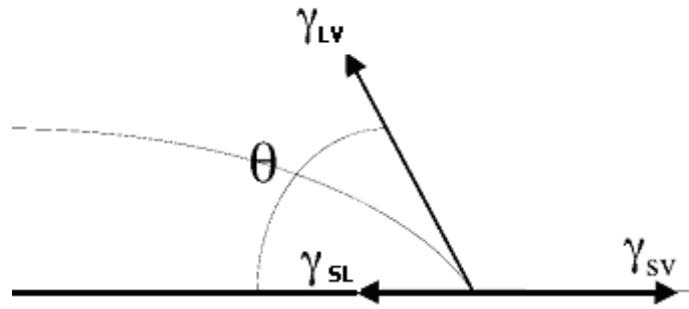


**Figure 2-10** A liquid drop on a solid substrate with three different phases.

Young's equation can also be interpreted as a mechanical force balance on the three-phase contact line; the surface tension is energy per unit area, equivalent to a force per unit length acting on the contact line. Where  $\gamma \equiv \gamma_{LV}$  denotes the liquid vapor surface tension when the three phases, solid, liquid and gas, are at least in mechanical equilibrium (force balance) with each other. Here  $s$ ,  $sl$  and  $\gamma$  are the interfacial free energy per unit area for the solid–vapour, solid–liquid and liquid–vapour interfaces. In addition, we consider chemical equilibrium (chemical potential matching for each component present) and thermal equilibrium (temperature matching) between liquid and gas, so that the gas is the saturated vapor of the liquid. Mechanical, chemical and thermal equilibrium together are referred to as thermodynamics equilibrium [76].

According to equation (2-13), angle  $\theta_{\text{equilibrium}}$  is understood to be measured macroscopically, on a scale above that of long-ranged intermolecular forces. If the three tensions are known, the wetting state of the fluid follows directly. If  $\gamma_{SV} < \gamma_{SL} + \gamma$ , a droplet with a finite contact angle minimizes the free energy of the system; we speak of partial wetting. On the other hand, if  $\gamma_{SV} = \gamma_{SL} + \gamma$ , the contact angle is zero. The system will consequently be in equilibrium when a macroscopic uniform liquid layer covers the whole solid surface and we speak of complete wetting.



The distinction between the different wetting states is usually made by considering the equilibrium spreading coefficient  $S_{eq} \leq 0$ , which represents the surface free energy  $\gamma_{sv}$  relative to its value for complete wetting:

$$S_{equilibrium} \equiv \gamma_{SL} - (\gamma_{SL} + \gamma) = \gamma (\cos \theta_{equilibrium} - 1) \quad (2-14)$$

Figure 2-10 shows the three wetting states that may exist in any three-phase system. For a solid-liquid-vapor system, complete drying would correspond to the intrusion of a macroscopic vapor layer between the solid and the liquid. From a thermodynamic point of view, the wetting and drying states are very similar, the only difference being that liquid and vapor are interchanged. In practice, drying is rather rare (with mercury on for instance, glass as a notable exception) since Van der Waals forces tend to thin vapor layers [76]. The research work focuses on wetting the steel substrate by intumescent coating material.

### 2.5.2 Adhesion Bonding Between Coating and Steel Substrate

The metal and the surface characteristics of metal can have major effects on adhesion. The surface tension of a clean metal surface (usually metal oxide) is higher than that of any potential coating. However, metal surface are frequently contaminated with oil and such surface can have very low surface tension. Steel can be cleaned by abrasive particle blasting such as sand blasting. The surface of steel, including rust, is removed, leaving a rough surface. The surface of clean steel is not iron; rather, hydrate iron oxides are present as a monolayer on the iron. The surface is rarely uniform on the molecular level. Adhesion to this surface is promoted by developing hydrogen bonds between groups on the resin molecules and the oxide and hydroxide groups on the surface of the steel [77].

It follows that adhesion is promoted by using resins having multiple hydrogen-bond donating and accepting groups, such as carboxylic acid (strongly hydrogen-coating), amine (strongly hydrogen-accepting), hydroxyl, urethane, amide (the latter three being both hydrogen-donating and hydrogen accepting), and the phosphate (hydrogen-donating and hydrogen accepting). One might assume that a large number of such substituent on a molecule would be desirable. However, it is known from adsorption studies that if there are

large numbers of polar groups, at equilibrium the absorbed layer can be very thin. At equilibrium, adsorption of adjacent polar groups is favored sterically, resulting in a thin absorbed layer with the polar groups on the steel surface and the only hydrocarbon groups exposed to the rest of the coating. The interaction between the rest of the coating and the hydrocarbon groups would be expected to be weak, resulting in a weak boundary layer and poor cohesion [77].

In general, the results of many studies of adsorption of polymer molecules in metal surface are consistent with Figure 2-10. Although strong interaction between coating and steel is critical for achieving good adhesion, it is also important to develop interaction that cannot be displaced easily by water. A reason that the presence of multiple groups in resin molecules, such as hydroxyl groups on epoxy resins, may be desirable is that some may remain bonded to the steel while others are reversibly displaced by water. This phenomenon has been termed cooperative adhesion [78].

It was found empirically that amine groups on the cross-linked resin molecules promote corrosion protection. Explanations for the effect are controversial; one hypothesis is that the amine groups interact strongly with the steel surface and are not easily displaced by water from the surface as are hydroxyl groups. Phosphate groups are another subsistent group that has been found to improve adhesion in the presence of water (wet adhesion). For example, the use of epoxy phosphate in epoxy coating has shown to improvement on both adhesion and wet adhesion [79].

## **2.6 Electrochemical Description of an Organic Coating on a Metal Substrate**

Electrochemical Impedance Spectroscopy is used to characterize a painted metal substrate - simultaneously measuring two phenomena: (1) the deterioration of the organic coating caused by exposure to an electrolyte and (2) the increase in corrosion rate of the underlying substrate due to the deterioration of the coating and subsequent attack by the electrolyte. In EIS, an AC voltage of varying frequency is applied to the sample [80].

The capacitance of a metal electrode in contact with an electrolyte gives an important information for any electrochemical system [81]. As the organic coating deteriorates with time during exposure to an electrolyte, EIS can track changes in the capacitance of the

coating. The capacitance will change as the coating swells or absorbs water, for example. In addition, changes in the porosity of the coating also can be measured. EIS can also simultaneously monitor the rate of corrosion of the metallic substrate which generally increases as the protective coating fails, allowing the electrolyte to contact the substrate. To quantify these physical and chemical processes with EIS, we need an appropriate equivalent circuit. The equivalent circuit that is most commonly used to describe an organic coating on a metallic substrate is shown in Figure 2-11. Figure 2-11, the equivalent circuit is overlaid on a schematic of a coated metal substrate.

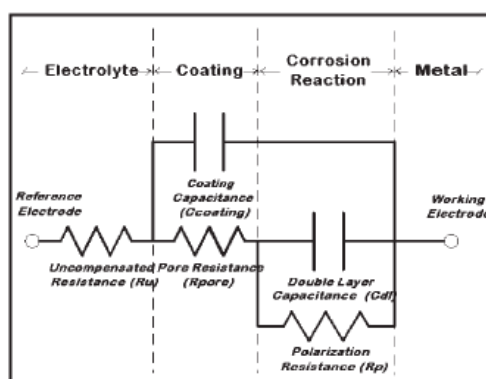


**Figure 2-11** Equivalent circuit of an organic coating on a metal substrate overlaid on a schematic of a painted metal surface.

$R_u$  (Uncompensated Resistance) is the resistance of the electrolyte between the working electrode and reference electrode. For studies of organic coatings, the electrolyte is very conductive, so  $R_u$  is usually very low (1-50 ohms) and can be ignored.  $C_{\text{Coating}}$  (Coating Capacitance) is the capacitance of the organic coating gives an important parameter to measure during coating failure. Because most coatings are relatively thick, the coating capacitance tends to be rather low, in the range of  $1 \text{ nF/cm}^2$ . The physical and chemical properties of the coating that affect the capacitance are [81]:

$$C_{\text{coating}} = (\epsilon) (\epsilon_0) (A)/t \quad (2-15)$$

Where  $\epsilon$  is the dielectric constant of the coating,  $\epsilon_0$  is  $8.85 \times 10^{-14} \text{ Farads/cm}$ ,  $A$  is the area ( $\text{cm}^2$ ), and  $t$  is the thickness (cm). The capacitance is related to the magnitude of the impedance ( $|Z|$ ):

$$(|Z| = 1 / (2\pi f C_{\text{coating}})) \quad (2-16)$$

$f$  is the frequency of the applied AC voltage.  $R_{\text{pore}}$  (Pore Resistance) is the resistance of the coating changes during exposure due to the penetration of electrolyte into the micro pores of the coating. Upon immersion, the pore resistance can be very high ( $>1010 \text{ ohm}$ ) and usually decreases with time of exposure to the electrolyte. However, it is not unusual for  $R_{\text{pore}}$  to increase after long exposure times; the increase is commonly attributed to corrosion products from the metal substrate blocking the pores.  $R_p$  (Polarization Resistance) is the Polarization Resistance describes the corrosion rate of the metal substrate beneath the coating. For a metal in the absence of a coating, the corrosion rate can be determined from the Polarization Resistance. The Polarization Resistance is inversely proportional to the corrosion rate. A typical Polarization Resistance for a bare metal is  $5000 \text{ ohm-cm}^2$ .  $R_p$  must be normalized because it is electrode area dependent.  $C_{\text{dl}}$  (Double Layer Capacitance) is the coating is not the only structural feature of the sample that gives rise to a capacitance. There is a charge on the metal electrode and a charge in the electrolyte that are separated by the electrolyte interface. Since this interface is commonly known as the double layer in electrochemical theory, the capacitance is called the Double Layer Capacitance and abbreviated  $C_{\text{dl}}$  [82]. The value of  $C_{\text{dl}}$  is usually in the range of  $10\text{--}40 \text{ }\mu\text{F/cm}^2$ . This capacitance is much higher than  $C_{\text{coating}}$  ( $\sim 1 \text{ nF/cm}^2$ , or  $10^{-9} \text{ F/cm}^2$ ), so the  $C_{\text{dl}}$  of even a small holiday will be apparent in the EIS response.

$$|Z| = 1/(C_{\text{dl}} \times R_t) \quad (2-17)$$

A metal covered with an undamaged coating generally has very high impedance. The equivalent circuit for such a situation is in Figure 2-12 and the Nyquist for this model is shown in Figure 2-13.

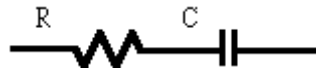


**Figure 2-12** Purely Capacitive Coating.

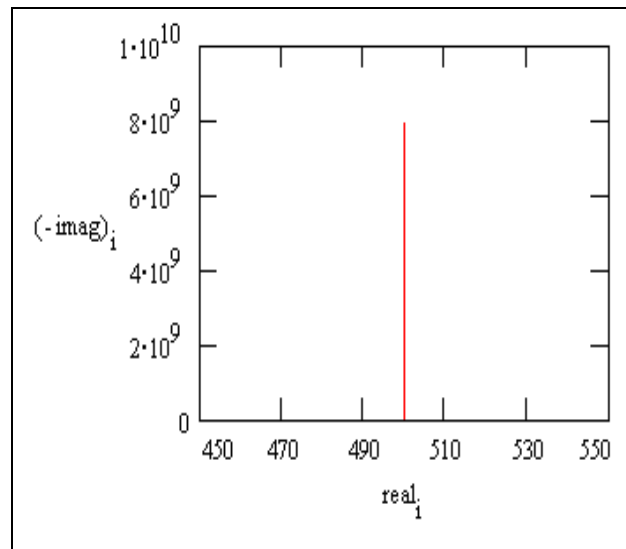


**Figure 2-13** Nyquist plot for excellent coating.

The Nyquist plot for the equivalent circuit in Figure 2-11 is shown Figure 2-14. The adhesion bonding strength can be observed by fitting a data curve to this Nyquist type of model.

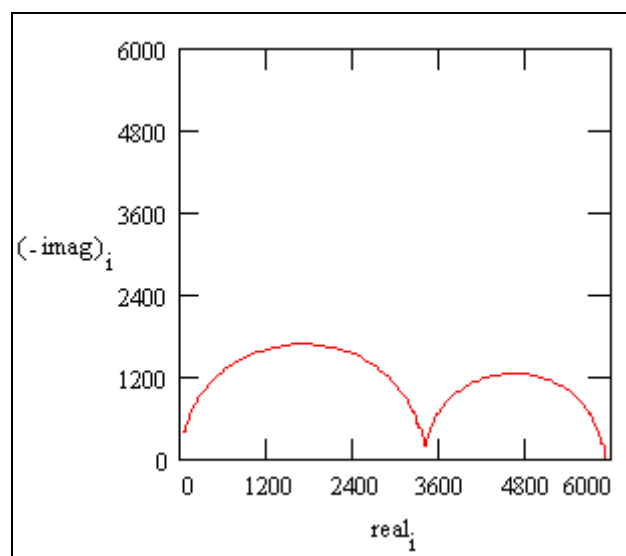


**Figure 2-14** Nyquist plot for damage coating.

## 2.7 Literature Review

### 2.7.1 Effect Thermo Oxidation to Adhesion

The past experimental data have shown that the contact thermo oxidation can have the considerable effects on the stability performance of the adhesive joints. The cohesive

characteristics of the boundary layers in the adhesive joints are affected by the contact thermo oxidation reactions of the polymer catalyzed by iron surface compounds [83]. As pointed out by Kalnins and Ozolins [84], oxygen from several sources can take part in the contact thermo oxidation, oxygen which diffuses through the polymer layer, oxygen captured at the interface, and finally, oxygen which is absorbed or chemisorbed by metal surface oxide. The main features of contact thermo oxidation (oxygen uptake, carbon dioxide evolution, change in the carbonyl group content, and change in the layer weight) under conditions of a free access of oxygen through the polymeric layer are kinetically interrelated with the change in peel strength. The rate of change of the individual kinetic parameters of contact thermo oxidation as well as of peel strength is dependent on the thickness of the adhesive layer and on the contact temperature. The dependence of peel strength on the contact time  $t$  can be described by an expression based on the assumption that the magnitude of peel strength is controlled by two main competing processes, the accumulation of oxygen-containing groups and the oxidation cross-linking which increase the peel strength values, on the one hand, and the reactions of oxidative destruction which decrease peel strength, on the other hand.

Water may affect both the chemical and physical properties of the adhesive and the nature of the interface that exists between it and substrate [85]. Brockmann [86] studied the change in strength and deformability of the adhesive (usually a polymer-based material) layer under hot and humid environmental conditions and concluded that, for aluminum adherents, the water stability is dependent on the adhesive and surface treatment. He pointed out that the two most effective ways to increase stability were: to change the surface condition through special surface pretreatment, and to use corrosion resistant primers.

### **2.7.2 Effect of Coating Thickness to Adhesion**

An interphase is created between the coating part with bulk properties and the metallic surface when epoxy-amine pre-polymers are applied onto metallic substrates. A partial dissolution of the metal oxide is observed. Then, metallic ions diffuse in the liquid monomers mixture (epoxy-amine) and react with the amine groups of either IPDA or DETA monomers to form organometallic complexes. The practical adhesion decreases because of the increase of the residual stresses when the interphase is formed [87]. The interphase figure is shown in Figure 2-15.

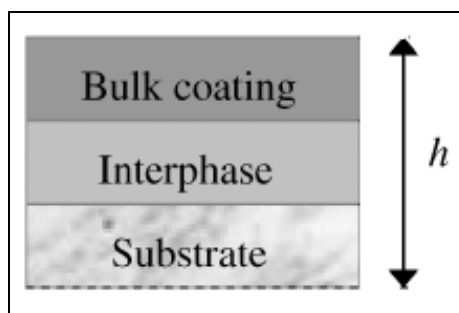


**Figure 2-15** Schematic drawing of tri-layer models [87].

In more recent work, Dillingham *et.al* [88] showed spectroscopically that the molecular structure in the interfacial region of an epoxy/aluminum joint varied with the curing agent and the curing temperature and was different from bulk cured resin. Interphase produced by purely physical process is also well known. Such a process produces the so called trans crystalline region. This region had properties that are different from bulk and these properties influence the mechanical behavior of joint system of materials which contain them [89].

### 2.7.3 Effect of Water Uptake to Adhesion

As is generally known and accepted, adhesively bonded joints will suffer a loss in joint strength when exposed to high humidity, liquid water and/or high temperatures. It can be seen from Figure 2-16 and Figure 2-17 that the young modulus, yield stress and ultimate stress decrease when the adhesive becomes wet, while the strain to failure increases. In other words, moisture increases the flexibility and ductility of the adhesive.

Abdel Wahab *et. al.* [90] have investigated the degradation in the joint strength due to water uptake in terms of the change in mechanical properties and swelling. There is evidence of swelling, which becomes significant as water uptake increases. The effect of moisture on the mechanical properties of adhesive was determined by testing bulk specimens in dumbbell form under dry and wet conditions. The wet specimens were immersed in water at 60°C until saturation. Both dry and wet specimens were subjected to tensile loading and the stress/strain diagrams were obtained. Figure 2-16 shows a comparison between these diagrams. It can be seen from Figure 2-16 that the E-modulus (the slope of the linear part), yield stress and ultimate stress decrease when the adhesive becomes wet, while the strain to

failure increases. In other words, moisture increases the flexibility and ductility of the adhesive.

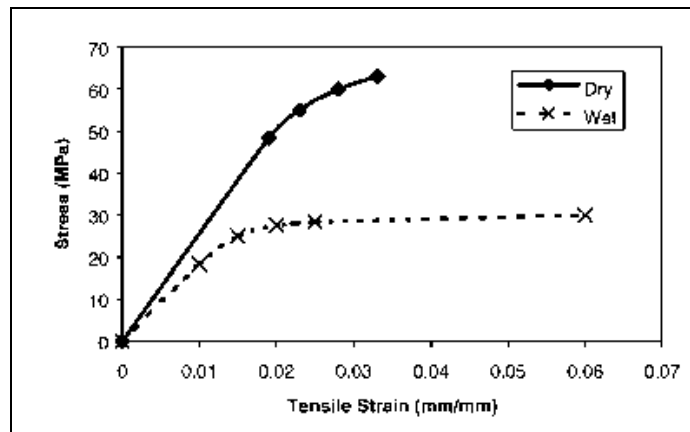


**Figure 2-16** Effect of moisture (wet and dry) on mechanical properties of adhesive joints [90].

The strength retention as a function of immersion time (in weeks) is shown in Figure 2-17 for the tensile butt joints, respectively. It can be seen that the silane improves the durability of the joint. The loss in strength is more significant in the first 3 weeks of ageing [91].

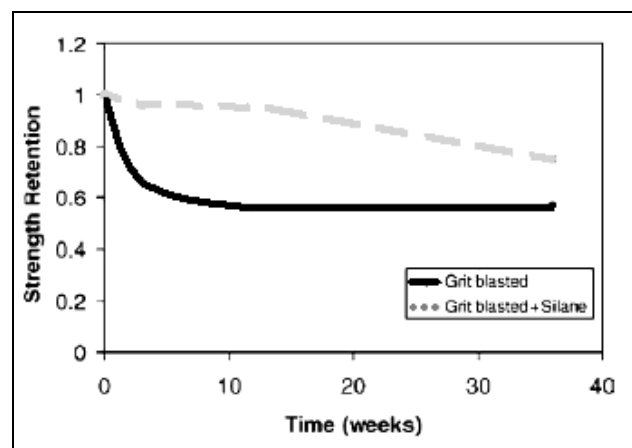


**Figure 2-17** Effect of water uptake on joint strength [91].



## CHAPTER 3

### MATERIALS AND METHODOLOGY

#### 3.1 Materials

##### 3.1.1 Intumescent Coating

The Chartek 7 intumescent coating and the Intergard 251 primer coating were supplied by International Paint Sdn Bhd. Chartek 7 is reinforced epoxy intumescent fireproofing coating, suitable for the protection of steel, aluminum and others from cellulosic and hydrocarbon (pool and jet) fires. The composition and properties of intumescent coating are given in Table 3-1 and Table 3-2.

**Table 3-1** Intumescent coating Chartek 7 resin and hardener composition [92].

Ingredient	Concentration range ( wt.% )
<b>PART A</b>	
Epoxy resin (av.mol.wt.<700)	25 - < 50
Triphenyl phosphate	2.5 - < 10
<b>PART B</b>	
Tetraethylenepentamine	1 - < 2.5

**Table 3-2** Technical data of intumescent coating Chartek 7 [92].

Property	Value	Unit
Tensile strength	12.8 (1850)	MPa (psi)
Lap shear strength	10.0 (1450)	MPa (psi)
Thermal conductivity at room temperature	0.123 (1.45)	W/moC (Btu-in/hr ft2°F)
Coefficient of thermal expansion	68 x 10-6 38 x 10-6	cm/cm°C (in/in°F)
Moisture Absorption	3.3% non topcoated 1.4% topcoated	
Flame Spread	25.0	
Smoke Generation	130.9	
Toxicity Index	1.3	
Hardness	Typically 70	Shore D

### 3.1.2 Primer Coating

Primer coating Intergard 251 is one of the preferred primers coating which have completed the primer qualification procedure from International Coatings. Intergard 251 is Zinc Phosphate based primer coating. The composition of primer coating is presented in Table 3-3.

**Table 3-3** Primer coating Intergard 251 composition [93].

Ingredient	Concentration Range ( wt. % )
<b>PART A</b>	
2-Methoxy-1-propanol	<1
Bis-amine wax	<1
Epoxy Resin liquid	10-25
Ethyl Benzene	2.5-10
Iron oxide	2.5-10
Propylene glycol monomethyl ether	2.5-10
Talc	10.-25
U.f. resin	<1
Xylene	10-25
Zinc phosphate	2.5-10
<b>PART B</b>	
2,4,6-Tris(dimethylaminomethyl)phenol	2.5-10
Xylene	>50

### 3.1.3 Steel Substrate

Carbon steel plate with thickness 15 mm was prepared according to the required standard NACE 2-SSPC-SP 10 [94] and supplier packing list as substrate [95]. Carbon steel is known as cheap material with various applications.

The steel substrate preparation is described on the next section. The chemical compositions of the steel substrate are given in XRF and XRD analysis in next chapter.

## 3.2 Material Preparation

### 3.2.1 Steel Substrate Preparation

The first step in the sample preparation was to clean the sample surface using thinner from grease, dirt and oil. After the surface was cleaned, sand blasting was performed using Air Compressor Airman 370 CFM. Garnet sand with particle size 30-60 mesh and 20-40 mesh were shot from nozzle size 3/8" for about 10 minutes to each steel surface. The steel substrate surface roughness was achieved 50-55  $\mu\text{m}$  while according to NACE SSPC-SP10 [94] and Swedish standard Sa 2.5, the surface roughness is 50-75  $\mu\text{m}$ . Figure 3-1 shows the result of measurement using MOHR Profilometer with testing distance 12.5mm and three times repetition.

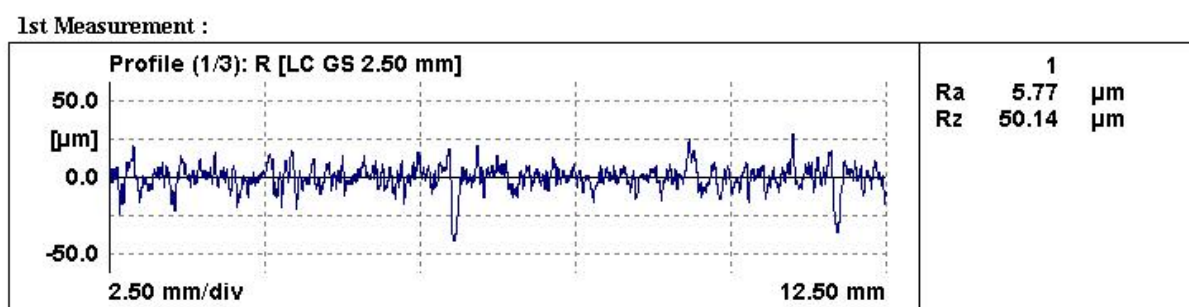


**Figure 3-1** Surface roughness of steel substrate using profilometer.

Ra is general surface roughness. This equipment measures average surface roughness by comparing all the peaks and valleys to the mean line, and then averaging them all over the entire cutoff length. Rz is mean roughness depth.

### 3.2.2 Intumescent Coating Preparation

Mixing of correct proportion of epoxy intumescent coating and hardener was performed according to application manual [92]. The mixtures were processed using the method described hereinafter. The ratio by weight of part A (resin) to part B (hardener) is 2.45: 1 and 4: 1 for intumescent coating and primer coating, respectively. The resin (Part A) was dissolved in hardener (Part B) with correct proportion, by using weighing scale. The coatings were prepared by mixing epoxy and hardener using mixer at 600 rpms and were applied onto steel surface of carbon steel using brush. After the homogenous mixture was achieved, this mixture was applied onto the steel substrate surface (20 x 20  $\text{cm}^2$ ). The

thickness of the coating was measured by automatic caliper before and after dry. A small amount of thinner as a solvent was added to the mixture to improve the flow ability to be applied to the steel substrate. This solvent evaporated and did not affect the coating properties. The schematic of intumescent coated steel is presented in Figure 3-2.

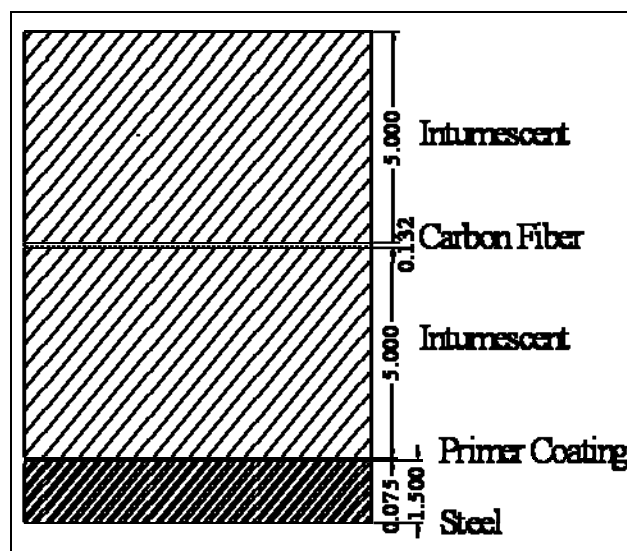


**Figure 3-2** Schematic of intumescent coated steel sample (all dimensions are in mm).

### 3.3 Physical Properties Characterization

#### 3.3.1 Microstructure Examination

Investigation of the physical condition of the samples before and after fire test was conducted using optical microscope and scanning electron microscope (SEM). Every intumescent coating coated sample was cut, cold mounted, and ground using silicon carbide paper grid 120-1200, polished with diamond suspension of 6 $\mu$ m and 1 $\mu$ m diameter and etched with 2% Nital. The cross section sample is given at Figure 3-2. The morphology of the interface layer of the steel substrate and the interface layer between the primer coating and the intumescent coating were observed using Optical Microscope Nikon Eclipse ME600 and Scanning Electron Microscope (SEM) Oxford Leo 1430.

For this study, the variable durations of fire test are 30 min, 45 min, 90 min and 120 min. In practice, people need one to two hours to evacuate to a safe place during fire accident. The microstructure of the steel substrate after fire test will show the quality of the coatings and also the strength of the steel.

### **3.4 Chemical Properties Measurement**

#### **3.4.1 Salt Spray Test**

The chemical resistant of the coating was examined using Salt Spray test chamber according to the required standard ASTM B117 [96]. Three types samples of the bare steel substrate, steel substrate coated with primer coating and steel substrate coated with intumescent coating were sprayed with 2% NaCl solution for 2 weeks. The temperature was maintained at 36-37°C.

#### **3.4.2 Electrochemistry Impedance Spectroscopy (EIS) Test**

The corrosion resistance of the bonding interface between the coating and steel substrate is important to be investigated. The corrosion resistance measurement was performed by measuring the impedance of the coated sample with graphite as auxiliary electrode and Ag/AgCl as the reference electrode. The set up was made of a Weld tester ACM machine with an ACM Instrument analyzer. The electrolyte solution was 2% NaCl, made from 20mg of 99.99 wt. % purity NaCl in 1 liter of water. The PH was around 6 and the temperature was 25°C. Every sample tested was connected with copper wire and mounted with cold mounting. The surface of the sample has to be flat and clean from dirt, oil or dust before the test. The surface of the samples was ground using SiC paper with grid 120-800, and then it was cleaned with water and ethanol to remove all the dirt.

The coating qualities of sample before fire test, after fire test and after three months immersion were tested using EIS test. The adhesion bonding condition also can be measured from the test. Three months immersion was chosen as average time allowance for repair the structure.

### **3.5 Lap Shear Test**

The aim of this test is to correlate the variable coating thickness to adhesive strength of the coating to steel substrate. The test procedure was according to ASTM 3163 [97], with pre load of 100 N, and speed of 0.05 in/min. Five samples of each thickness were tested for more accurate data. The lap shear test sample dimension is shown in Figure 3-3.

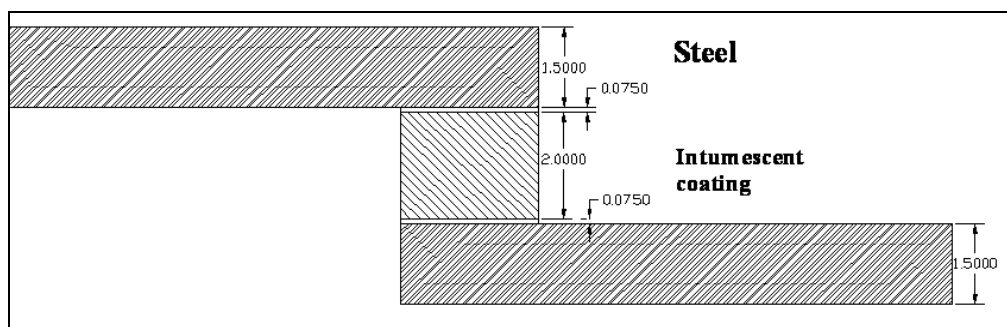


**Figure 3-3** The schematic of lap shear test sample dimension (all dimensions are in mm).

The thickness of intumescent coating depends with the application. In real life, Chartek 7 is used to apply on the steel structure with 10 mm while other brands only around 1 mm to 5 mm of thickness. Therefore, in order to understand about the adhesion bonding on intumescent coating to steel substrate, the variables of thickness were 1 mm, 2 mm, 3 mm, 4 mm, 10 mm and 22 mm.

### 3.6 Coating Characterization

#### 3.6.1 Thermal Properties Characterization

##### 3.6.1.1 Thermo Gravimetric Analysis (TGA)

The thermo gravimetric analysis of samples (approx. 10 mg) were carried out at a heating rate of 10°C /min of gas Nitrogen with flow rate 20 ml/min over the whole range of temperature 25°C to 800°C. The data was recorded using Pyris Player Data Analyzer.

##### 3.6.1.2 Differential Scanning Calorimetry (DSC)

DSC thermo grams were performed using Perkin Elmer Instruments Pyris 1 to determine the thermal history of the intumescent coating. The sample weight was about 10 mg and encapsulated in an aluminum pan. The DSC instrument was heated from -40°C to 400°C at a heating rate of 10°C/min under the nitrogen flow of 20 ml/min.

##### 3.6.1.3 Fourier Transform Infrared Spectroscopy (FTIR)

The functional group of intumescent coating powder before and after fire was analyzed by FTIR, model Perkin Elmer. The powder samples were ground and mixed with KBr to form

pellets and attached to FTIR instrument. Then, the spectra were analyzed using Spectrum One data acquisition system. The FTIR spectra data were recorded in the range of 4000-300  $\text{cm}^{-1}$ , the number of scanning is 8.

### **3.6.2 Coating Composition Measurement**

#### **3.6.2.1 Energy Dispersive X-Ray (EDX) and X-Ray Fluorescence (XRF)**

The combination of EDX and XRF results not only improve the accuracy of the analysis but also the range of elements that can be detected [98]. EDX was employed to determine the chemical composition of the intumescent, primer coating and steel substrate.

The chemical analysis was conducted using XRF testing machine, Bruker AXS, XRF S4 Pioneer. The steel sample was in the form of 40 mm circle, while the intumescent coating and primer coating were in the form of fine powder, of 20 g each in weight. The surface of the steel sample was cleaned using thinner and ground with SiC paper grid 800-1200.

### **3.7 Mechanical Properties Characterization**

#### **3.7.1 Hardness Test**

The mechanical properties of intumescent coating were conducted using Shore D Scale Durometer Hardness. Five indentations on intumescent coating sample were taken to get accurate result. For the steel substrate, hardness test was performed using Micro hardness Vickers tester, Leco LM 247AT. The steel surface was ground with silicon carbide paper grid 240-1200 and polished with diamond suspension 6  $\mu\text{m}$  and 1  $\mu\text{m}$  in order to get flat and smooth surface. An example of the indentation is presented in Figure 3-4.

Vickers hardness is a measure of the hardness of a material, calculated from the size of an impression produced under load by a pyramid-shaped diamond indenter. The indenter employed in the Vickers test is a square-based pyramid whose opposite sides meet at the apex at an angle of 136°. The diamond is pressed into the surface of the material with 300 kilogram-force, dwelling time of 15 seconds and the size of the impression is measured with the aid of a calibrated microscope. The Vickers number (HV) is calculated using the following formula [99]:

$$HV = 1.854 \left( \frac{F}{D^2} \right) \quad (3-1)$$

With  $F$  being the applied load (measured in kilogram-force) and  $D^2$  the area of the indentation (measured in square millimeters). The applied load is usually specified when the HV is cited.

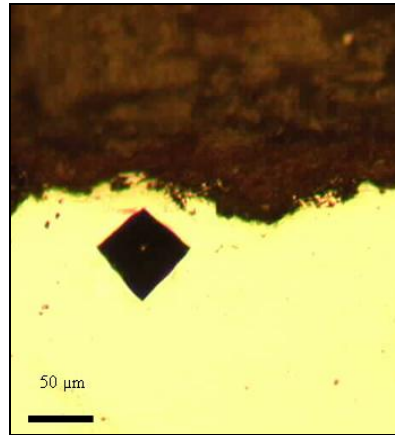


**Figure 3-4** The hardness indentation on steel substrate of the sample using Vickers hardness tester, Leco LM 247AT.

### 3.8 Fire Test

Fire test was conducted to evaluate the penetration of fire to the steel substrate according to standard ASTM E119 [100]. The fire test is schematically presented in Figure 3-5.

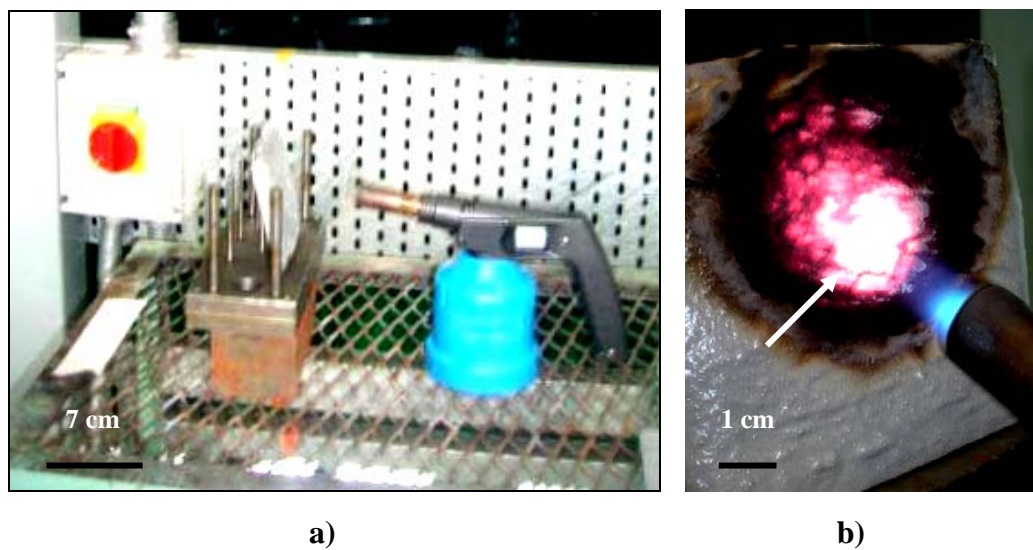


**Figure 3-5** a) The experimental set up the fire test, b) The center of the sample (arrow) taken for further examination.



The test was carried out for 30, 45, 90 and 120 minutes. The heat of the fire was set up according to hydrocarbon fire temperature. The fire was shot from LPG Bunsen burner with temperature of 1000°C at a distance of 7 cm from the intumescent coating surface. The steel substrate surface was monitored every second for 300 seconds and the temperature was measured using Hanna Thermocouple. The thermocouple was used to measure the temperature on the sample surface, at the back of the sample and at 15 cm behind the sample (environment).

## CHAPTER 4

### RESULTS AND DISCUSSION

#### 4.1 Physical Properties Characterization

Physical properties of the steel substrate and the adhesion bonding of intumescent coating to steel were analyzed under optical microscope and scanning electron microscope. These physical properties in this section are divided into two sections, before and after fire test. The effect of heat from burner influences coating adhesion to steel substrate. Therefore, the time variables for fire tests from 30 minutes to 120 minutes are sufficient to investigate the adhesion at interface between steel and intumescent coating. A good mixture of intumescent coating is a key to have satisfying property profile of the produced material and enable the whole process to be much more efficient.

##### 4.1.1 Optical Micrographs Analysis Before Fire Test

The microstructure of the steel substrate and the cross section of the intumescent coated steel are shown in Figure 4-1a and Figure 4-1b. Figure 4-1a shows that the steel substrate contains ferrite structures with elongated grains. The evidence of this phase was further confirmed with XRF and XRD result which indicate that the substrate is a carbon steel.

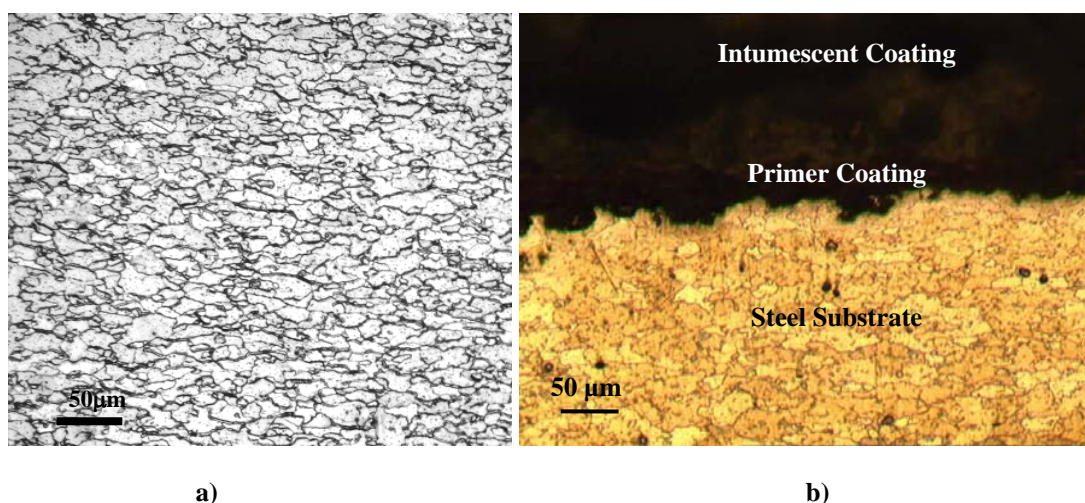


**Figure 4-1** Optical micrographs, a) steel substrate, b) cross section of intumescent coated steel. Magnification : 100x.

Figure 4-1b shows the intumescent coating formed uniform surface with the primer indicating good wetting of the intumescent on the zinc phosphate primer surface. The jagged interface of the steel substrate surface is the result of blasting during surface preparation. The surface roughness aids in developing adhesive bonding between the steel and the primer coating with interlocking effect.

A thin layer of primer was applied on the steel surface in order to enhance the adhesion bonding between intumescent coatings to steel substrate. The successfulness of primer coating fulfill the jagged interface on steel depends on the surface tension of primer coating and steel substrate. Flaws and dirt would increase the surface tension on steel surface and resulted to bad adhesion with primer coating. In order to eliminate the flaws on the jagged steel surface, good wetting of the surface is important. Intimate contact occurs when the adhesive spontaneously spreads over the surface. Spreading (spontaneous or not) can be examined by contact angle measurement [101].

#### **4.1.2 Optical Micrographs Analysis After Fire Test**

The intumescent coated steel was burnt out for 30, 45, 90 and 120 minutes using LPG burner. As seen in Figure 4-2, the structure integrity of primer coating and steel substrate surface were well performed and these are shown by stable microstructures on the steel substrate surface although induced heat from LPG gas. The grain size on the surface shows that grain shape was not affected by heat and there was no phase transformation on the surface.

Figure 4-2a shows the interface between steel substrate, primer coating and intumescent coating after burnt for 30 minutes. The structures remained stable by showing no gap formation after 30 minutes exposure. The steel microstructures remain the same as before the fire test. The intumescent coating has successfully protected the steel from the heat.

Figure 4-2b shows the interface of steel, primer coating and intumescent coating and the structures are also remained unchanged by showing no gap formation after 45 minutes fire test. The figure shows no phase changed created for 45 minutes of fire test.

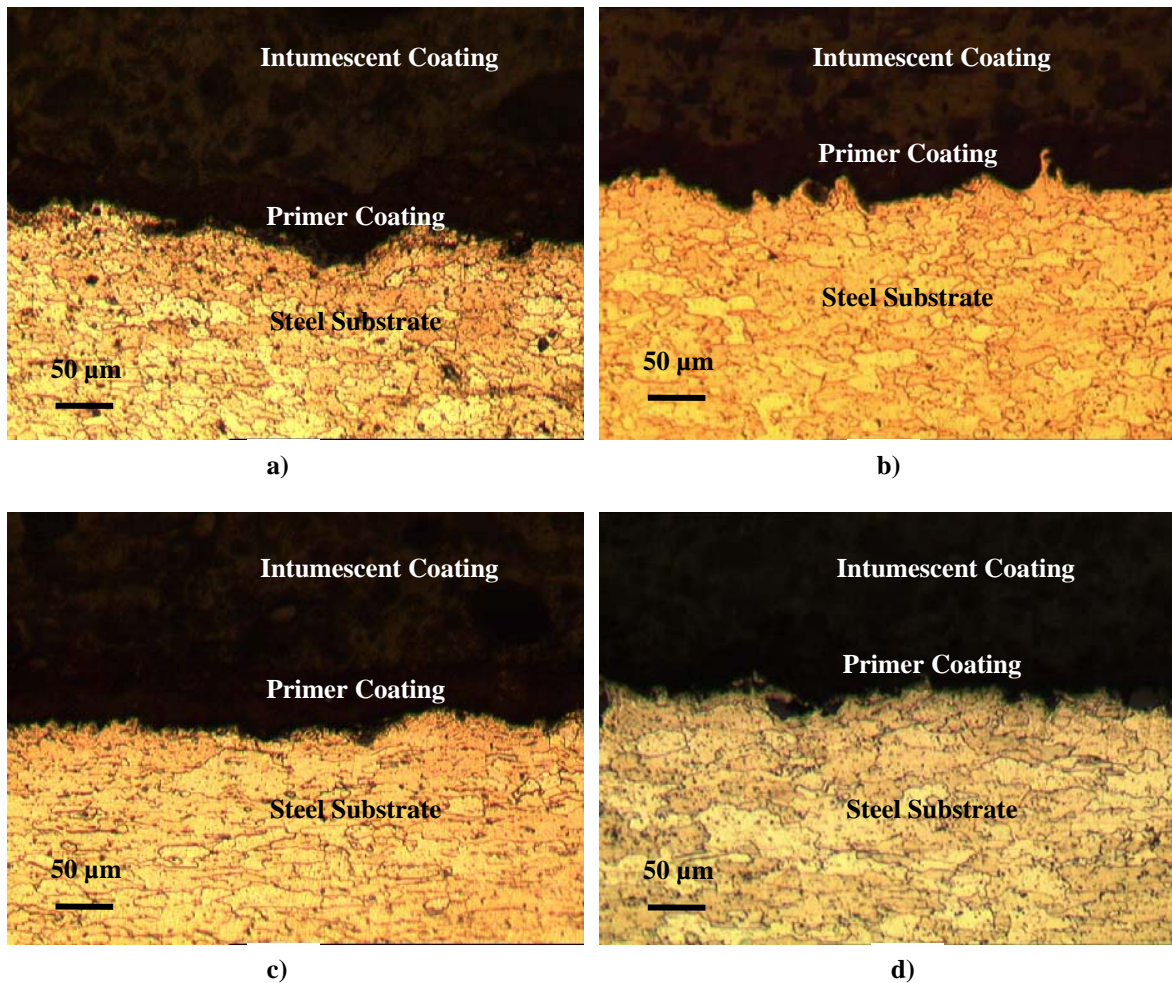


**Figure 4-2** Microstructure of steel substrate conditioned with different fire test duration of a) 30 min, b) 45 min, c) 90 min and d) 120 min of fire test duration. Magnification: 100x.

Figure 4-2c shows the interface of steel, primer coating and intumescent coating after 90 minutes fire test. It could maintain the structure by showing no debonding and no new phase formed after fire test.

Figure 4-2d shows interface of steel substrate, primer coating and intumescent coating remained stable and no gap was formed after 120 minutes of fire duration. The ferrite phase remained stable and the grain size was slightly increased. No crack has occurred on the steel surface after two hours of exposure time.

Referring to Figure 4-3, the effect of annealing will occur at temperature above 400°C. The optical micrographs show that the intumescent coating and primer coating could protect the steel substrate from softening by holding the temperature at the interface below 400°C.

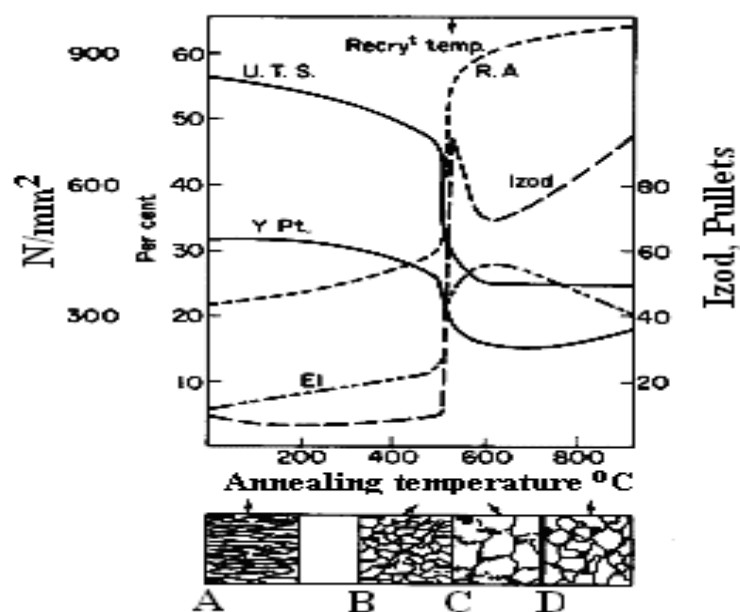


**Figure 4-3** Effect of annealing cold-worked carbon steel [102].

The re-crystallization temperature of pure iron is in the region of 500°C consequently the higher temperature of 650°C brings about rapid re-crystallization of the distorted ferrite [102]. Therefore, the optical micrographs of steel substrate after fire test were inline with the theory.

#### 4.1.3 Electron Micrographs Analysis Before Fire Test

Further investigation on adhesion bonding of steel substrate, intumescent coating and carbon fiber performance before fire test are presented in Figure 4-4. The Electron Micrographs of Figure 4-4a shows the cross section of intumescent coated steel sample. The thickness of primer coating is 75  $\mu\text{m}$  while the thickness of intumescent coating is 10 mm, both created during experiment. This figure shows that all the elements are uniformly bonded together.

Figure 4-4b shows good bonding between intumescent coating and primer coating. This is achieved since both are using the same binder, epoxy based. The presence of additives will be revealed using EDX in next section.

Figure 4-4c shows the small gap between the primer coating and the steel substrate and this is due to the effect of mechanical interlocking. The primer coating viscosity and jagged profile of the steel substrate determine the size of the gap created at the interface.

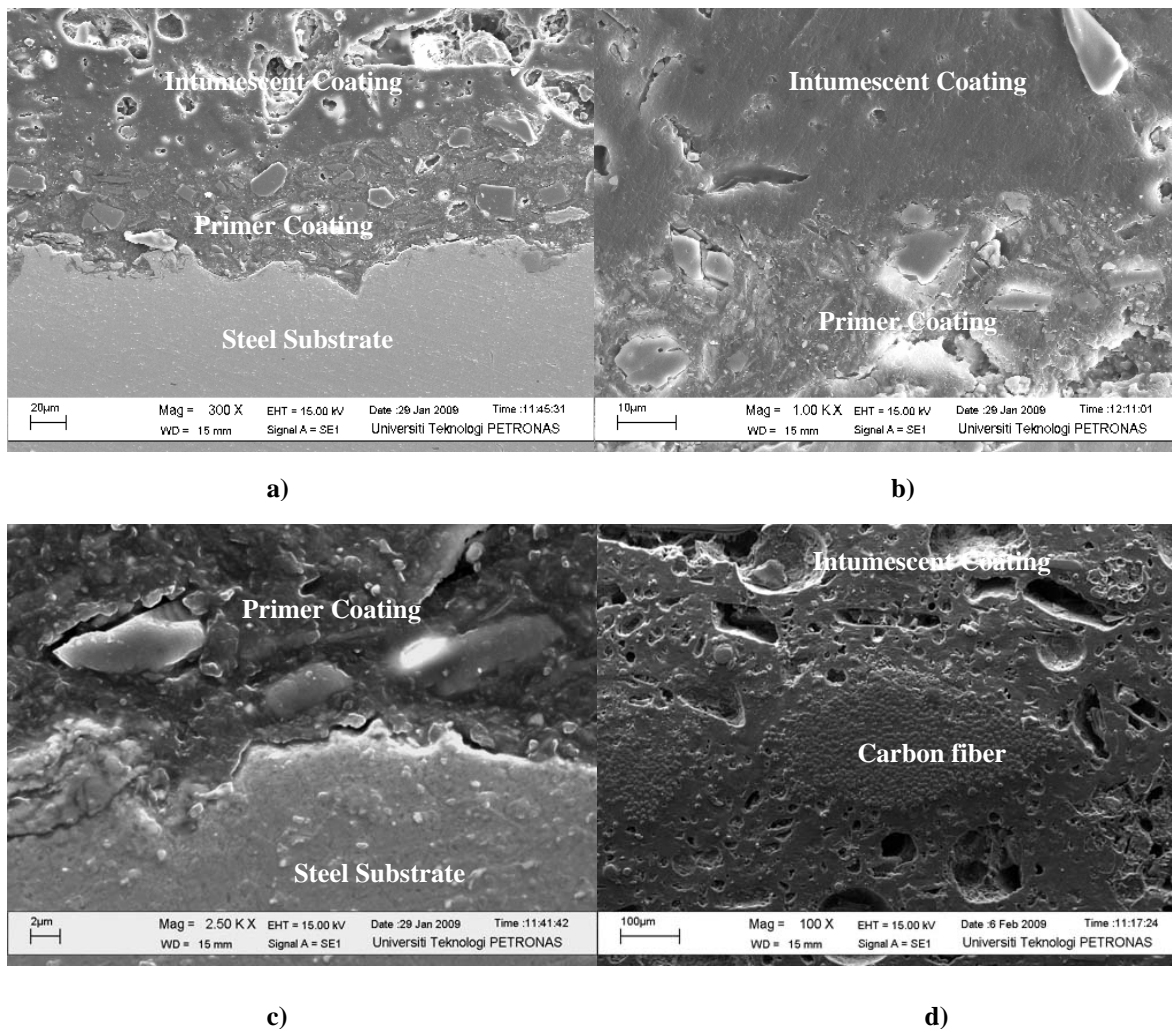


**Figure 4-4** Electron micrographs for sample before fire test. a) Overall sample structures, b) interface of intumescent coating and primer coating, c) interface of primer coating and steel substrate, d) carbon fiber in intumescent coating.

The mechanical bonds involve solely mechanical interlocking at the steel substrate surface and primer coating. Mechanical anchoring promoted sand blasting produces a large number of pits and corrugations. According to tortuous surface profile, contact angle of the liquid polymer decreases with an increase in roughness. The surface roughness alone may change the advancing contact angle ( $\theta_a$ ) on a rough surface compared with the contact angle ( $\theta$ ) on a smooth surface of identical surface chemistry. This change can be expressed by [103]:

$$\cos \theta_a = r_f \cos \theta_{eq} \quad (4-1)$$

Where,  $r_f$  is the roughness factor which is the ratio of actual to nominal surface areas of the solid. The roughness ( $r > 1$ ) will reinforce the wetting properties of the smooth substrate. If  $\theta_{eq}$  is more than  $90^\circ$ , roughening will result in a bigger  $\theta_a$ . This will decrease the apparent surface tension of the solid surface,  $\gamma_{sv}$ . Therefore, the sand blasting treatment is very important to achieve good mechanical bonding between steel and intumescent coating since it created new surfaces.

Figure 4-4d shows carbon fibers were embedded in the middle of intumescent coating. The carbon fiber formed a good bonding with intumescent coating without creating any defect between them.

#### 4.1.4 Electron Micrographs Analysis After Fire Test

The intumescent coating, primer coating and steel substrate integrity after fire test are presented in Figure 4-5 to Figure 4-8, respectively.

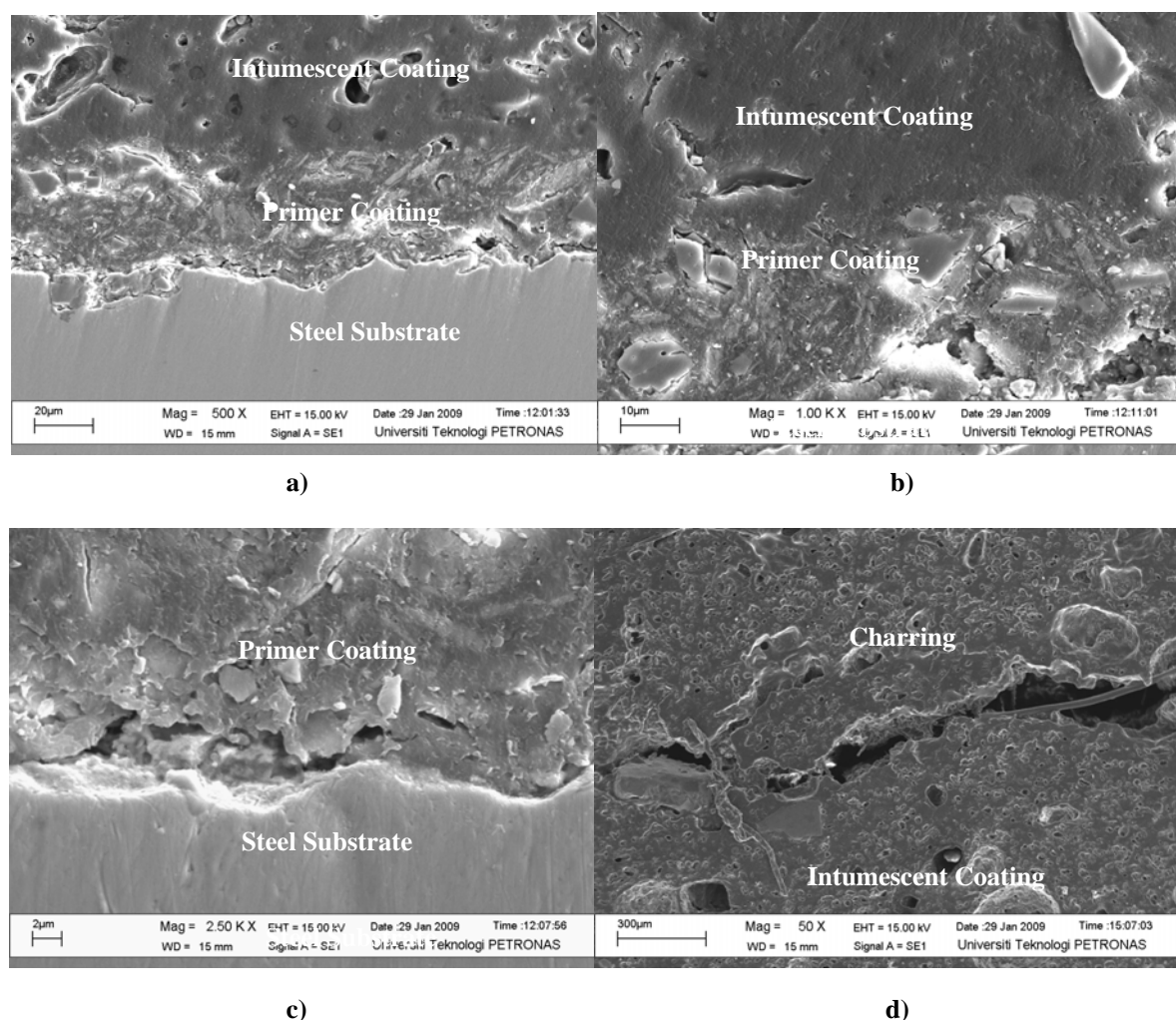
Figure 4-5a shows the cross section of intumescent coated steel after 30 minutes of the fire test. Comparing to sample before the fire test, the adhesion bonding on the steel surface and the intumescent coating degraded by showing a small gap on it.

Figure 4-5b shows the interface of primer coating and intumescent coating remained stable and no crack has occurred. The adhesion bonding was strong enough to hold the heat.

Figure 4-5c shows the gap along the steel surface and primer coating formed and this is due to different in thermal expansion of the material and adhesion properties. According to literature, the thermal expansion of steel is  $12 \times 10^{-6} / ^\circ\text{C}$  while intumescent coating has higher value as  $68 \times 10^{-6} / ^\circ\text{C}$  [104]. Therefore, by increasing the temperature, the intumescent coating would easily expand wider than the steel. The jagged surface on steel surface locked the intumescent coating from debonding.



Figure 4-5d shows the carbon fiber within the intumescent coating after fire test. The TGA result shows that the carbon fiber melting point was higher than intumescent coating. Therefore, the carbon fiber protected the lower side intumescent coating at high temperature.



**Figure 4-5** Electron micrographs for sample after fire test for 30 minutes. a) Overall sample structures, b) interface of intumescent coating and primer coating, c) interface of primer coating and steel substrate, d) carbon fiber in intumescent coating.

The Electron Micrographs in Figure 4-6 show the intumescent coated steel after 45 minutes of fire test. The big pores were formed on intumescent coating due to the escaping blowing agent which is shown in Figure 4-6a. Figure 4-6b shows the adhesion bonding of intumescent coating and primer coating remaining stable and still able to maintain its integrity after the fire test for 45 minutes. No gap formed along primer and steel substrate surface.



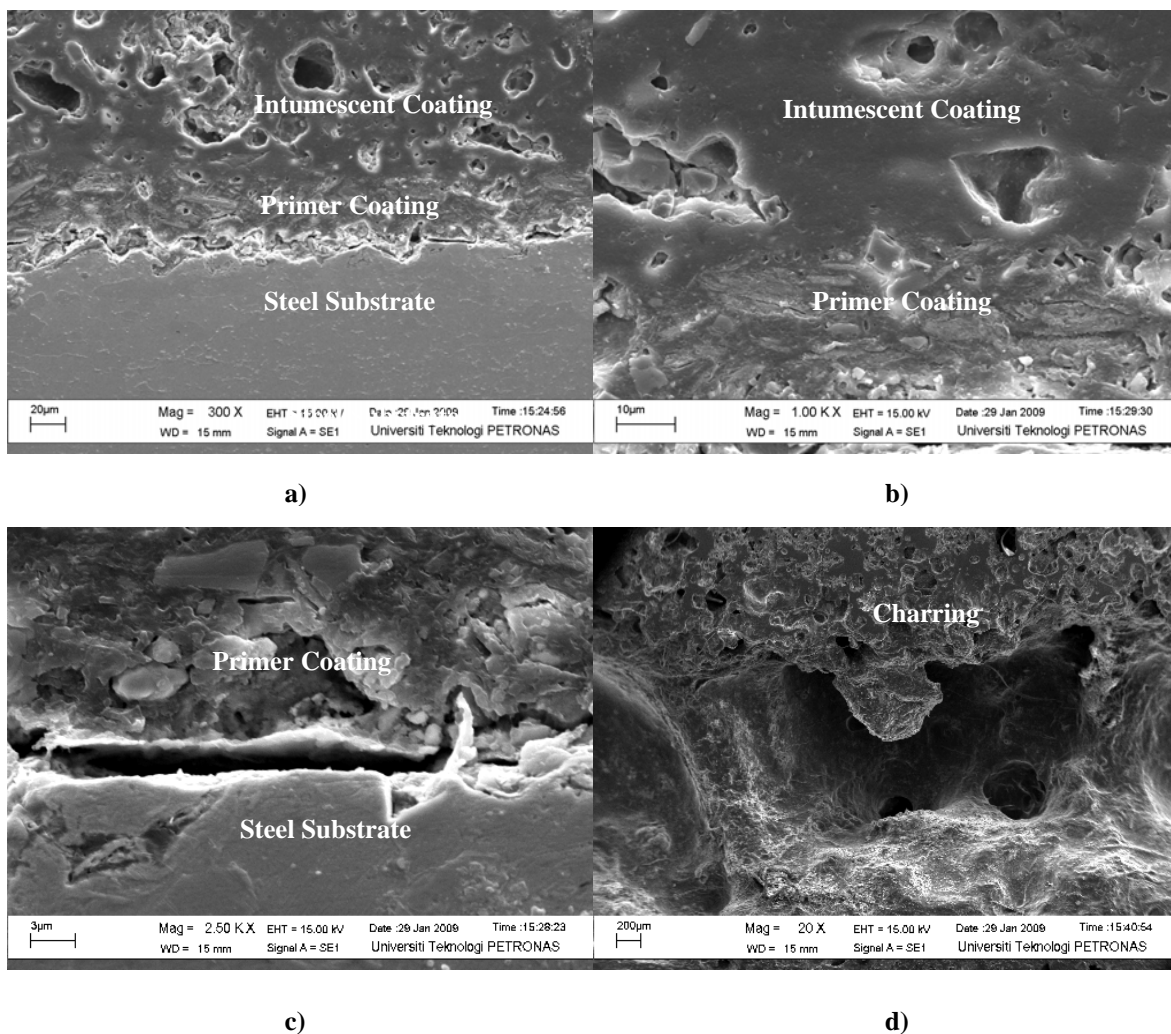


**Figure 4-6** Electron micrographs for sample after fire test for 45 minutes. a) Overall sample structures, b) interface of intumescent coating and primer coating, c) interface of primer coating and steel substrate, d) charring layer.

A bigger gap formed along the interface of steel substrate and primer coating which is shown in Figure 4-6c. The gap might be a site for oxygen or hydrogen entrapped due to the environment between the primer coating and steel substrate. The oxygen may form FeO, Fe<sub>2</sub>O<sub>3</sub> or other iron oxides with steel substrate on the steel surface. In addition, the oxygen may also cause to form some bonding between hydroxyl groups of the epoxy binder which may causes the debonding of the coating by increasing the temperature and time. Figure 4-6d shows the creation of charring layer of intumescent coating on the surface after 45 minutes of fire test duration. The cracks in the charring layer indicated that heat at this location place reached the melting point of intumescent coating.

The intumescent coated steel condition after 90 minutes fire test is shown in Figure 4-7. Figure 4-7a shows that the intumescent coating was able to protect the steel substrate from changes in structure and properties after 90 minutes of fire test.

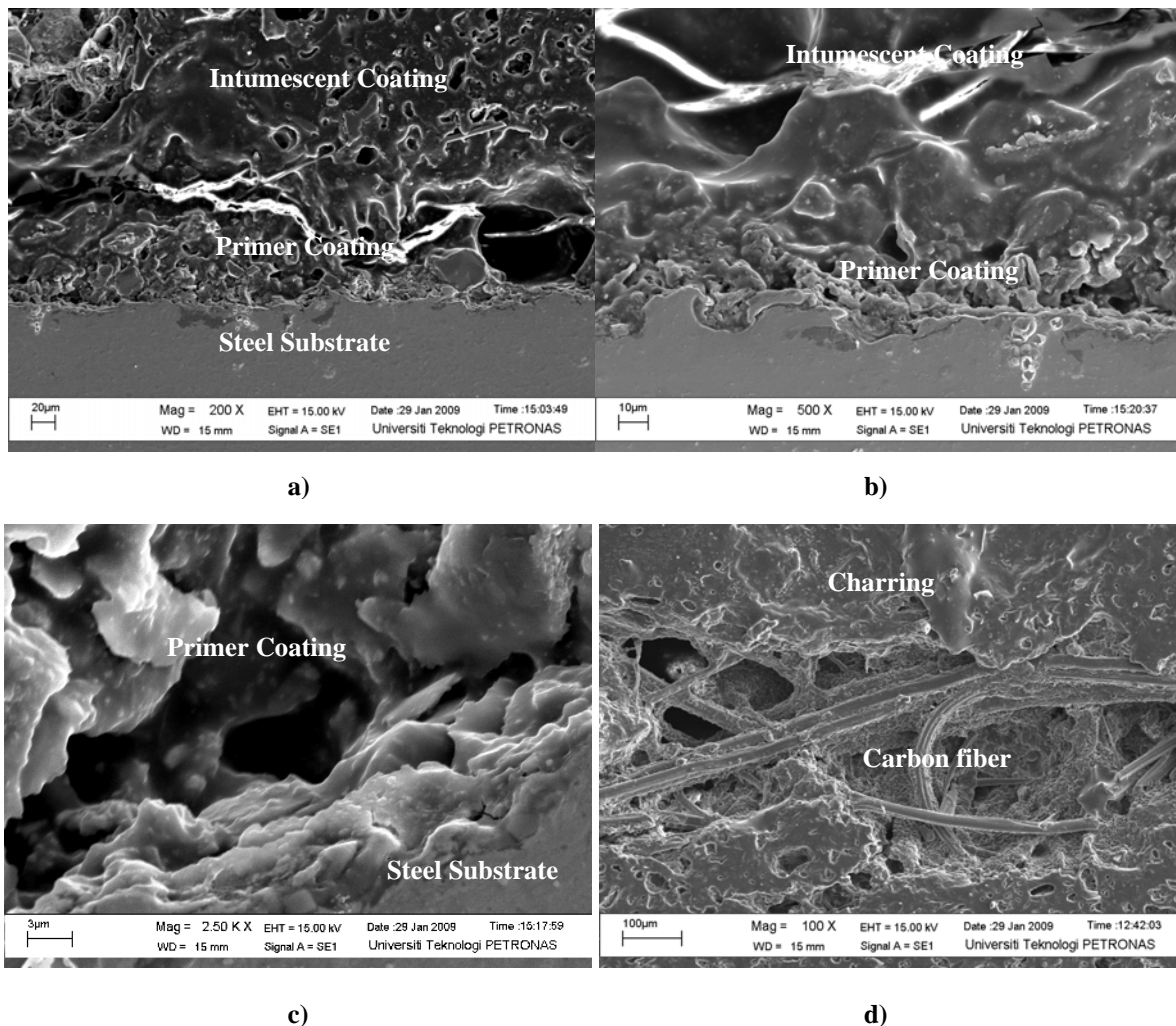


**Figure 4-7** Electron micrographs for sample after fire test for 90 minutes. a) Overall sample structures, b) interface of intumescent coating and primer coating, c) interface of primer coating and steel substrate, d) carbon fiber and charring layer in intumescent coating.

Figure 4-7b shows that after 90 minutes of fire test, the adhesion bonding between primer coating and steel substrate remained stable and no crack was formed along the surface.

Figure 4-7c shows the gap between primer coating and steel substrate with some amount of primer coating embedded on steel surface. This is probably due to the lock and key mechanism of mechanical interlocking system on steel surface and the additives that enhance the adhesion bonding to steel substrate.

Figure 4-7d shows that the heat started to destroy the carbon fiber after 90 minutes of fire test and formed char on it. The carbon fiber reinforced the intumescent coating to maintain its structure at high temperature.

The longest fire test duration was 120 minutes and the electron micrographs can be seen in Figure 4-8. Figure 4-8a shows the structure remained stable with no crack formation on steel surface. From this figure, the intumescent coating successfully protected the steel at temperature 1000°C up to two hours.

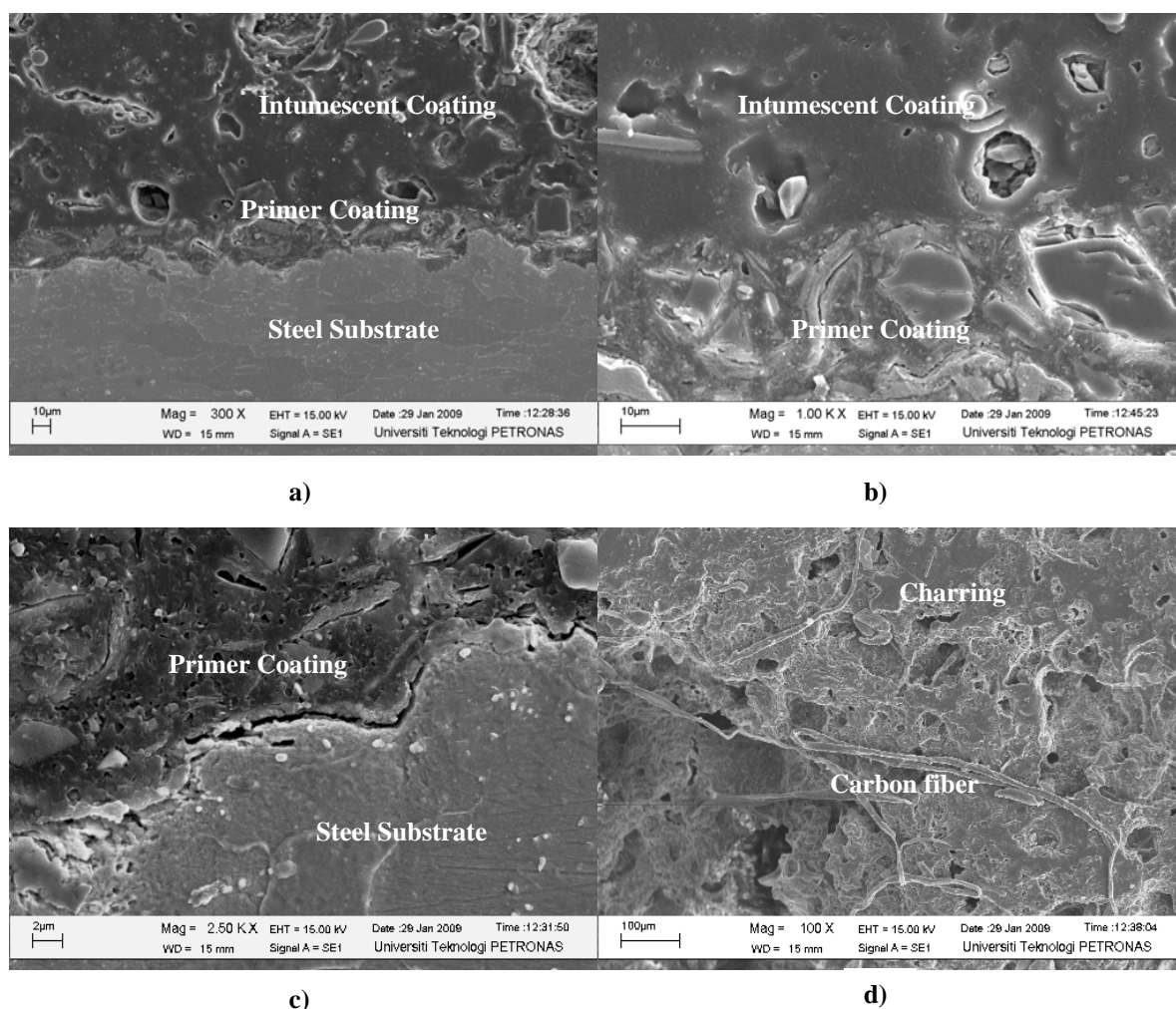
Figure 4-8b shows the stable interface layer between intumescent coating and primer coating by showing no crack and debonding. The primer coating degradation is shown by small cracks in the structure of primer coating. This was probably due to the heat reaching the melting temperature.

Figure 4-8c shows no crack was formed on steel substrate surface but a gap was formed along the surface. The steel substrate microstructure remained stable by showing no phase changes. The degradation of primer coating was observed by forming pores on the surface after the two hour fire test.

Figure 4-8d shows the carbon fiber successfully degraded after two hours fire test. The degradation of the carbon fiber was due to the heat was reaching the carbon fiber's  $T_g$  (glass temperature). This figure also indicates that the carbon fiber is not only a good reinforcement but also good capacitor. The intumescent coating acted as a fire retardant coating unless the carbon fiber is melted and the entire charring layer was formed.

The higher melting point of carbon fiber than intumescent decomposition temperature is useful to maintain the charring structure. The thickness of the coating applied to the steel substrate is an important parameter which limits the performance of the coating. The intumescent coating thickness should be chosen correctly to protect the fiber from environmental attack, minimize the residual stress, minimize the lost in strength, optimize the toughness, and induce a none brittle failure modes [105]. Based on literature, the carbon fiber is useful for structural application due to their high specific strength, high modulus and near zero coefficient thermal expansion. Many composite which contain carbon fibers can

be used at high temperature with less degradation and a good resistance to corrosive environment except for oxygen at high temperature [106].



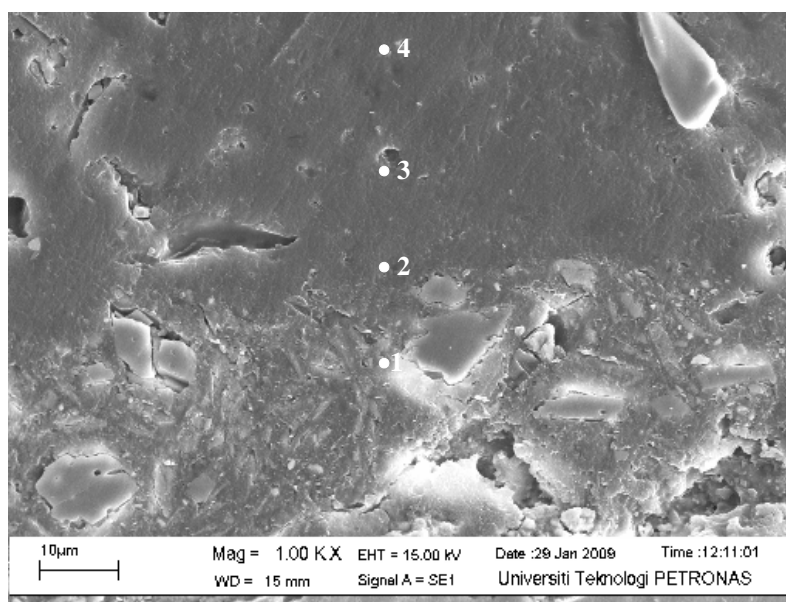
**Figure 4-8** Electron micrographs for sample after fire test for 120 minutes. a) Overall sample structures, b) interface of intumescent coating and primer coating, c) interface of primer coating and steel substrate, d) carbon fiber and charring layer in intumescent coating.

Figure 4-5 to Figure 4-8 show that the weakest region is at interface between the steel substrate and the primer coating. As this will be evidence for the lap shear test results, the interface strength between steel and primer coating is high since fracture happened at the interface layer between the intumescent coating and the primer coating. This means the adhesion strength of the steel substrate and the primer coating is primarily due to mechanical interlocking mechanism. Surface preparation before applying the coating becomes important part since the steel surface roughness can promote the adhesion strength of the interface.

#### 4.1.5 Energy Dispersive X-Ray Analysis

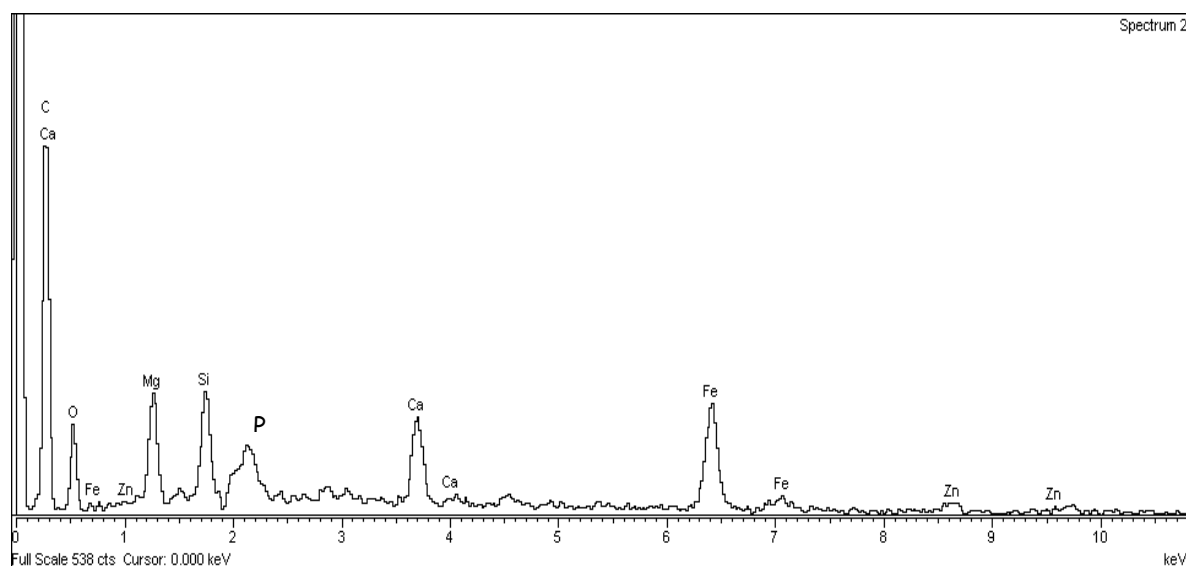
Referring to electron micrographs at previous section, the interface between intumescent coating and primer coating maintained stable after two hours exposed with fire. EDX was used for further investigation on the interface between intumescent coating and primer coating.

Figure 4-9 shows the some points on electron micrograph which refers to 1) primer coating, 2) the interface between intumescent coating and primer coating, 3) intumescent coating, and 4) intumescent coating, before exposed to fire. The EDX analysis on every point depict in Figure 4-10 and Figure 4-11.

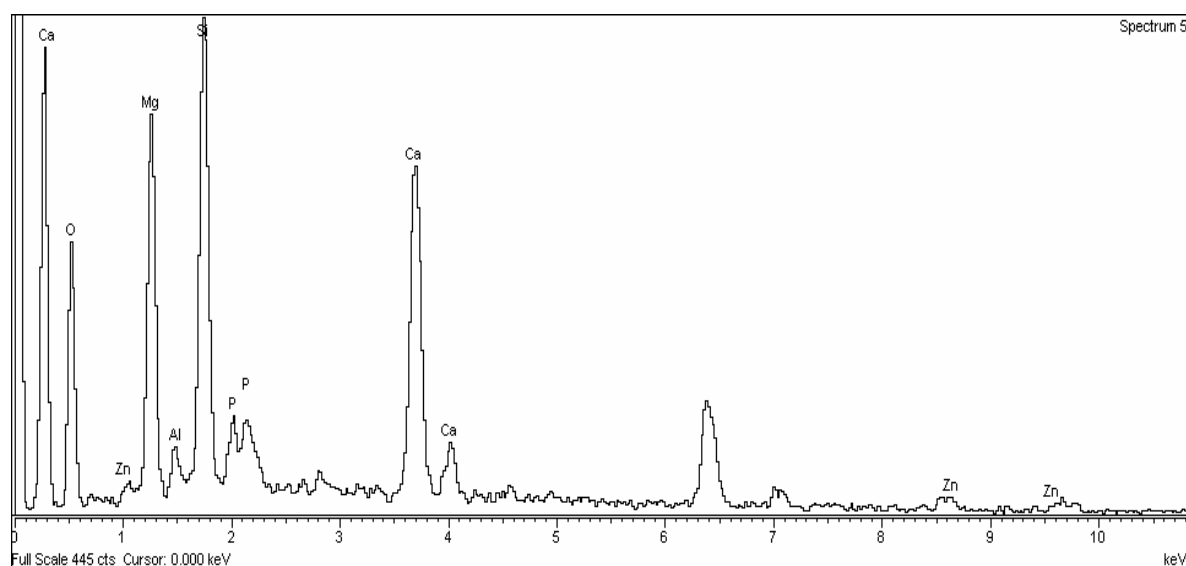


**Figure 4-9** Electron micrographs on interface of intumescent coating and primer coating before fire test. Points 1-4 refer to the EDX analysis.

Figure 4-11 shows the graph of EDX result of primer coating, at the interface of primer coating and intumescent coating. The primer coating at point analysis no 1 shows that the coating consist of high phosphate and zinc. Some additives such as Ca, Ti and Fe were found. These elements were added as a mixture and as fluxing agent. The interface of primer coating and intumescent coating shows high silicon and phosphate elements.



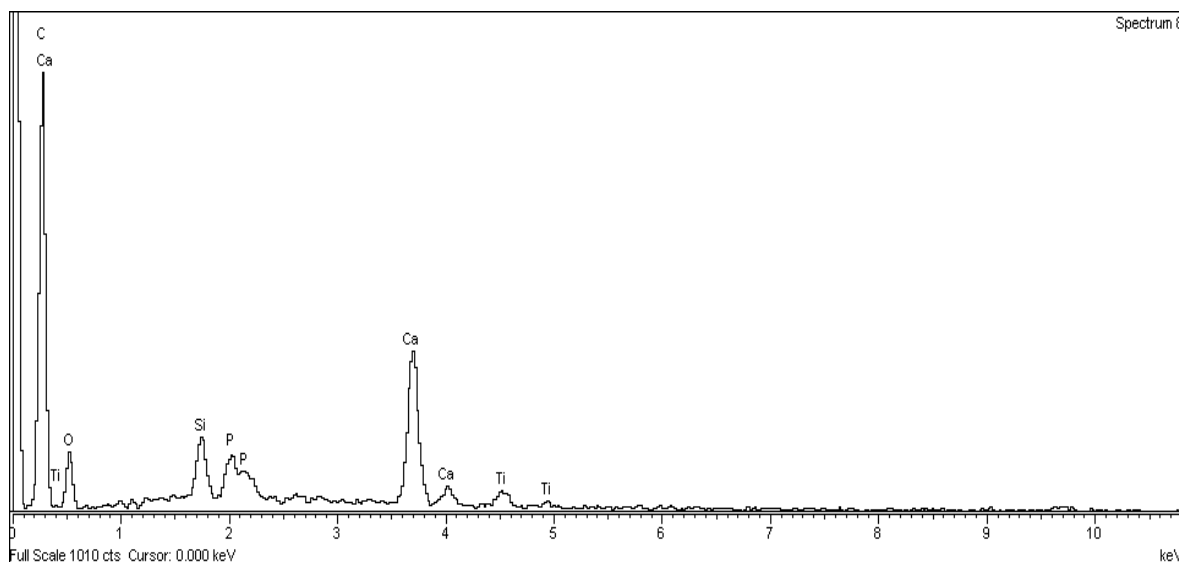
1)



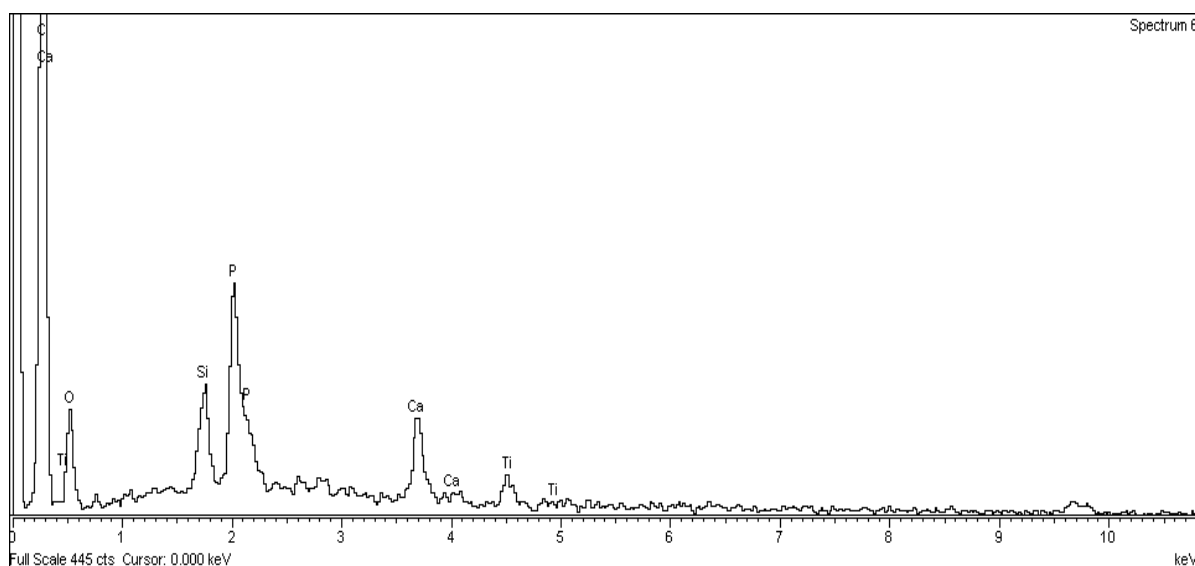
2)

**Figure 4-10** Energy Dispersive X-Ray analysis, 1) primer coating and 2) at the interface between primer coating and intumescent coating before fire test.

Figure 4-11 shows the intumescent coating EDX analyses at point no 3 and 4. Both points consist of high phosphate, titanium, calcium, silicon and other additives. The function of phosphate content in intumescent coating is as char forming agent. A char forming agent will promote the formation of a char when the intumescent is exposed to fire, typically by acting as a fire retardant which controls the rate and mechanism of thermal decomposition of the cured epoxy.



3)



4)

**Figure 4-11** Energy Dispersive X-Ray analysis of intumescent coating before fire test at point no 3 and 4.

The high amount of silicon is believed as the adhesion promoter and wetting agent. Silicon could reduce the surface tension therefore; the coating would wet uniformly the substrate. In addition, the electronegative and ionization energies of silicon and other metalloids are between metals and nonmetals. Thus, the metalloids have characteristics of both classes. The reactivity of the metalloids depends on the element with which they are reacting [107]. This properties make silicon become an essential element must be added especially in coating. The high melting point of silicon (1410°C) may give an advantage as thermal barrier. The EDX result resume for each point before fire test is provided at Table 4-1.

Figure 4-12 shows electron micrographs analysis of the interface between intumescent coating and primer coating after fire test.

**Table 4-1** Energy Dispersive X-Ray results for sample before fire test.

No	Element (wt. %)									
	C	O	Mg	Si	Al	P	Ca	Fe	Ti	Zn
<b>Primer Coating</b>										
1.	60.90	22.41	3.80	2.53		1.17	1.18	6.59		1.42
<b>Intumescent Coating</b>										
2.	40.32	29.82	10.24	12.84	0.59	1.72	2.65			1.83
3.	63.36	27.20		1.67		0.96	5.47		0.84	
4.	70.68	23.50		1.23		2.55	1.35		0.96	

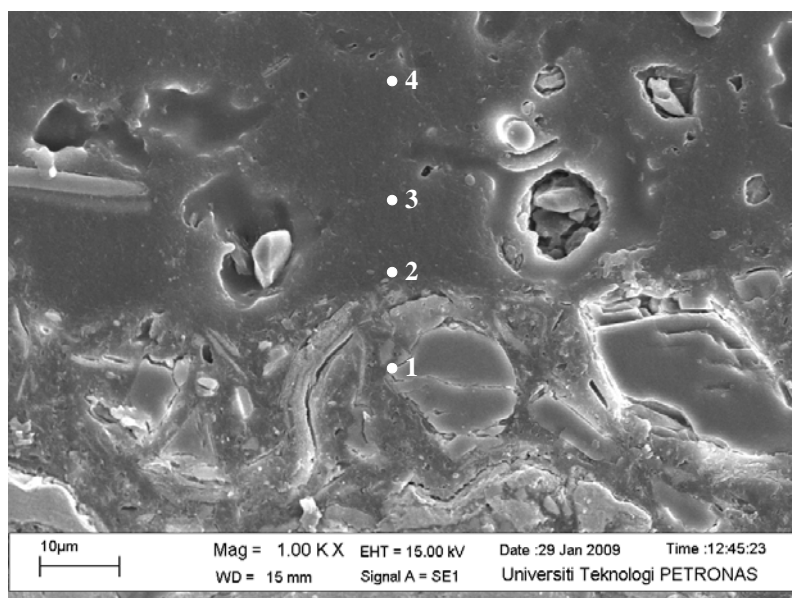
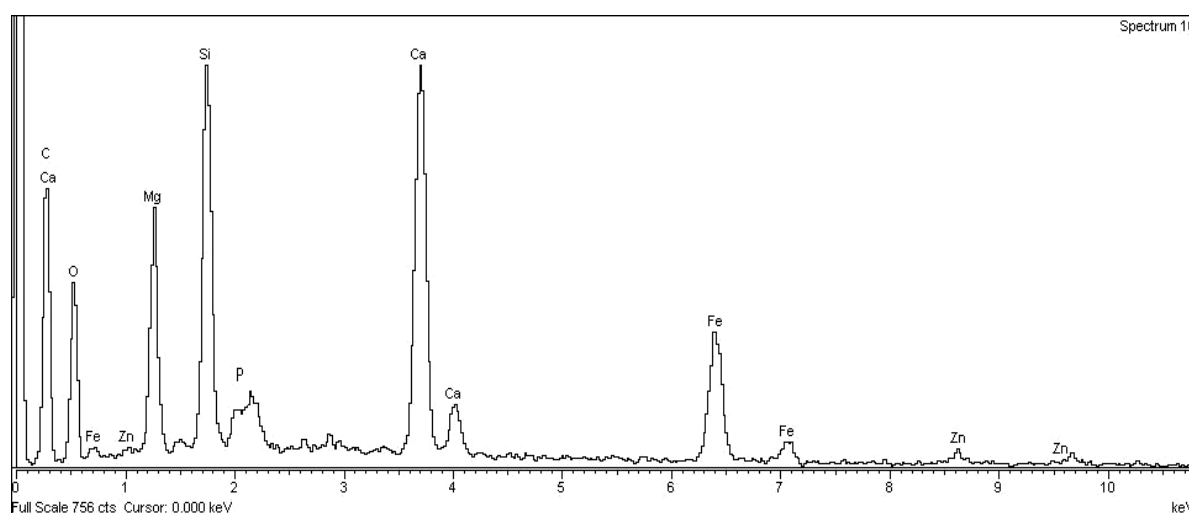


**Figure 4-12** Electron micrographs on interface of intumescent coating and primer coating after fire test. Points 1-4 refer to EDX analysis.

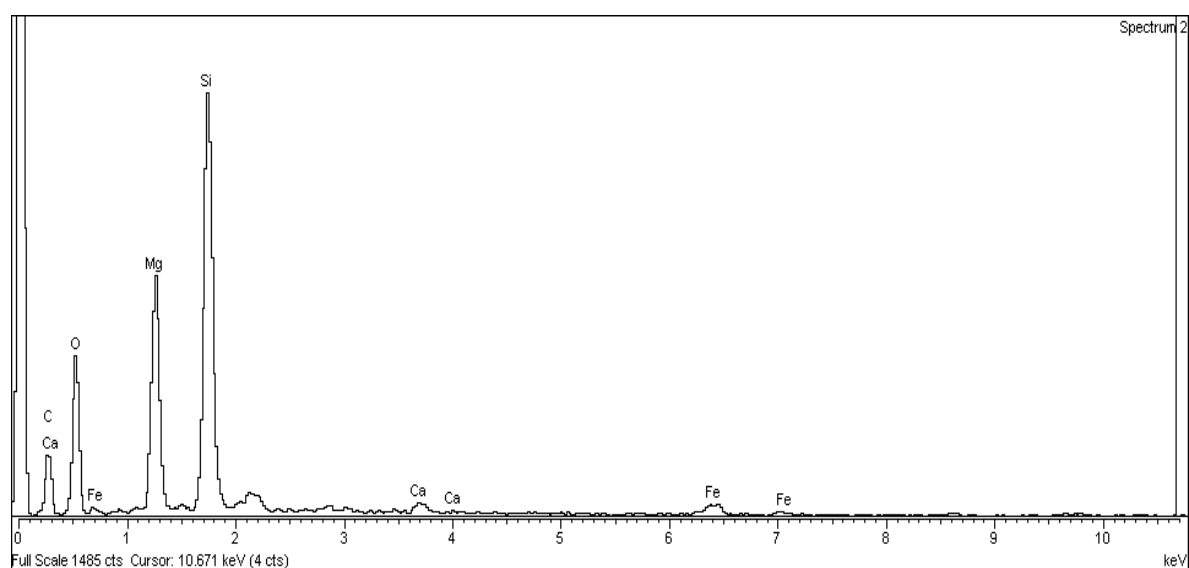
Figure 4-13 shows the EDX analysis result on the interface of intumescent coating and primer coating after fire test. The EDX analysis at the interface between intumescent coating and primer coating (point analysis no 2) indicates the silicon content might form covalent bonding with carbon and iron. This is because silicon is metalloid element which can bond with metal and non metal. The covalent bonding of silicon and iron has great adhesion strength due to a mixture of metallic and multiple covalent bonds that are responsible for the very strong adhesion at the interface. According to the literature, the interface region has been used to refer to the region which is formed because of the bonding



and reaction between strengthening particulate in the intumescent coating and primer coating. The morphological, chemical reaction and thermo-mechanical properties of the interface are distinct from the intumescent coating and primer coating. Combination of dissimilar material in a composite created inevitably interface region since residual stress was generated during fabrication and in service due to the difference in thermo-mechanical characteristic [105]. The graphs show the quantity of silicon remain high after fire test on the interface while the oxide slightly decreased compare with the result before fire test. This is because during fire test, some of the elements reacted with others to form char layers while silicon remain stable due to the high melting point.



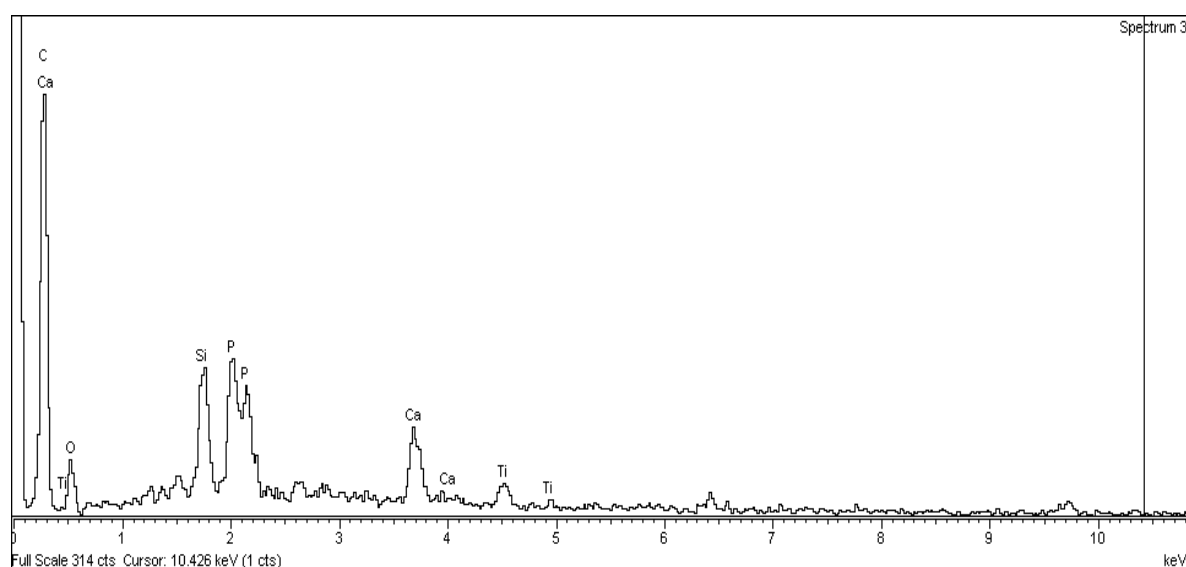
1)



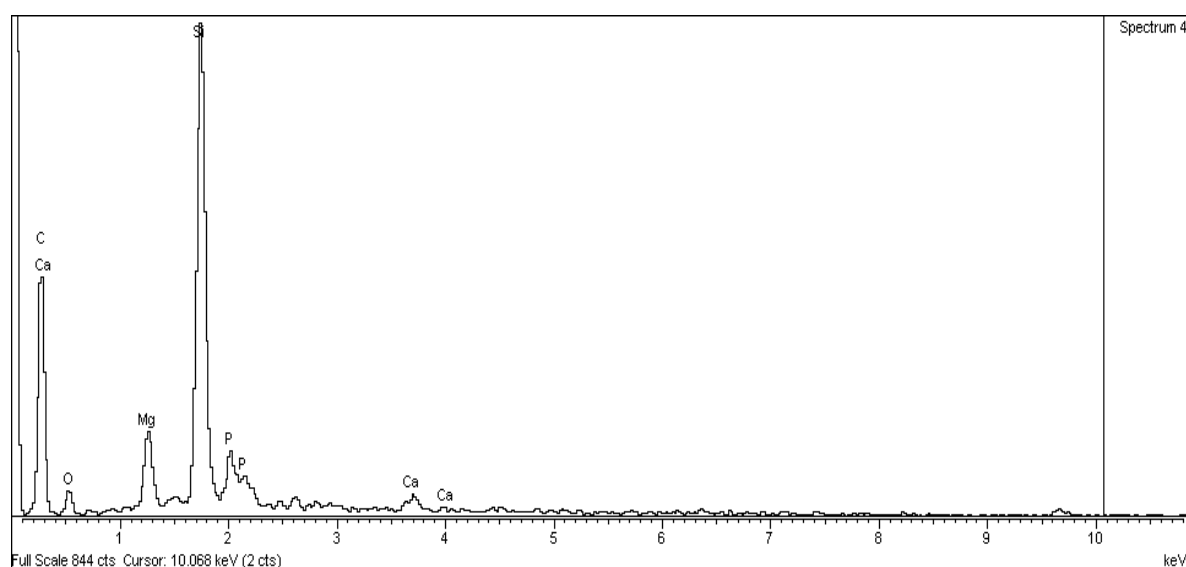
2)

**Figure 4-13** Energy Dispersive X-Ray analysis, 1) primer coating and 2) interface of intumescent coating and primer coating after fire test.

The EDX result at Figure 4-14 shows that the intumescent coating contains high silicon and phosphate after fire test. Point analysis no 3 and 4 indicate that intumescent coating contains some fluxing agent, such as aluminum, iron and magnesium. According to literatures [108,109], beside in order to enhance the adhesion bonding, fluxing agents also are added to intumescent coating as char formation char. During char formation, these fluxing agents react with phosphorus and silicon component forming phosphorosilicate glass which expands and foams due to gases released by thermal decomposition of the intumescent coating. Fluxing agent includes such as metal oxide of titanium, molybdenum, calcium, iron, aluminium, zinc and tin [110].



3)



4)

**Figure 4-14** Energy Dispersive X-Ray analysis of intumescent coating after fire test.

$\text{Fe}_2\text{O}_3$  can stabilize the carbon backbone and increase the char residue by promoting an early cross linking reaction of thermoset carbon chain, which indicates that it might be used as modifiers to improve the thermal stability of intumescent coating system. The higher composition of  $\text{TiO}_2$  and  $\text{Fe}_2\text{O}_3$  among other fluxing agents in this intumescent coating system is to enhance the formation of char layer at an elevated temperature.  $\text{TiO}_2$  also acts as wetting agents and anti foaming agents [110].

The continuation of EDX result after fire test is presented at Table 4-2. The high amount of silicon at point analysis no 2 (14.95 wt.%) shows that the adhesion bonding of intumescent coating and primer coating was due to the presence of silicon. The phosphate element indicates that phosphate is the main element for char formation during fire test. The reaction as follows [10]:

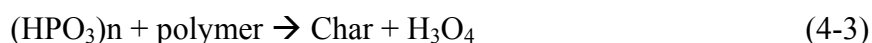


**Table 4-2** Energy Dispersive X-Ray result for sample after fire test.

No	Element Weight (wt.%)								
	C	O	Mg	Si	P	Ca	Ti	Fe	Zn
<b>Primer Coating</b>									
1.	43.18	29.50	5.19	6.29	1.19	7.61		6.13	0.90
<b>Intumescent Coating</b>									
2.	32.9	41.16	10.30	14.95		0.45		1.05	
3.	67.67	23.48		3.00	2.51	2.19	1.16		
4.	73.32	10.10	2.55	12.25	1.26	0.52			

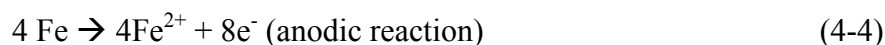
The carbon content was increased for point analysis no 3 to 4. This is probably because the charring layer of intumescent coating was formed up to nearly the interface after 120 minutes of fire test. This indicates the intumescent reaction was continuously forming a char layer by synergist reaction of each substance as the time went by. The degradation of primer coating after 120 minutes of fire test indicates that heat was reached primer coating therefore the possibility to transfer to steel substrate is higher. The heat may affect the adhesion bonding although the adhesion bonding after fire test shows unchanged the structure. The Electrochemistry Impedance Spectroscopy (EIS) test will investigate further about the adhesion bonding to corrosion resistance on next section.

## 4.2 Chemical Properties Measurement

### 4.2.1 Salt Spray

#### 4.2.1.1 Bare Steel Substrate

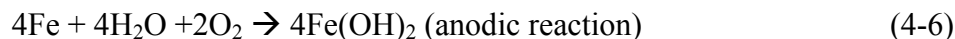
Carbon steel is such technologically important substrates where there were many studies carried out on the adhesion to it of organic system, predominantly in the form of coating. The limitation of carbon steel is the production of copious amount of corrosion product in an aqueous environment. The surface was ground and cleaned with ethanol before conducting the test which is shown in Figure 4-15a. Figure 4-15b shows that oxide fully covered the surface of steel substrate after salt spray test with 2% NaCl concentration for two weeks. A simplified view of what happens when a piece of iron corrodes is summarized below [111]:



Water and oxygen are also needed for corrosion:



After overall corrosion of the iron is thus a combination of (4-4) and (4-5):



The iron hydroxide reacts further with air to form hydrated ferric oxide – rust:

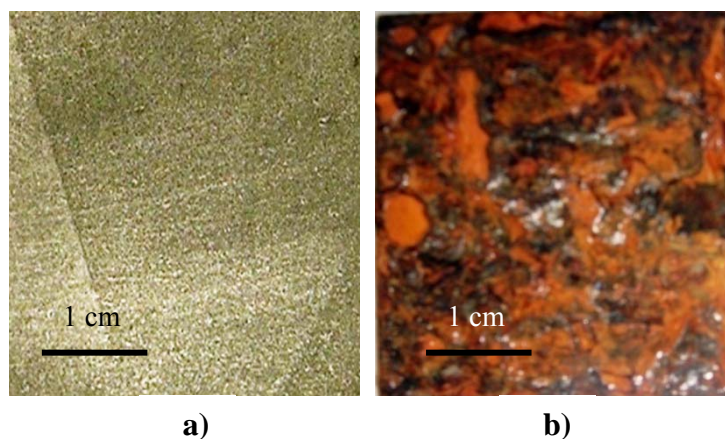
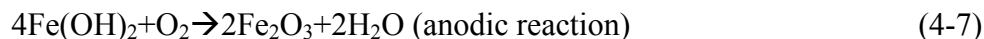


**Figure 4-15** Steel substrate was sprayed with 2% NaCl, a) before salt spray test, b) after salt spray.

The copious corrosion product on steel substrate shows that low carbon steel has poor corrosion resistance. The actual mechanism in the corrosion of iron and steel is extremely complex and embraces the fields of chemistry and electrochemistry. Iron will corrode only in the presence of both water and oxygen.

#### 4.2.1.2 Primer Coating Coated Steel Substrate

Figure 4-16 shows the macrographs of steel substrate coated with zinc phosphate as primer coating. Figure 4-16a shows the zinc phosphate primer coating that was applied to the steel substrate surface as corrosion resistant coating and also as an adhesion promoter. The side along the sample is uncoated. According to Figure 4-16b, the corrosion product was formed starting from the uncoated side. It indicates that the steel still can be corroded unless the primer coating uniformly covered the surface and no defect on the coating.

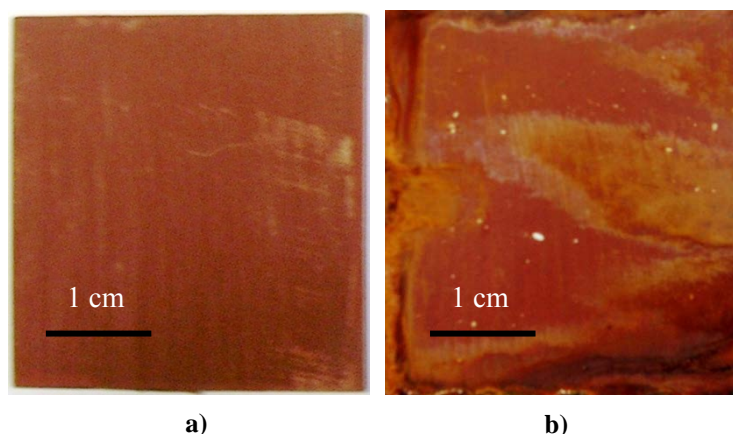


**Figure 4-16** Steel substrate coated with zinc phosphate primer coating, a) before salt spray test, b) after salt spray.

#### 4.2.2 Steel Substrate Coated with Intumescent Coating

Figure 4-17 shows the samples of intumescent coated steel before and after salt spray. The intumescent coating was applied on the surface of primer coating and steel substrate. The epoxy based intumescent coating is known to have excellent corrosion properties since epoxy has hard and durable structure.

Figure 4-17a shows the surface of intumescent coating was uniform and no defect on the surface. The sodium chloride was sprayed to the sample and the result is shown in Figure

4-17b. The figure shows that there is no corrosion product was produced on the surface after the exposure to salt spray. This is because the electron can not easily transfer to the coating structure due to the crosslink structure of epoxy.

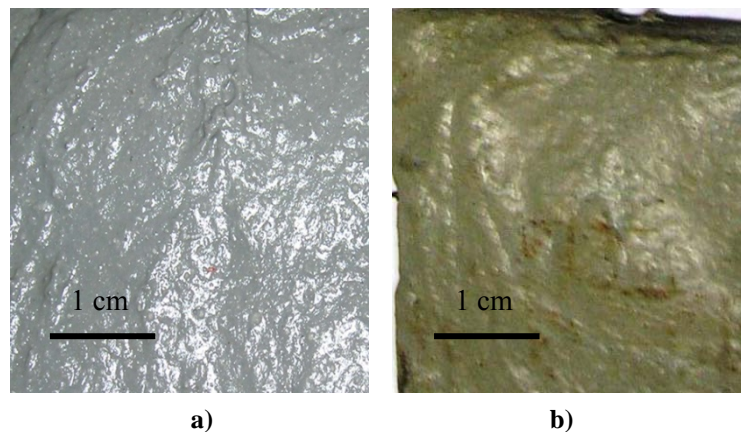


**Figure 4-17** Steel substrate coated with intumescent coating, a) before salt spray b) after salt spray.

### 4.2.3 Electrochemistry Impedance Spectroscopy (EIS)

The effect of the duration of fire test to adhesion bonding between steel substrate and intumescent coated steel was revealed by EIS test. Measurements were performed in the EIS mode in the 0.5 Hz to 100 kHz frequency range. The Nyquist graphs are shown Figure 4-18 and Figure 4-19. The summary of Polarization Resistance and Rest Potential are given in Table 4-3.

#### 4.2.3.1 After fire test

Figure 4-18 shows Nyquist graph of intumescent coated steel before and after fire test. According to the theory, coating impedance higher than  $10^7 \Omega \cdot \text{cm}^2$  indicates the coating has excellent corrosion resistance while coating impedance between  $5 \times 10^5$  to  $10^6 \Omega \cdot \text{cm}^2$  indicates the area of steel to be corroded is increased to 0.3% to 1 % [112]. The coating impedance before fire test is  $43.7 \times 10^7 \Omega \cdot \text{cm}^2$ . After fire test, the impedance was reduced to  $32.3 \times 10^7 \Omega \cdot \text{cm}^2$ ,  $20.4 \times 10^7 \Omega \cdot \text{cm}^2$ ,  $17.1 \times 10^7 \Omega \cdot \text{cm}^2$ ,  $15.2 \times 10^7 \Omega \cdot \text{cm}^2$  for 30, 45, 90 and 120 minutes of fire test duration. However, the coating was still able to maintain the corrosion resistance up to two hours exposure to fire test. The degradation most probably

happen because a thicker char was formed by increasing the time, hence the cross linking structure of epoxy was broken, thus water easily penetrated to the steel substrate.

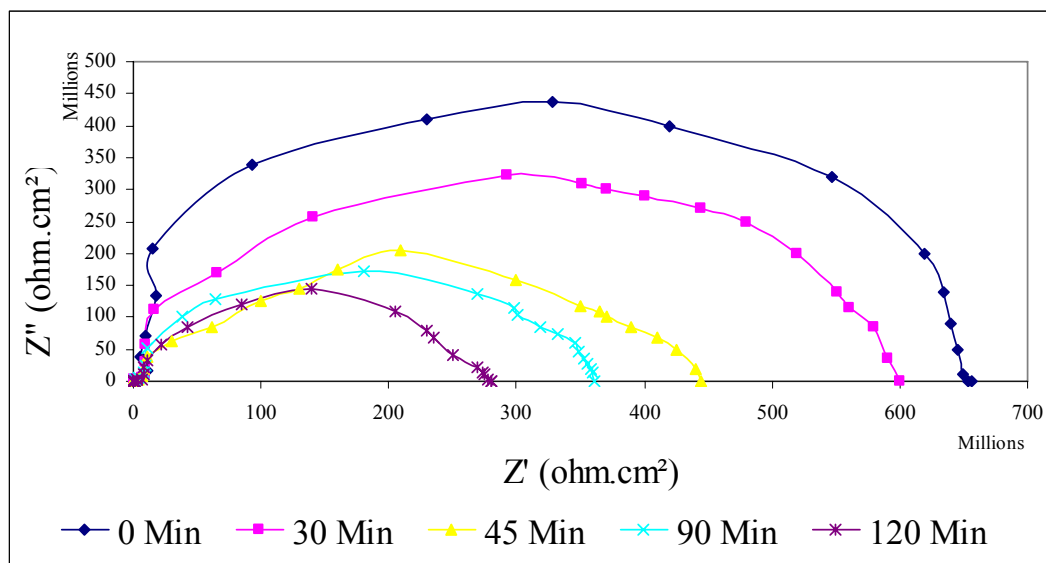


**Figure 4-18** Nyquist plot of intumescent coated steel sample before and after exposure for 30 to 120 minutes of fire test.

#### 4.2.3.2 After three months immersion in sodium chloride

The Nyquist plot in Figure 4-19 shows that the coating impedance is dramatically decreased to  $1.43 \times 10^7 \Omega \cdot \text{cm}^2$ ,  $1.03 \times 10^7 \Omega \cdot \text{cm}^2$ ,  $9.55 \times 10^6 \Omega \cdot \text{cm}^2$ ,  $8.94 \times 10^7 \Omega \cdot \text{cm}^2$ ,  $4.52 \times 10^6 \Omega \cdot \text{cm}^2$  after three months immersion in sodium chloride for sample before fire and after fire test for 30, 45, 90 and 120 minutes. Obviously, the chemical properties of intumescent coating, primer coating and steel substrate gradually degraded and lost the corrosion resistance after applying the heat on the coating surface. The EIS results in Figure 4-19 reveal that the higher quantity of water uptake in intumescent coating and primer coating will reduce the impedance of the coating and result in reduction quality of the coating. The significant reduction of impedance after immersion is believed that the corrosion occurred on the steel during immersion.

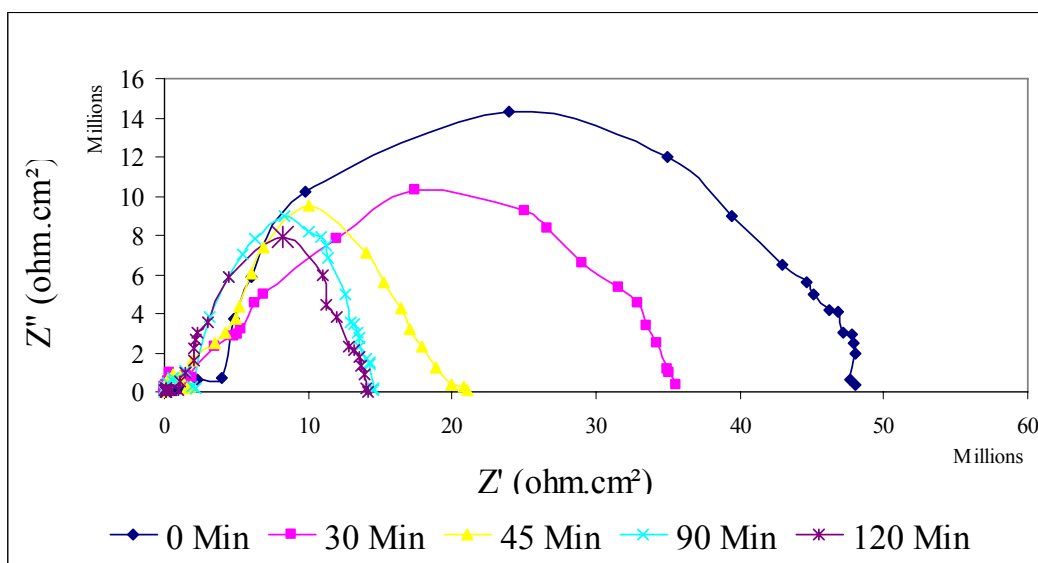


**Figure 4-19** Nyquist plot of intumescent coating resistance of before and after fired samples for three months immersion in 2% NaCl.

Table 4-3 shows the polarization resistance (corrosion rate) and rest potential of the samples. The reduction of polarization resistance and rest potential indicates the resistance of steel substrate to be corroded is increased. The primer coating was getting weaker to protect steel from corrosion by increasing the fire test duration and also immersion in electrolyte solution.

**Table 4-3** Coating degradation observation through  $R_p$  and Rest Potential.

Duration	$R_p (\Omega.cm^2)$		Rest Potential (mV)	
	After Fire Test		After Immersion	
0	4.37E+08	1.43E+07	574.27	-225.28
30	3.23E+08	1.03E+07	328.42	-217.06
45	2.04E+08	9.55E+06	220.03	-305.01
90	1.71E+08	8.94E+06	168.97	-352.62
120	1.45E+08	7.92E+06	66.232	-465.22

The decreasing of coating resistance also shows that the electrolyte solution was contacted with the steel and corrosion is initiated. The SEM micrograph on interface of primer coating and steel shows a narrow gap was created and also the degradation of primer steel occurred along the time. This gap could be a corrosion site since corrosion will only happen by the presence of oxygen and water.



#### 4.2.4 Electron Micrographs of EIS Sample

Figure 4-20 shows the electron micrographs of two hours exposure with fire test before and after three months immersion sample in sodium chloride. Figure 4-20a shows the surface degradation of intumescent coating and primer coating after fire test might be the reason of the decreasing of the coating performance. The arrows indicate the coating structure has failed even before immersion in electrolyte solution.

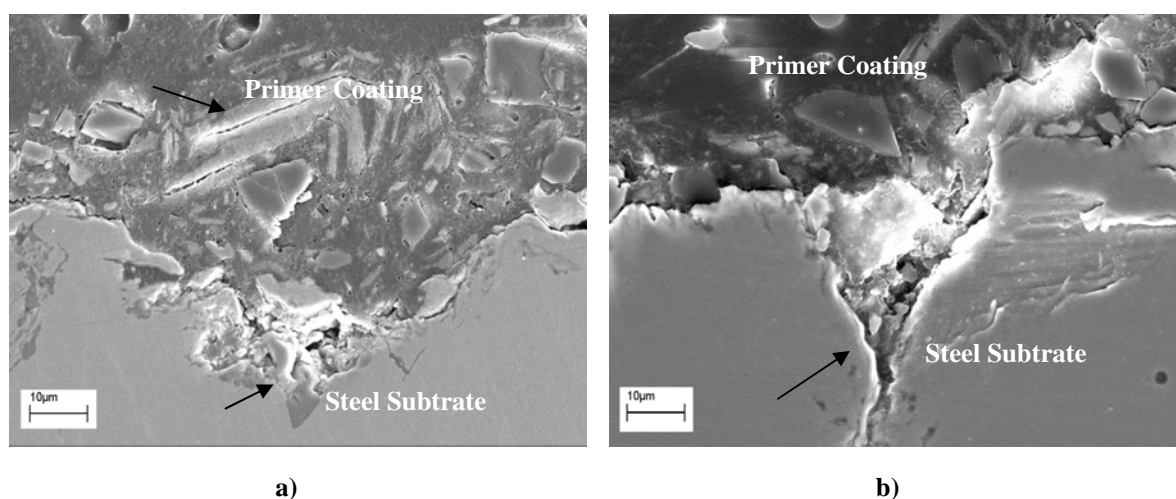


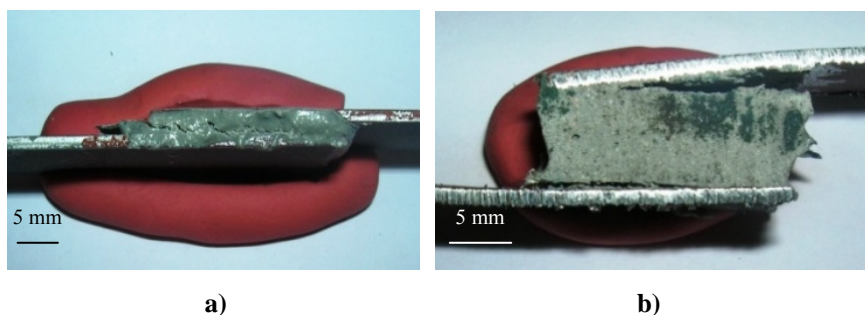
**Figure 4-20** Electron micrographs of intumescent coated sample, a) before immersion and b) after 3 months immersion in 2% NaCl.

The evidence of crack of the coating and the corrosion occurred after three months immersion in sodium chloride is shown Figure 4-20b. The dramatic decrease of impedance is due to the primer coating failed to protect the steel by letting the steel surface to be corroded. This figure also shows that the jagged surface could be a high risk location for pitting corrosion. The three months immersion in sodium chloride prove that water uptake could break down the adhesion bonding between intumescent coating, primer coating and steel substrate. The resistance of the coating changes during exposure due to the penetration of electrolyte into the micro pores of the coating.

#### 4.3 Lap Shear Test

In this study, the adhesion strength of steel substrate to epoxy coating was studied. Figure 4-21 shows the fracture mode with different thickness. The mode of fracture depends with

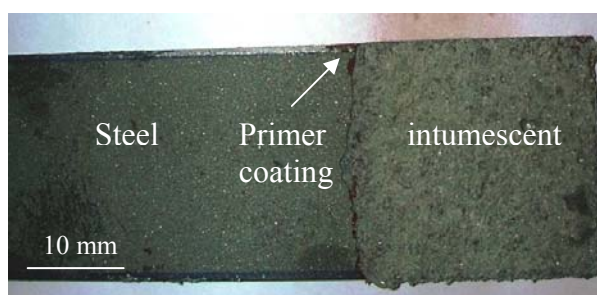
the thickness of the intumescent coating. The sample with thicker coating will fracture on the interface with steel substrate while the thinner coatings fracture mode is in the middle.



**Figure 4-21** Lap shear test sample, a) 1 mm thickness and b) 10 mm thickness.

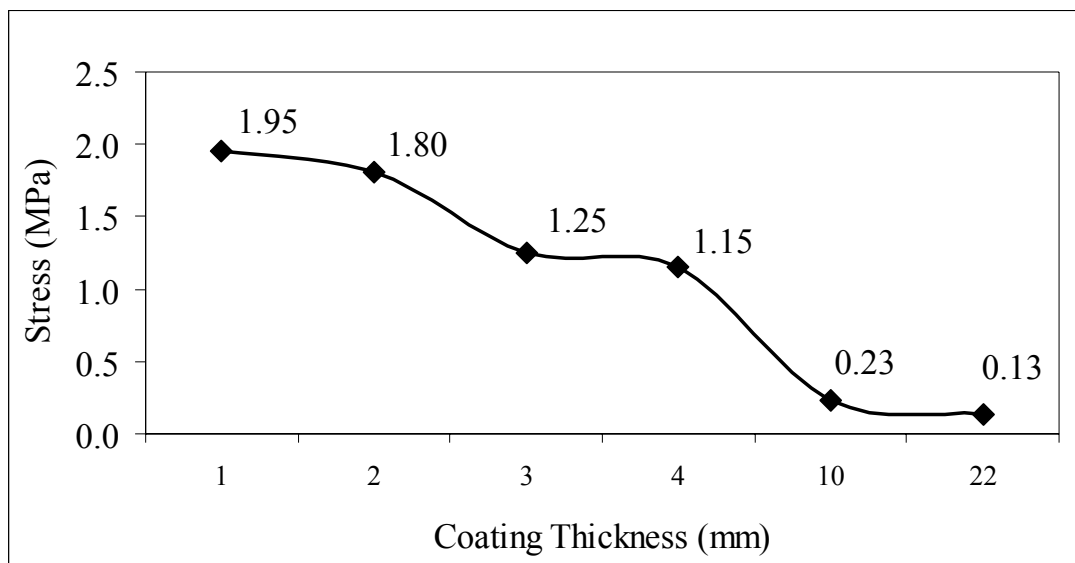
Traditionally, stress redistribution is achieved by optimizing the interfacial strength so that partial debonding occurs [113]. The stress is transferred by shear at the interface due to the differences in the modules of the fibers and resin. Thus, by increasing the thickness of the coating, the stress distribution on the surface also increases.

Figure 4-22 shows that primer coating is used as adhesion promoter to intumescent coating. The thin layer of intumescent coating on primer coating surface also showed that this coating successfully spread to the primer coating surface and the mechanism is cohesive bonding.



**Figure 4-22** Primer coating respond as adhesion promoter to intumescent coating.

Figure 4-23 shows that the lap shear strength is inversely proportional to the intumescent thickness on steel substrate. The shear strength continuously decreased and achieved 0.13 MPa for 22mm intumescent coating thickness. The maximum lap shear strength for this coating is 1.95 MPa.



**Figure 4-23** Lap shear test result of six different intumescent coating thickness.

The lower lap shear strength compared to standard (10 MPa) is due to the lower adhesion bonding strength between the epoxy and fillers in intumescent coating. In addition, the porous morphology on the intumescent coating also reduced the strength. The cohesive fracture indicates that the bonding between the coatings to steel substrate is strong.

Figure 4-24 shows the tortuous surface on steel substrate and adhesion interaction between the coatings to steel substrate. Lap Shear determines the shear strength of adhesives for bonding materials. The strength of adhesive bonds depends on the conditions under which the adhesion bonding process is carried out. Therefore, variations in this process lead to variations in the accuracy of the results acquired from strength tests of these adhesion bonds. The important properties of a protective coating are wear resistance (high hardness), high-temperature robustness (high melting point), corrosion resistance (formation of a protective oxide scale), and strong adhesion to the substrate being protected [114].

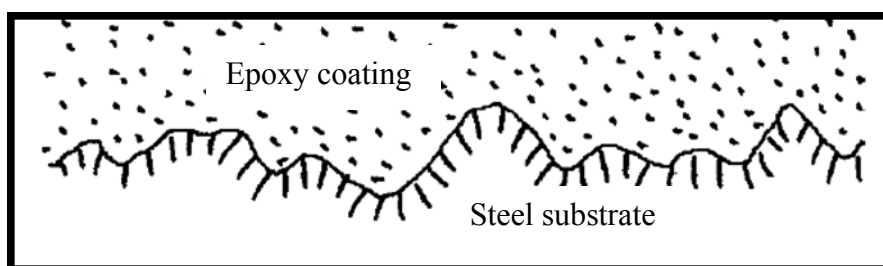


**Figure 4-24** The adhesion interaction pulls the epoxy coating into complete contact with the rough steel substrate surface.

The bonding between the coating and the steel substrate metal is mainly determined by mechanical interaction and welding of coating particles with the metal [114]. The tortuous surface on steel substrate is to enhance the adhesion strength with polymer. Figure 4-24 shows that the polymer completely fills the pores on the surface of the substrate. At these pores, the exit of the polymer is partially blocked by part of the steel substrate. This place in the interface will exhibit a so-called lock and key effect. A key, when turned into the tumblers of a lock, can not be removed from the lock because of the physical impediment provided by the tumblers. In the same way, a solid adhesive in a pore can not move pass the locking of the pore without physically deforming. Plastic deformation acts as an energy absorbing mechanism and the strength of the adhesive bond appears to increase [115].

The intrinsic work of adhesion or cohesion is independent of the shear rate, peel angel, thickness of the adhesive and thickness of the steel substrate [116].

## **4.4 Coating Characterization**

### **4.4.1 Thermal Properties Measurement**

The thermal properties of intumescent coating, primer coating and carbon fiber are important to identify their act at high temperature and its effect to adhesion bonding to steel substrate. The formation of the charring layer and the heat insulation of intumescent coating to steel depends with these properties.

#### **4.4.1.1 Thermo Gravimetric Analysis (TGA)**

The TGA curves of intumescent coating, primer coating and carbon fiber are presented in Figure 4-25.

From the TG curves in Figure 4-25, it can be seen that the weight loss of the intumescent coating is 5 wt. % at the beginning of the experiment within 20°C to 160°C. The small decomposition at this stage is due to softening epoxy and solvent vaporization. The softening stage is crucial since intumesce reaction will occur after this stage. The softening temperature is determined by cross link reaction of epoxy with hardener. This reaction will affect the mechanical, physical and chemical properties of the intumescent coating. Therefore, the physical significance of the glass transition for epoxies is at temperatures

above the  $T_g$ . The values of the physical properties such as tensile strength, lap shear and adhesive bonding strength are substantially reduced. The coefficient of thermal expansion on the other hand greatly increases.

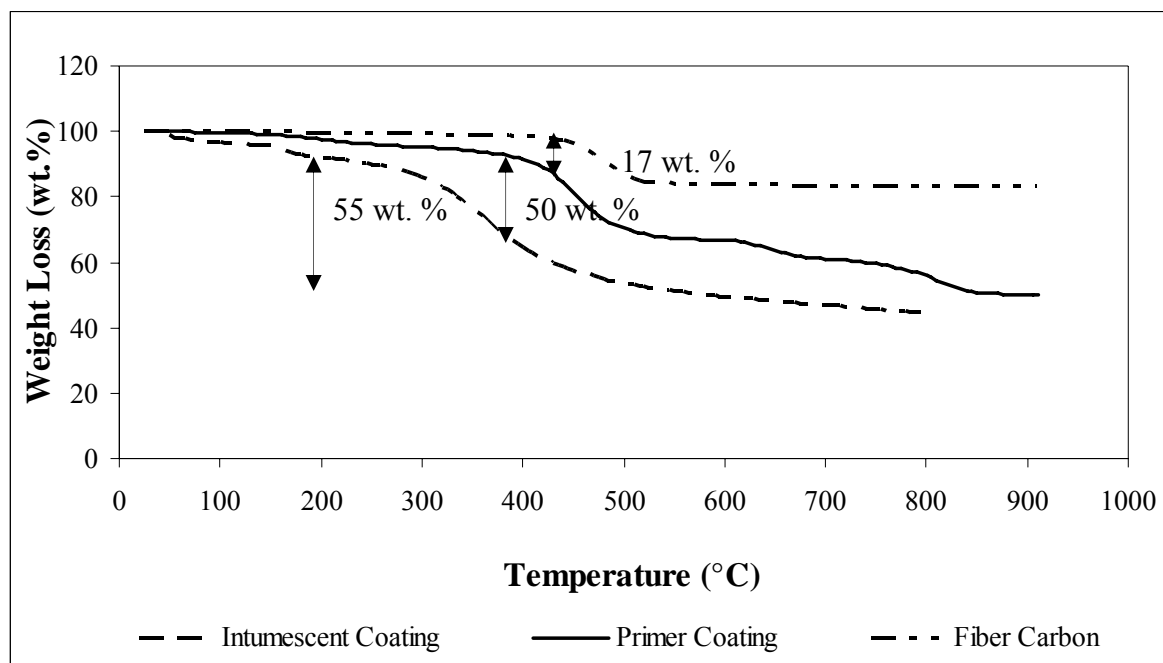


**Figure 4-25** The thermal degradation of intumescent coating, primer coating and carbon fiber by using Thermo Gravimetric Analyzer with range temperature 30°C to 850°C.

The next stage of the experiment (150–500 °C) is the key weight loss region that the coating begins to decompose largely, the weight loss is 55 wt. %. The biggest loss is due to the reaction of some ingredients to form char layer within the temperature. At this stage, the intumescent coating started to release the acid source (Triphenyl Phosphate (TPP)), carbon source (char forming) and blowing agent to form charring layer. The acid source decomposed upon thermal exposure to release an expansion gas such as nitrogen, carbon dioxide or water vapor, thereby expanding the char to increase the char thickness. This gas should be released before the charring layer is formed otherwise the coating could not insulate the steel.

In the later stages of experiment, the weight loss of the intumescent coating is 18 wt. % at temperature 470°C to 800°C. At this stage, it can be seen that charring layer formation consumed approximately 60 wt. % of the intumescent coating and gradually decreased by increasing the temperature.

According to Jun Wei *et. al* [117], the coating melts at the second stage, when the acid source decomposes to release  $\text{NH}_3$ ,  $\text{H}_2\text{O}$  and phosphoric acid thermally degrades, dehydrates to release poly-metaphosphoric acid and pyrophosphoric acid, moreover reacts with pentaerythritol and other organic materials which contains hydroxyl groups, dehydrates, to form the charring framework. At the same time, the ammonia gas begins to release  $\text{NH}_3$  gas when the temperature is over  $296^\circ\text{C}$ . The  $\text{NH}_3$  gas blows the charring layer to form a compact, firm and multiple charring layers.

Jun Wei *et. al* and Duquesne *et. al* [118,119] also stated that the opposite high temperature and high pressure air current occasion on the surface resulted the carbon in the charring layer is oxygenized to  $\text{CO}_2$  by  $\text{O}_2$ . The weight loss under  $370^\circ\text{C}$  is due to the decomposing blowing agent and  $\text{NH}_3$  releasing. The ammonia released by blowing agent can dilute the oxygenous concentration, blow the charring layer and form intumescent, microporosite foam charring layer. Some charring layer is off by gas because of the weak strength of adhesion on the structure. Some inorganic framework maintains at last, the most important components of the rudimental are the matter of inorganic phosphate. The released inorganic elements release will also be confirmed by FTIR in next section.

The glass transition of primer coating can be seen in Figure 4-25. This figure shows that the primer coating started to decompose at around  $120^\circ\text{C}$ - $250^\circ\text{C}$ . The small decomposition is due to epoxy softening and it is confirmed that the binder is epoxy, same with the intumescent coating. This will enhance the adhesion bonding between two coatings since they have same chemical structure. The primer coating decomposed larger from  $250^\circ\text{C}$  to  $600^\circ\text{C}$  and continuously degradable by increasing the temperature. The higher glass transition than intumescent coating is probably because of the additives inside the primer coating which is able to resist at high temperature. The benefit for adhesion is at high temperature when the intumescent coating already melted, the primer coating is still able to absorb the heat for some time thus protect the steel from overheating and weakening.

From Figure 4-25 also, the decomposed temperature of carbon fiber is the highest among intumescent coating and primer coating. The carbon fiber started to decompose from  $400^\circ\text{C}$  and above. This evidence shows that carbon fiber acts as reinforcement and strengthens the char and up until it reached the glass transition temperature. The carbon fiber weight loss is

also very small, 17 wt. %. The use of carbon fiber aside from strengthening the char proved cost effective since the residue is relatively small.

#### 4.4.1.2 Differential Scanning Calorimetry (DSC)

The DSC curve of intumescent coating is presented in Figure 4-26. The endothermic reactions can not occur spontaneously but it needs energy. Some works must be done in order to get the endothermic reactions to occur. The endothermic reaction occurs when the energy is absorbed. Thus, a temperature drop is measured during the reaction.

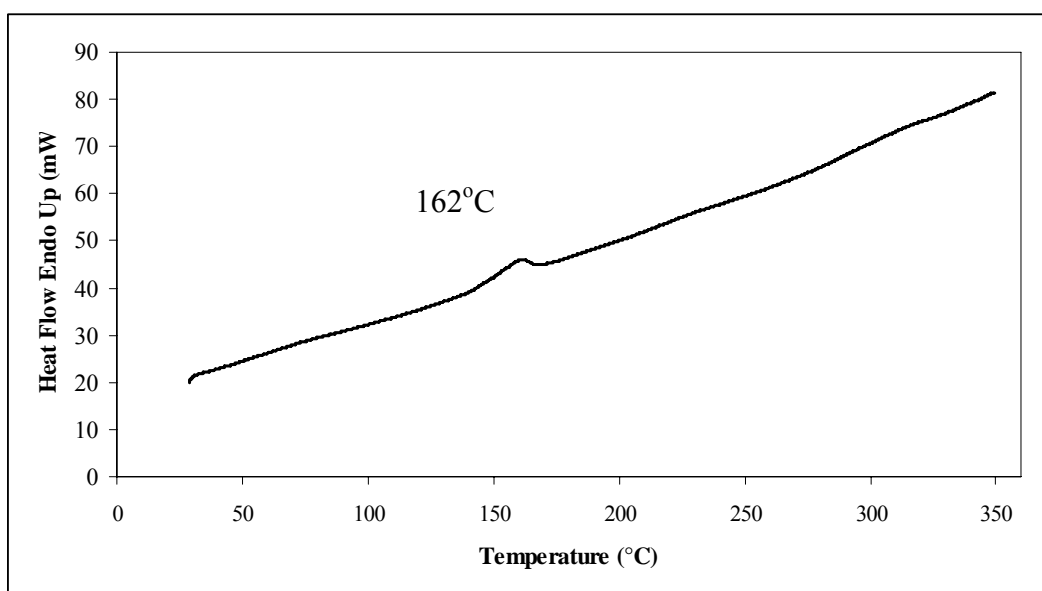


**Figure 4-26** Thermal decomposition of Intumescent coating analysis using DSC.

The elimination of water and heat absorption of epoxy binder of intumescent coating required energy 47 mW and it occurred at 162°C. The softening of epoxy binder started from this temperature. The softening of epoxy is important as a starting point to perform a synergist reaction between the acid source, carbon source and gas source. Only a small quantity of reaction mixtures transforms into solid foam charring layer at high temperature.

However, the majority loses is in the forming of gas products. The lack of matrix materials influences the flame-retardant performance and the matrix plays a very important role in the course of charring foam. The release of pyrolysis gases such as H<sub>2</sub>O, NH<sub>3</sub>, CO<sub>2</sub> and hydrocarbons are essential factor to create effective production of large amount of multi

cellular charring layer during combustion [117]. With the increase of temperature, water of crystallization and epoxy resin in the intumescent coating are gradually decomposed and eliminated, and the dehydration can form steam and absorb heat from the system. The heat can not be freely released from the system due to high viscosity of the epoxy resin matrix, so the melted matrix triggered by the heat can form a porous structure.

The DSC curves are continuously rising and no major peaks were observed below 350°C for primer coating and carbon fiber. The several minor endothermic peaks that are observed are irregular. It indicates that the melting point of primer coating and carbon fiber are above 350°C. The TGA result of primer coating and carbon fiber confirm that both materials have higher temperature to degrade than intumescent coating.

#### **4.4.1.3 Fourier Transform Infrared Spectroscopy (FTIR)**

The organic and inorganic substance in intumescent coating can be observed using FTIR spectra. Figure 4-27 shows the char residue contains fewer group of organic substances and inorganic simple substances than that of the intumescent coating.

From Figure 4-27 and Table 4-4, the FTIR spectra present the elongation of some bands. The strong characteristic vibration peak at  $3217.04\text{ cm}^{-1}$  (O-H) implies the fire retardant has good system since the epoxy functional group remain stable after fire test.

The bands near  $2200\text{ cm}^{-1}$  can be assigned to the characteristic vibration peaks of nitriles groups (C=N). This is an evidence of the presence of nitrogen gas as the blowing agent of the intumescent coating. The stretching vibration peaks of the P-O-C band from  $1000\text{ cm}^{-1}$  to  $1200\text{ cm}^{-1}$  and P=O band from  $900\text{ cm}^{-1}$  to  $1050\text{ cm}^{-1}$  can keep shifting to lower frequency sharply, respectively.

According to Jun Wei *et.al* [117], phosphides make some organic materials drastic degrade irregularly, reduce flammable gas, and make the high-carbon compounds dehydrate, char to form compact charring-layer structure by bridging reactions in the heat degradation in the solid phase.



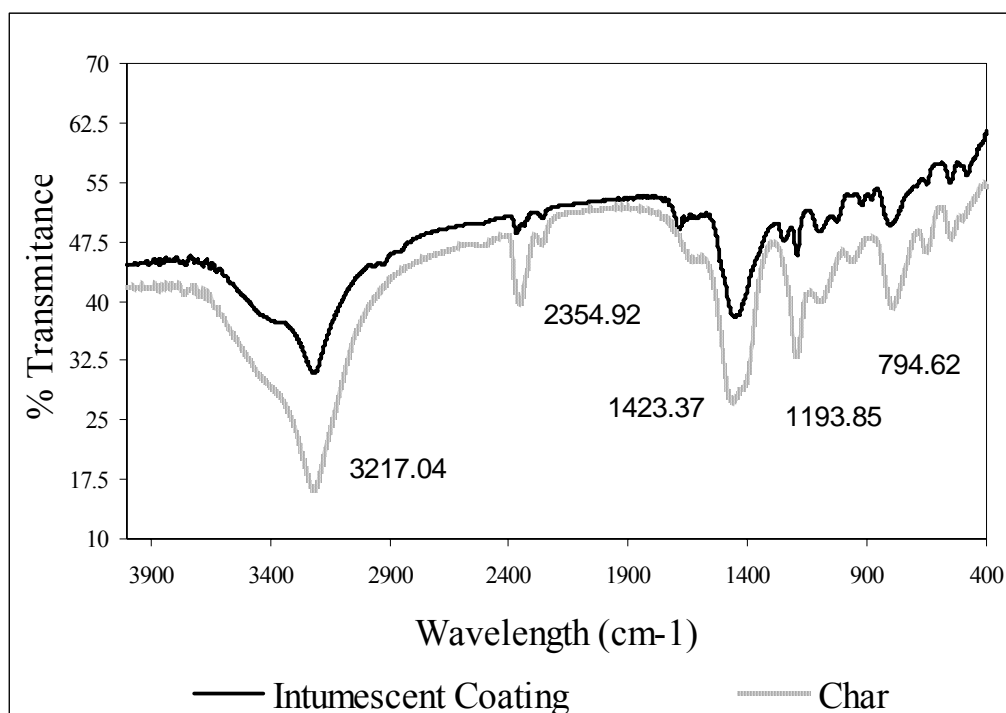


**Figure 4-27** FTIR results of functional group structural changes of intumescent coating and char.

**Table 4-4** The FTIR analysis of intumescent coating and char [120].

Functional Class	Wave Length (cm <sup>-1</sup> )	Assignment	Intumescent Coating wave length (cm <sup>-1</sup> )	Char wavelength (cm <sup>-1</sup> )
Alcohol and Phenols	3200-3550	O-H (H-Bonded)	3218.97	3217.04
Nitriles	2240-2260	C=N (sharp)	2374.21	2354.92
Ketone	1690	R-CO-R	1689.53	-
Alkena	1350-1470	CH <sub>2</sub> & CH <sub>3</sub>	1446.51	1423.37
Sulfate (str)	1350-1450	S=O	1245.93	-
Phospsonate	1230-1260	P=O		
Phosphoramide	1200-1275	P=O		
Silicon function	1250±10	Si-CH <sub>3</sub>		
Amine Oxide aromatic	1250±50	N-H	1193.85	1193.85
Phosphate	1100-1200	P=O		
Esters	900-1050	P-OR	923.84	-
Alkena	880-995	C-H & =CH <sub>2</sub>	883.34	-
Alkena	780-850	C-H & =CH <sub>2</sub>	794.62	794.62

## 4.4.2 Coating Composition Measurement

### 4.4.2.1 X-Ray Fluorescent (XRF) : Intumescent Coating

The flame retardant CHARTEK 7 delivers the maximum degree of thermal efficiency with a thinner, lighter coating with faster, easier, less expensive installation. The composition of the intumescent coating as obtain from XRF is presented in Table 4-5. According to the results, the compounds present in decreasing order is P<sub>2</sub>O<sub>5</sub> (43 wt. %), CaO (25.10 wt. %), SiO<sub>2</sub> (13.40 wt. %), TiO<sub>2</sub> (10.20% wt. %), Fe<sub>2</sub>O<sub>3</sub> (2.99 wt. %), Al<sub>2</sub>O<sub>3</sub> (1.06 wt. %) and some small percentages of additives.

The high amount of phosphorus oxides confirmed that the intumescent coating is a phosphorus based flame retardant. All of the phosphate in intumescent coating can be viewed as an acid source which releases phosphoric acid or polyphosphoric acid during char formation. Referring to the material data sheet from supplier (Chapter 3), the intumescent coating consist of epoxy resin as binder, triphenyl phosphate and tetraethylenepentamine. The existence of carbon chain and gases form (CO<sub>2</sub>, N<sub>2</sub>, etc) can not be detected by XRF equipment since carbon (12.011 amu), nitrogen (14.007 amu) and hydrogen (1.008 amu) have low atomic weight.

The high concentration of CaO (25.10 wt. %) is believed to absorb moisture from the atmosphere. It was estimated that about 1.3% of the water in the epoxy resin reacted with CaO. The curing acceleration mechanism and the flame retardant mechanism of CaO were as follows [121]:



Water is absorbed in an epoxy compound during its production and storage processes. The water exists near the hydroxyl group of the epoxy resin and inhibits the curing reaction. If CaO is added to the compound, it will absorb water from the epoxy resin during the formation and storage processes as well as during the curing process. Consequently, the curing reaction proceeds are faster than in epoxy compounds without CaO. Also, Ca(OH)<sub>2</sub> formed from the absorbed water is considered to improve flame retardancy by releasing water at a high temperature. The degree of cure of epoxy resin promoted by CaO is considered to enhance the flame-retardation properties [121,122].

**Table 4-5** Intumescent coating composition by using XRF

Compound	wt. %
Al <sub>2</sub> O <sub>3</sub>	1.06%
SiO <sub>2</sub>	13.40%
P <sub>2</sub> O <sub>5</sub>	43.00%
Cl	0.72%
K <sub>2</sub> O	1.22%
CaO	25.10%
TiO <sub>2</sub>	10.20%
Cr <sub>2</sub> O <sub>3</sub>	0.17%
MnO	0.13%
Fe <sub>2</sub> O <sub>3</sub>	2.99%
CuO	0.68%
ZnO	0.14%
others	1.20%
Total	100.00%

Silicon dioxide, SiO<sub>2</sub> is an amorphous mineral fiber that acts as fiber and filler in intumescent coating system and has superior property as impact resistance improver. SiO<sub>2</sub> used to strengthen the char formed from intumescent coating at an elevated temperature, forms phosphorosilicates glass within the char which improves the insulation of the coated steel substrate and the durability of the char, SiO<sub>2</sub> could also be used to improve anti aging [123 ,124]. It is believed that mix of SiO<sub>2</sub> and Al<sub>2</sub>O<sub>3</sub> will partly forms a compound oxide and partly forms particles having a multi-phase structure composed of a silicon dioxide phase and an aluminum oxide phase (mullite). Mullite (3Al<sub>2</sub>O<sub>3</sub>-SiO<sub>2</sub>) is an excellent structural material due to its high temperature stability, strength and creep resistance. It has a low dielectric constant and high electrical insulation capabilities [125,126]. These properties will increase the corrosion resistance of the coating due to hard and high thermal stability.

The chlorine element was found in this intumescent coating with 0.72 wt. %. It might come from acid source that was used in this study. Organochlorine flame retardant emits hydrogen halide (HX) gas during their decomposition. This interferes with the flame reactions by promoting scavenging of the high energy H<sup>+</sup> and OH<sup>-</sup> chain branching radicals [127]:



These reactions compete with those occurring in the absence of halogen. The halogen atom produced is a low energy radical which is incapable of propagating the oxidation process. This reduces the rate of heat transfer back to polymer, which decrease the burning rate and leads to extinction of the flame [127]. The disadvantage of halogen containing system is releasing more smoke than the untreated polymer formulations, a part of which is corrosive hydrogen halide. The function of chlorine element in this intumescent coating is to release  $\text{Cl}^\cdot$  radical to the environment and produces water, thus it will slow down the thermal degradation of intumescent coating. The corrosion resistance of the coating will be affected by hydrogen chlorine amount during charring formation.

The current researches indicate no significant connection between chronic exposure to low concentrations of chlorine and adverse health effects. Finnish [128] showed an increase in chronic coughs and a tendency for hyper-secretion of mucous among workers. However, these workers showed normal pulmonary function in tests or chest X- Rays. One of the most comprehensive studies, involving 300 chlorine plant workers chronically exposed to 0.006 to 1.42 ppm, showed no statistically significant increase in abnormal chest X-Rays, electrocardiograms, or pulmonary function tests. Other studies of workers in the chlor-alkali industry have resulted in similar observations. No significant effects have been indicated for chlorine levels normally found in work places where chlorine is handled. Those levels typically are well below one ppm. As for the air breathed by the general population, chlorine levels in ambient air are so low that they are either can not measured or no toxicological importance [128].

#### **4.4.2.2 X-Ray Fluorescent (XRF): Primer Coating**

The use of primer coating is to promote adhesion and fill in voids in the substrate that can help to improve quality. The major composition for this primer coating is  $\text{ZnO}$  (22 wt. %),  $\text{Fe}_2\text{O}_3$  (25.90 wt. %),  $\text{SiO}_2$  (20.10 wt. %),  $\text{CaO}$  (19.2 wt. %) and  $\text{P}_2\text{O}_5$  (2.98 wt.%). The composition test result is presented in Table 4-6.

According to material data sheet from the supplier, this primer coating is zinc phosphate epoxy based. Zinc phosphate which is used with epoxy resin binders has provided excellent adhesion to steel substrate. All extenders and pigments, in addition to the active anticorrosive ones, have a role to play in the formulations improvement. For example,

lamellar extenders are used to provide a barrier to the moisture permeation, so increasing corrosion protection [129]. Silicon oxide has been used in coatings for many years, in various applications. Silicon oxide in water-based coatings improves corrosion protection and reduces cracking and pigment sedimentation. Other pigments employed were titanium dioxide, barium sulphate and talc [130].

**Table 4-6** Zinc phosphate primer coating composition by using XRF.

Compound	wt. %
MgO	8.35%
Al <sub>2</sub> O <sub>3</sub>	0.28%
SiO <sub>2</sub>	20.10%
P <sub>2</sub> O <sub>5</sub>	2.98%
Cl	0.04%
K <sub>2</sub> O	0.04%
CaO	19.20%
Cr <sub>2</sub> O <sub>3</sub>	0.05%
MnO	0.04%
Fe <sub>2</sub> O <sub>3</sub>	25.90%
CuO	0.07%
ZnO	22%
Br	0.29%
SrO	0.06%
Others	1%
Total	100.00%

The pigment material in the formulation which colors the formulation and provides it with corrosion inhibiting properties is zinc chromate and strontium chromate. The extender material which is filler that provides some tooth for adhesion for subsequent topcoat application is a natural fibrous magnesium silicate or a porous low micron particle size silica-magnesium oxide material. The results in the above table shows this coating contains of high percentage of SiO<sub>2</sub> (20.10 wt. %), CaO (19.2 wt. %), MgO (8.35 wt. %), Fe<sub>2</sub>O<sub>3</sub> (25.90 wt. %) and small amount of P<sub>2</sub>O<sub>5</sub> (2.98 wt. %). The presence of these elements are also believed as fire retardant additives in primer coating. Thus, for certain duration, primer coating still can stand up from softening of steel substrate.

#### 4.4.3 Mechanical Properties

The hardness of intumescent coating is presented in Table 4-7. The hardness of the intumescent coating was measured by using Shore D hardness test which refer to ASTM D

2240-03. The hardness result test was taken for 7 different locations on the intumescent coating surface. The result shows that the coating hardness was 71 Shore D while compared to the data from supplier; the hardness was 70 Shore D [92].

**Table 4-7** Hardness of intumescent coating (Shore D).

Indentation	Shore D
1	70
2	70
3	75
4	70
5	75
6	70
7	70
Average	71
stdev	2.44

Therefore, the coating that was used in this study had same property with the standard. The high hardness of polymer does not guarantee that the others properties are also good, since in polymer, there are some additives added which will influence the properties.

## 4.5 Steel Substrate Characterization

### 4.5.1 Hardness of Steel Substrate

The data of hardness test is presented at Table 4-8 and the graph is showed at Figure 4-28. Referring optical and SEM micrograph, the strength of steel substrate remained stable by showing no new phase and re-crystallization formation during fire test up to two hours. The hardness test result for sample before fire test, after 30 min, 45 min, 90 min and 120 min of fire test show that the hardness are gradually increased.

The critical core temperature of steel substrate depends with carbon concentration in the material. It is known that small heat on the steel surface will have effect to its properties. The optical and electron micrographs confirm that the intumescent coating was able to protect steel from weakening for up to two hours of firing.

**Table 4-8** Hardness of steel substrate before and after fire test.

No	Fire Test Duration				
	0 min	30 min	45 min	90 min	120 min
1	114.8	123.3	132.5	143.3	167.4
2	110	124.2	124.7	140.8	169.1
3	111.9	129.6	131.7	134.9	164.5
4	111.6	125.7	128.7	136.6	165.5
5	113	129.4	124.9	137.5	163.5
Average Hardness (HV)	112.26	126.44	128.5	138.62	166
Standard Deviation	1.78	2.92	3.66	3.38	2.25

The increased hardness on steel substrate has a correlation with the time limit for heat to reach the steel. If the temperature is continuous across the coating, therefore the velocity and thermal conductivity will also do the same. The frontal model was derived to assist understanding of intumescent reaction mechanism [13].

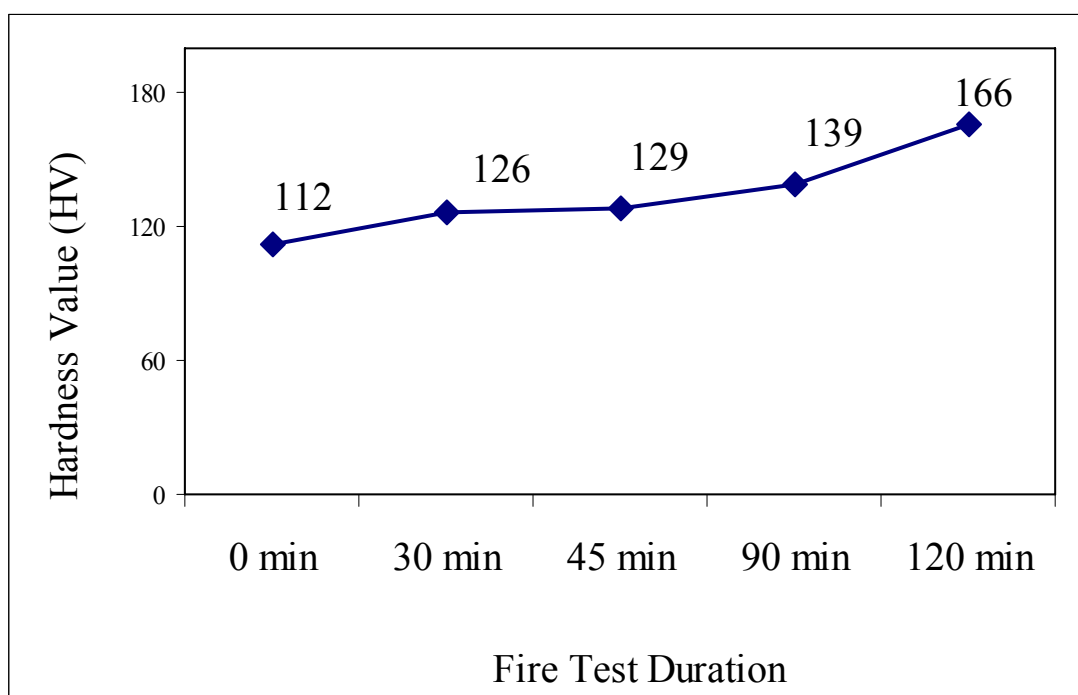


**Figure 4-28** Graph of hardness measurement of steel substrate for 0, 30, 45, 90 and 120 min of fire test.

According to this theory, it is obviously seen that the interface between steel and coating can be destroyed if the heat reach the substrate. The heat transfer to the substrate is limited by the temperature gradient between front and substrate. The surface hardening could happen easily if the heat temperature reaches 450°C which is in the austenite phase.

The increase hardness of steel substrate in this experiment might be achieved due to normalizing heat treatment on the surface substrate. Normalizing is a process whereby iron base alloys are heated to approximately 100°F (56°C) above the upper critical temperature, followed by cooling to room temperature in still air. According to the result, the steel substrate hardness was still within the range of carbon steel hardness, 120 - 164 HV [131]. Therefore the use of coating will protect the steel from weakening and extremely useful to safe money.

## 4.5.2 Chemical Properties Measurement of Steel Substrate

### 4.5.2.1 Energy Dispersive X-Ray (EDX)

Figure 4-29 shows the chemical composition of steel substrate using EDX. According to this figure, the steel that was used in this study contained Fe and C. This graph supports the microstructure of steel substrate that shows ferrite structure. The chemical compositions of other element were analyzed using XRF.

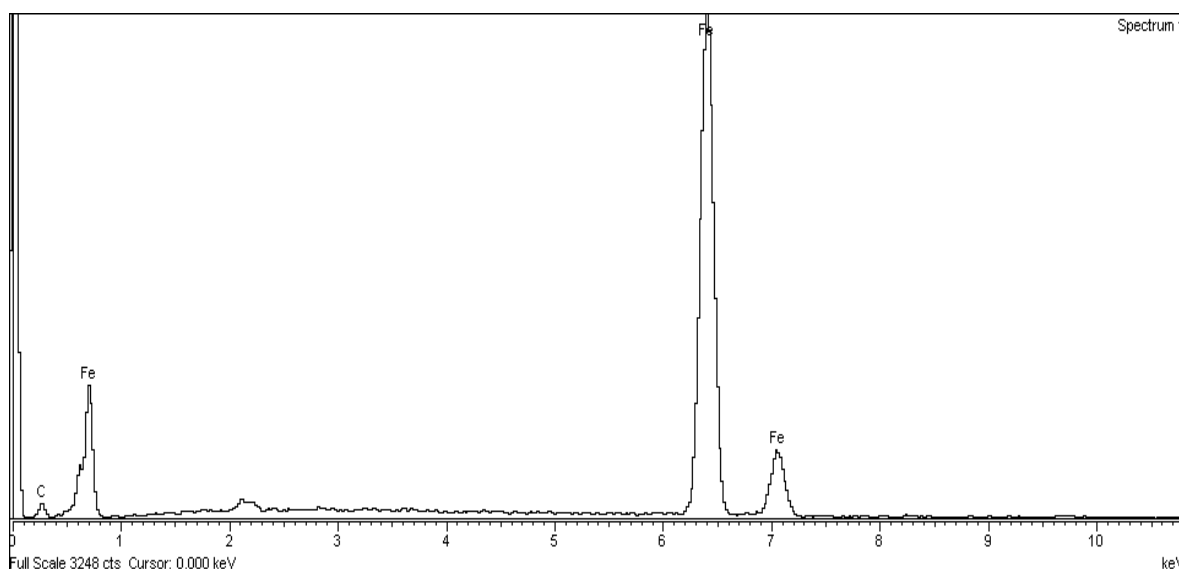


**Figure 4-29** Energy Dispersive X-Ray analysis of steel substrate.



#### 4.5.2.2 X-Ray Diffraction (XRD)

Figure 4-30 shows chemical composition result of steel substrate using XRD. The graph shows the steel substrate consist of iron and carbon. Thus, the steel substrate is carbon steel.

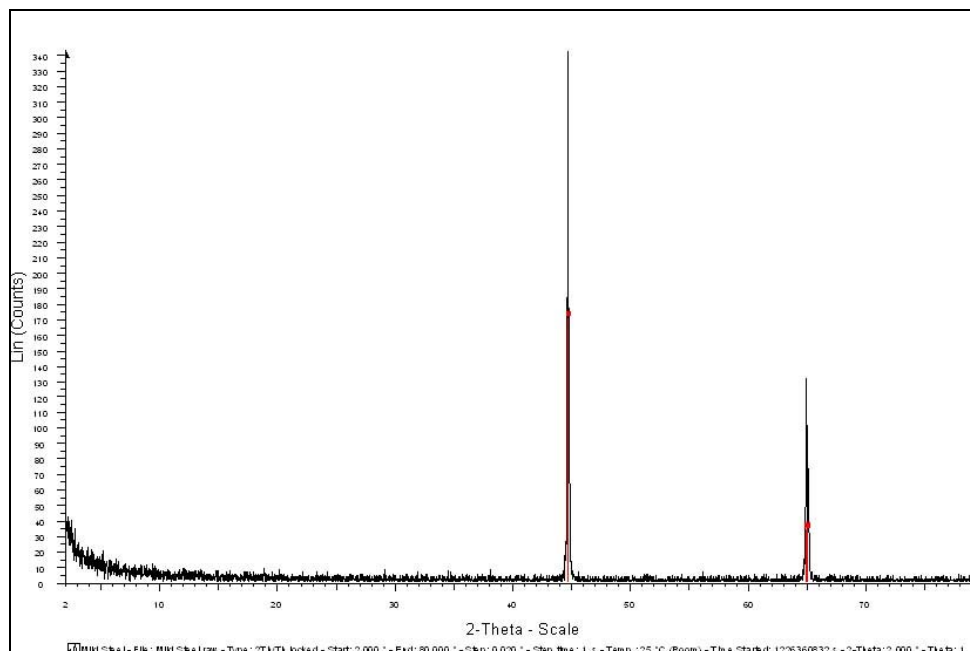


**Figure 4-30** X-Ray Diffraction (XRD) graph of steel substrate.

#### 4.5.2.3 X-Ray Fluorescent (XRF)

Steel is usually defined as alloy of iron and carbon, containing not more than 2% carbon, with or without other alloying elements. With more than 2 wt.% carbon, the material comes into the category of cast iron. The composition of steel was analyzed using XRF and shown in Table 4-9.

**Table 4-9** XRF chemical composition analysis of steel substrate.

Element	wt.%
O	2.01%
Al	0.10%
Si	1.45%
Cr	0.05%
Mn	0.15%
Fe	77.30%
Cu	0.14%

This table shows that the steel composition major elements are iron with small percentage of Si, Mn, and Cu. Residual elements such as chromium, aluminium and copper, which are unavoidably retained from raw materials, may present in small quantities, in addition to impurities such as oxides. In addition, the presence of these elements will improve the properties of the steel. Comparing to the MATWEB material database [131], the substrate that was used for this experiment is low carbon steel.

#### 4.6 Fire Test

The summary of temperature of fire, back steel and environment are given in Table 4-10.

**Table 4-10** Fire test of uncoated steel for 60 minutes duration.

Time (min)	Temperature (°C)		
	Flame	Back of Steel Substrate	Environment
5	887	221	20
10	892	228	21.8
15	912	245	21.5
20	915	278	21.5
25	930	372	22.7
30	940	390	24.3
35	974	408	25
40	940	416	25.3
45	1006	420	25.9
50	1004	424	25
55	1004	424	25.8
60	1005	420	25.3
Average Temperature (°C)	950.75	353.83	23.68
Fire Spread (°C/min)	15.85	5.90	0.39
Temperature Reduction	62.78%		

Five plates were evaluated: uncoated steel, intumescent coated steel for fire test duration 30, 45, 90 and 120 min. The surface of the sample was burnt with LPG gas butane for 30 min,

45 min, 90 min and 120 min for the thickness of 10 mm. The temperature is maintained at above 1000°C to have, at least, almost similar experience with hydrocarbon fire in the real condition.

Table 4-10 shows the result of fire test of uncoated steel. Average temperature has reached 950.75°C with fire spreading on the steel surface at 15.85°C/min. According to Figure 4-31 and Table 4-11, the heat transferred to steel substrate was minimized by 95% while to environment was 98 % when using this intumescent coating. The intumescent coating is able to insulate the steel from weakening for about two hours at above 1000°C flame temperature.

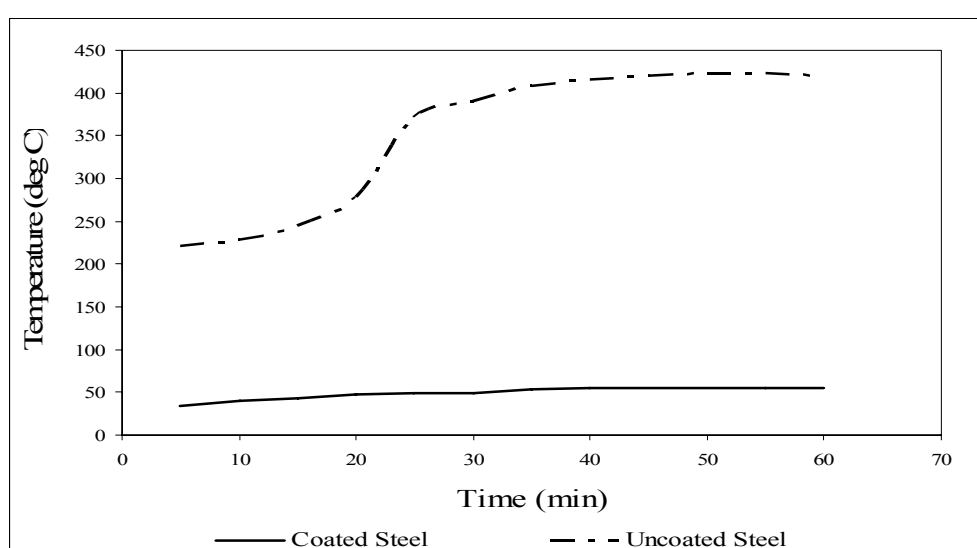


**Figure 4-31** The fire test result of uncoated and intumescent coating coated steel after one hour fire test.

The charring layer formation was successful to inhibit the heat during the test. However, the disadvantage is flame temperature from fire depends on the air flow and the pressure from fire equipment. The smoke extinguisher which was used during the experiment to absorb the smoke also influences the flame temperature. How far the air flow effect the flame temperature can be seen at Figure 4-32. This chart shows that flame temperature decreased gradually during the fire test but still above 1000°C. The maximum temperature was around 1025°C while the lowest was 995°C. In the real life, the hydrocarbon fire temperature will be kept constant at around 1100°C by using fire jet machine [132].

**Table 4-11** The temperature of flame from fire, back of steel substrate and environment during fire test.

Time (min)	Temperature (°C)		
	Flame	Back of Steel Substrate	Environment
5	900	34	20
10	920	40	20
15	925	43	20.2
20	1003	48	20.2
25	1005	49.5	20.2
30	1006	49.2	21.4
35	1015	53.2	20.3
40	1017	54.8	20.1
45	1018	55	36
50	1018	55.2	23.3
55	1019	55.6	23.3
60	1011	55.5	23.3
65	1012	50.7	20
70	1014	54	20.4
75	1015	54.5	20.1
80	1016	53.9	23.6
85	1018	54.7	20.2
90	1016	53.3	21
95	1018	58.9	20
100	1008	69.2	21.2
105	1009	64.7	20
110	1005	61.5	20
115	1005	68.6	20.2
120	1009	67.3	21.8
Average Temperature (°C)	1000	54	22
Fire Spread (°C/min)	8.33	0.45	0.18
Temperature Reduction	94.6%		

Hydrocarbon fire protection has to respond to a very rapid temperature increase and extreme turbulence fuelled by the burning of hydrocarbon products such as oil and gas. This type of fire often found in severe environmental conditions such as the oil, gas and petrochemical processing industries, places very high demands on the fire protection coating system. Thick

film epoxy intumescent coatings were used to protect substrates against high and rapid flame temperature.

The temperature at the back of the steels gradually increased during fire test because the coating has limited time to insulate the steel. The intumescent coating element works as a synergy and forms carbonaceous layer on the surface. Figure 4-33 shows sample before and after fire test.

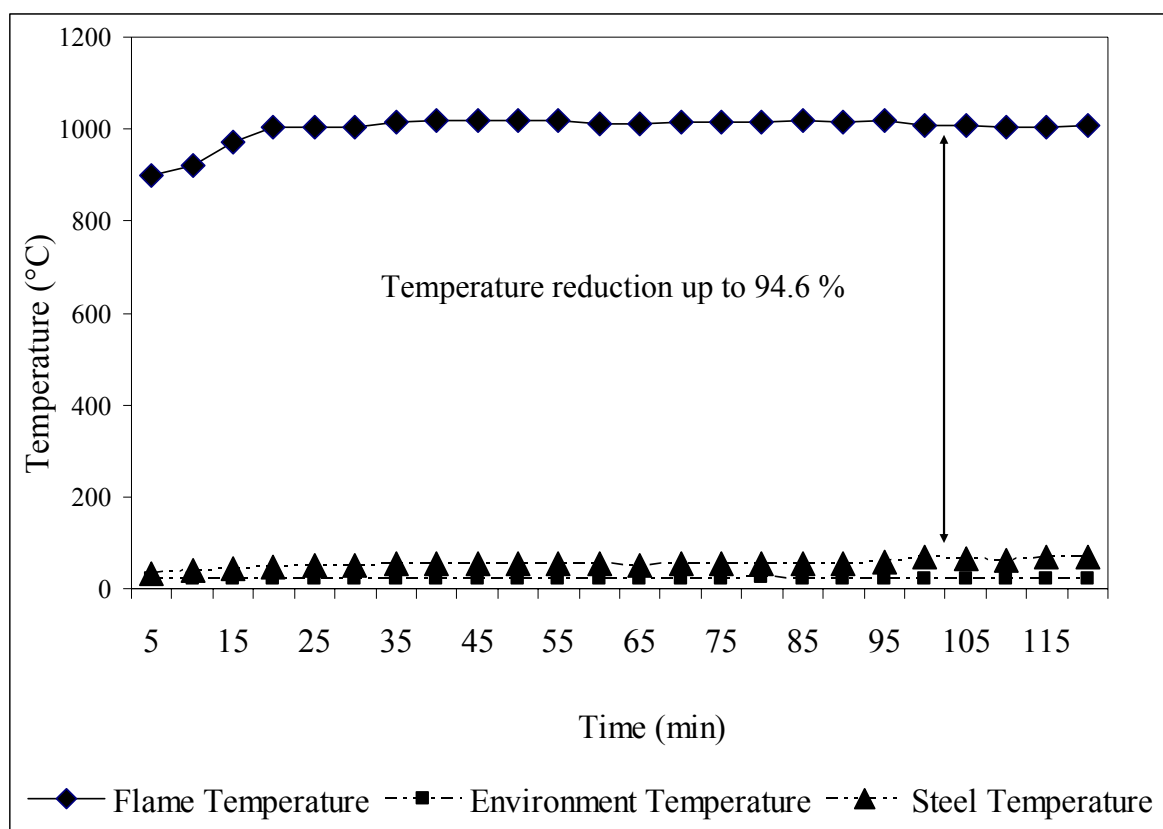


**Figure 4-32** The temperature of flame, back of steel substrate and environment during fire test.

When the temperature of the coating surface reached the critical temperature under the heat of flame, the surface begins to melt and is converted into highly viscous liquid. Simultaneously, reactions are initiated that resulted in the release of inert gases with low thermal conductivity. These gases were trapped inside the viscous fluid (formation of bubbles).

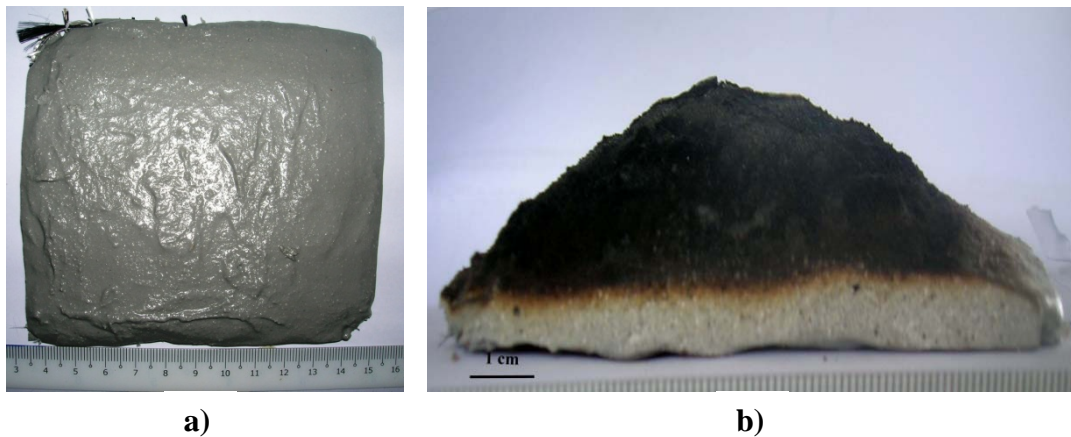


**Figure 4-33** Intumescent coated steel fire test sample, a) before fire test and b) after fire test.

The result is the expansion of foaming, sometimes up to several times its original thickness (2-10mm), to form a protective carbonaceous char (Figure 4-33) that acts as an isolative barrier between the fire and the substrate [13]. The char formed with the char thickness almost reached 4 times the original thickness of the intumescent coating. The thick char has a much lower thermal conductivity than in the intumescent coating before burn out.

The constant environment temperature showed that the coating has an excellent insulation with the formation of multi carbonaceous layer during the two hour fire test and the low hardness strength of intumescent coating can be balanced with the presence of various level additives in the material.

## CHAPTER 5

### CONCLUSION AND RECOMMENDATIONS

#### 5.1 Conclusions

The study on adhesion bonding of intumescent coating to steel substrate was observed. The main conclusions can be derived as follows:

The intumescent coating has a good thermal barrier by showing temperature reduction up to 94.6% for up to two hours of firing. Adhesion bonding on the steel substrate and coatings was broken due to the attainment of the glass temperature ( $T_g$ ) of the heat of the coatings and carbon fiber. Further observation shows that the adhesion bonding broke due to the penetration of water to steel substrate especially after immersion. The mechanical properties show that the steel substrate strength maintained by showing no new phase formation and no re-crystallization, though the hardness is increased. Lap shear strength decreased inversely proportional by increasing the coating thickness and showing cohesive fracture on intumescent coating surface. The surface treatment of the steel is important to promote the adhesion bonding since the tortuous surface increases the surface area. The type of adhesion bonding between the coatings and steel substrate are mechanical interlocking and adsorption bonding. The intumescent coating and primer coating contains non hazardous element, therefore this coating is safe to use. The additives elements such Silicon, Phosphate and Calcium are useful to promote the adhesion bonding of the coatings to steel substrate. In addition, the compatibility of the primer coating and intumescent coating will result in a good adhesion bond by forming diffusion adhesion bonding.

## **5.2 Recommendations**

The investigation of silicon presence and other additives to adhesion bonding strength is recommended for further study.

Though the lap shear strength is poor; the intumescent coating has excellent thermal barrier. Thus, the suitable application for the intumescent coating is on the wall and surface without any load. The improvement on lap shear strength of the intumescent coating will result in great thermal barrier and can be applied in any area, such as rig platform, bridge or building.

The development in chemical composition of intumescent coating is also needed to produce a thin coating thickness with excellent thermal barrier.



## REFERENCES

- [1] W. Zhenyu, H. Enhou, and W. Ke, "An investigation into fire protection and water resistance of intumescent nano-coatings", *Journal of Surface and Coatings Technology*, vol. 201, pp. 1528-1535, 2006.
- [2] "The workplace (health, safety and welfare) regulations 1992", Statutory Instrument, Ed. United Kingdom, 1992.
- [3] J.A. Seiner and T. A. Ward, "Fire protective coatings for structural steel", *Polymer Paint Colour Journal*, vol. 178, pp. 75, 1988.
- [4] G. K. Castle, "Fire Protection of Structural Steel", *Loss Prevention Journal*, vol. 8, pp. 57, 1974.
- [5] S.C. Upadhyaya, Asian Paints (I) Ltd., Paintindia, vol. 50, pp. 45–52, 2000.
- [6] S. Duquesne, S. Magnet, C. Jama, and R. Delobel, "Intumescent paints: fire protective coatings for metallic substrates", *Surface Coating Technology*, vol. 302, pp. 180-181, 2004.
- [7] H. L. Vandersall, "Intumescent coating systems, their development and chemistry," *Fire Flammability*, vol. 2, pp. 97-140, 1971.
- [8] J. A. Rhys, "Intumescent coatings and their uses", *Fire and Material Journal*, vol. 4, pp.154-156, 1980.
- [9] G. Jun-wei, Z. Guang-cheng, D. Shan-lai, Z. Qiu-yu, and J. Kong, "Study on preparation and fire-retardant mechanism analysis of intumescent flame-retardant coatings", *Surface and Coating Technology*, vol. 201, pp. 7835-7841, 2007.
- [10] S. Bourbigot, M. Le Bras, S. Duquesne, and M. Rochery, "Recent advances for intumescent polymers", *Macromolecular Materials and Engineering*, vol. 289, pp. 499, 2004.
- [11] M. Jimenez, S. Duquesne, and S. Bourbigot, "Characterization of the performance of an intumescent fire protective coating", *Surface and Coating Technology*, pp. 981, 2006.
- [12] J. Charles E. Anderson and D. K. Wauters, "A Thermodynamic Heat Transfer Model for Intumescent System", *International Journal of Engineering Science*, vol. 27, pp. 881-889, 1984.
- [13] J. Charles E. Anderson, D. Jeremo, M. William A, and J. Buckmaster, "Intumescent reaction mechanism", *Journal of Fire Sciences*, vol. 3, pp. 161, 1985.
- [14] Websites of fire retardant coating companies, Leighs Paints, 2008.  
url : <http://www.leighspaints.co.uk/>

- [15 ] R. Rose A and P. V. Yaneff, *Coatings of Polymers and Plastics*. New York: Marcel Dekker, Inc, 2003.
- [16] S. Yawei, J. Cao Jia, M. Guozhe, Z. Tao and W. Fuhui, "The role of a zinc phosphate pigment in the corrosion of scratched epoxy-coated steel", *Corrosion Science*, vol. 51, pp. 371-379, 2009.
- [17] M. Zubielewicz and W. Gnot, "Mechanisms of non-toxic anticorrosive pigments in organic waterborne coatings", *Prog. Org. Coat.* Vol. 49, pp. 358, 2004.
- [18] A.C. Bastos, M.G. Ferreira, and A.M. Simões, "Corrosion inhibition by chromate and phosphate extracts for iron substrates studied by EIS and SVET", *Corros. Sci.* vol. 48, pp.1500, 2006.
- [19] F. Uwe, H. Fred, M. Hiroaki and Y. Wei, "Flame Retardants", Sri Consulting, Ed., December 2008. url:<http://www.sriconsulting.com/SCUP/Public/Reports/FLAME000/>
- [20] A. Holt, "Fire-resistant coatings market sees 200 % growth in the UAE", *AME Info. The Ultimate Middle East business resource*, Al Gurg Leigh Paints, 2001.
- [21] R.F. Gibson, "Principles of composite material mechanics", McGraw-Hill, New York, pp.1-3,1994.
- [22] R.F. Gibson, "Principles of composite material mechanics", McGraw-Hill, New York, pp.11, 1994.
- [23] R.F. Gibson, "Principles of composite material mechanics", McGraw-Hill, New York, pp. 13, 1994.
- [24] European Flame Retardants Association "How do they work?", 2006.  
url : <http://www.flameretardants.eu/Content/Default.asp?PageID=130>
- [25] S. Posner, "Guidance on alternative flame retardants to the use of commercial pentabromodiphenylether (c-PentaBDE)", 2009.
- [26] "Flame retardants - a general introduction", *Environmental Health Criteria*, vol. 192, 1997.
- [27] G. A. Skinner, "Smoke-the hazard, the measurement and the remedy", *Journal of Chemical Technology and Biotechnology*, vol. 31, pp. 445-456, 1981.
- [28] G. A. Skinner, "Smoke-the hazard, the measurement and the remedy", *Journal of Chemical Technology and Biotechnology*, vol. 31, pp. 457, 1981.
- [29] G. Camino, "Fire retardant polymeric materials in Atmospheric oxidation and anti Oxidant", *Elsevier*, vol. Chapter 10, pp. 461-494, 1993.

- [30] J. Hao and W. K. Chow, "A brief review of intumescent fire retardant coatings", *Architectural Science Review*, 2003.
- [31] K. Russell, "Fire retardant coatings," *Handbook of Fire Retardant Coatings and Fire Testing Services*, Lancaster: Technomic Publishing Co, pp. 265, 1994.
- [32] L.C. Camino and G. Martinasso, *Polymer Degradation Stabilisation*, vol. 23, pp. 359-376, 1989.
- [33] A. R. Horrocks, "Developments in flame retardants for heat and fire resistant textiles – the role of char formation and intumescence", *Polymer Degradation Stabilisation*, vol. 54, pp. 143-154, 1996.
- [34] W. D. Callister, "*Materials Science And Engineering : An Introduction*", seventh edition, 2007.
- [35] J. Xu and J. Hao, "The Combustion and Thermal Behavior of PA-6/PP Blends with added Nano-LDH and APP," *Polymer Materials Science and Engineering*, 2001.
- [36] J. Wang, W. Ping, and J. Hao, "Comparative study of the effect of aluminosilicates on intumescent flame retardancy of PP/APP/PER systems by CONE/LOI/XPS", *Am. Chem. Soc. 220th*, 2000.
- [37] S. Duquesne, M.L. Bras, and S. Bourbigot, "Analysis of fire gases released from polyurethane and fire-retarded polyurethane coatings", *Journal of Fire Sciences*, vol. 8, pp. 456-482, 2000.
- [38] R.L. Buxton and E. M. Parker. vol. US Patent 6245842 United States, June 12, 2001.
- [39] P. Penczek and, R. Ostrysz, "Expandable graphite as a fire retardant in unsaturated polyester resins", *Proceedings of the Flame Retardants 2000 Conference, Interscience Communications*, pp. 105-111, 2000.
- [40] S. Duquesne, M. Le Bras and S. Bourbigot, "Thermal degradation of polyurethane and polyurethane/expandable graphite coatings", *Polymer Degradation Stabilisation*, vol. 74, pp. 493-499, 2001.
- [41] DIN 4102-18, "Fire behaviour of building materials and components; fire barriers, verification of automatic closure (continuous performance test)", *German National Standard: German National Standard*, 1991.
- [42] W.D. Pirig, S. Rothkamp, and V. Thewes, "Intumescent coatings stable in tropical climates", *Europe Patent 902062 A1*, 1999.
- [43] H. Bennett, "Fire retardant coating composition comprising fly ash and polymer emulsion binder", vol. US Patent 4229329 United States, 1980.
- [44] R. Vitaly, "Fire-protective coatings, paints and varnishes", vol. US Patent 4849298 United States, 1989.

- [45] B. Li and J. Wang, "A cone calorimetric study of flame retardancy and smoke emission of PVC. I. The effect of cuprous and molybdic oxides", *Journal of Fire Sciences*, vol. 15, pp. 341-357, 1997.
- [46] R.P. Lattimer and W. J. Kronke, "The functional role of molybdenum trioxide as a smoke retarder additive in rigid poly(vinyl chloride)", *Journal Applied Science*, vol. 26, pp. 1191-1210, 1981.
- [47] M. S. Deogon, "Intumescent fireproofing compositions", vol. WO patent 9111498 A1, 1991.
- [48] K.K. Shen and T. S. Griffin, "Fire and Polymers", *ACS Symposium Series 425*, American Chemical Society, pp. 157, 1990.
- [49] Y. Niu and Y. Xie, "Fire and waterproof coatings for fibers", vol. Chinese Patent 1061610 A, China, 1992.
- [50] Y.N. Shebeko, I.A. Bolodian, V.N. Filippov, and E. A. Navzenya, "Explosion prevention of LPG vessels using fire retardant coatings and safety valves", *Proc. Asia-Pac. Int. Symp. Combust. Energy Util*, vol. 5, pp. 215-226, 1999.
- [51] Y.N. Shebeko, I.A. Bolodian and V.N. Filippov, "A study of the behavior of a protected vessel containing LPG during pool fire engulfment", *J. Hazard. Mater*, vol. 77, pp. 43-56, 2000.
- [52] A. R. Hochstim, "Fire retardant coatings for group electric cables and the testing methods", *New Adv, Flame Retard. Technol., Fall Conf*, 1999.
- [53] N.K. Saxena, S. Singh, and T. P. Sharma, "Fire retardant coatings for electric cables", *Paintindia*, vol. 49, pp. 35-37, 1999.
- [54] D.M. Bishop and D. Bottomley, "Fire-retardant paints", *J. Oil Colour Chem. Assoc*, vol. 66, pp. 373-396, 1983.
- [55] I. Broutier and F. Damour, "Halogen-free fire-retarding composition, yarn fire-retarded with the latter and fire-resistant textile structure comprising such yarns", vol. US Patent 630974 United States, 2001.
- [56] T. Subyakto, K. Takeshi, H. Toshimitsu, I. Shigehisa, K. Shuichi and G. Hideo, "Improving fire retardancy of fast growing wood by coating with fire retardant and surface densification", *Fire Material*, vol. 22, pp. 207-212, 1998.
- [57] S. Gottfried, "Intumescent fire-retardant composition for high temperature and long duration protection", vol. US Patent 5723515 United States, 1998.
- [58] F. Liu and W. Zhu, "Fire retardant intumescent coating for lignocellulosic materials", vol. US Patent 5968669, 1999.

- [59] M.K.Yalinkilic, Y. Imamura, M. Takahashi, and Z. Demirci, "Effect of boron addition to adhesive and/or surface coating on fire-retardant properties of particle board", *Wood Fiber Science*, vol. 30, pp. 348-359, 1998.
- [60] L.G. Eskind and Petersburg, "New improvements in intumescence," *Plastic Engineering*, vol. 56, pp. 29-30, *Brookfield*, 2000.
- [61] ISO 834:1985, "Fire-resistance tests –Elements of building construction", International Organization for Standardization, 1975.
- [62] UL 1709:1994, "Rapid Rise Fire Test of Protection Materials for Structural Steel", Underwriters Laboratories, 1994.
- [63] BS 476-22:1987, "Fire tests on building materials and structures. Methods for determination of the fire resistance of non-load bearing elements of construction", British Standard Institution, 1987.
- [64] BS 476-20:1987, "Fire tests on building materials and structures. Method for determination of the fire resistance of elements of construction general principles)", British Standard Institution, 1987.
- [65] ASTM E119:2008, "Standard Test Methods for Fire Tests of Building Construction and Materials", ASTM International, vol. 04.07, 2008.
- [66] C.F. Cullis and M. M. Hirschler, "The combustion of organic polymers", 1981.
- [67] J. Buckmaster, A. Charles, and A. Nachman, "A Model for intumescent paint", *International Journal of Engineering Science*, 1971.
- [68] A. Charles and D. K. Wauters, "A Thermodynamic Heat Transfer Model for Intumescent System", *International Journal of Engineering Science*, vol. 27, pp. 881-889, 1984.
- [69] G. K. Castle. vol. US Patent 3913290 United States, 1995.
- [70] B. George and G. K. Castle, "Reinforcement System For Mastic Intumescent Fire Protection Coatings Comprising a Hybrid Mesh fabric", vol. US Patent 5433991 United States, 1995.
- [71] C. A. Harper, *Handbook of Building Materials For Fire Protection*: Mcgraw Hill, 2004.
- [72] R. Cornell and H. K. D. H. Bhadeshia, "Decarburization of Steel", United Kingdom: University of Cambridge, 2002.
- [73] B. Daniel A and J. C. Warner, "Material Properties", *Metallurgy Fundamentals*: The Goodheart-Willcox Company, Inc., 2005.
- [74] J. Toth, "Adsorption: Theory, Modeling, and Analysis " 2002.

- [75] Website Special Chemical for Polymer, "Adhesion", 2008.  
url:<http://www.specialchem4polymers.com/>.
- [76] T. Young, *Phil. Trans. R. Soc*, vol. 95, pp. 65, 1985.
- [77] W. Zeno W, N. Frank, P. Jones, and D. A. Wicks, "Adhesion in Organic coatings", Wiley-Interscience, 2006.
- [78] W. Funke, "Towards Environmentally Acceptable Corrosion Protection by Organic Coatings - Problems and Realisation", *Journal of Coatings Technology*, Vol: 55, No: 705, p. 31-38, 1983.
- [79] J. Massingill, *Journal Coating Technology*, vol. 62, pp. 31, 1990.
- [80] L. David, P. Pete, and B. Rodgers, "Evaluation of Organic Coatings with Electrochemical Impedance Spectroscopy, Part 2: Application of EIS to Coatings", *Gamry Instruments. JCT Coatings Tech*, pp. 88, 2004.
- [81] L. David, P. Pete, and B. Rodgers, "Evaluation of Organic Coatings with Electrochemical Impedance Spectroscopy, Part 2: Application of EIS to Coatings", *Gamry Instruments. JCT Coatings Tech*, pp. 89, 2004.
- [82] L. David, P. Pete, and B. Rodgers, "Electrochemical Impedance Spectroscopy Theory: A Primer", Gamry Instruments, 2007.
- [83] M. Kalnins, "Adhesive Interaction of Polyethylen with Steel", *International Journal Adhesion Adhesives*, vol. 143, 1990.
- [84] M. Kalnins and J. Ozolins, "Kinetics of Adhesion Interaction of Polyolefins with metals under Conditions of Contact Thermo oxidation", *International Journal Adhesion Adhesives*, vol. 22, pp. 179, 2002.
- [85] M. R. Bowditch, "The durability of adhesive joints in the presence of water", *International Journal Adhesion Adhesives*, vol. 16, pp. 73, 1996.
- [86] W. Brockman, "The Environmental Resistance of Metal Bonds in New Industries and Applications for Advanced Materials Technology", *19th SAMPE Symposium*, Exhibition, Azusa, CA, 1974.
- [87] A. Maëlenn and A. A. Roche, "Residual stresses and practical adhesion: effect of organo-metallic complex formation and crystallization", *Journal Adhesion Science Technology*, vol. 20, pp. 1889 - 1903, 2006.
- [88] R. G. Dillingham and F. J. Boerio, "Interphase Composition in Aluminium/Epoxy Adhesive Joints", *Journal Adhesion*, vol. 24, pp. 313-335, 1987.
- [89] T. K. Kwei, H. Schonhorn, and H. L. Frisch, "Dynamic Mechanical Properties of The Transcrystalline Regions in Two Polyefins", *Journal Applied Polymer Science*, vol. 38, pp. 2512-2516, 1967.

- [90] M. M. Abdel Wahab, A. D. Crocombe, A. Beevers, and K. Ebteha, "Coupled stress-diffusion analysis for durability study in adhesively bonded joints", *International Journal Adhesion Adhesives*, vol. 22, pp. 62, 2002.
- [91] M. M. Abdel Wahab, A. D. Crocombe, A. Beevers, and K. Ebteha, "Coupled stress-diffusion analysis for durability study in adhesively bonded joints", *International Journal Adhesion Adhesives*, vol. 22, pp. 63, 2002.
- [92] "Material Data Sheet Chartek 7 Part A and B", International Paint, Azko Nobel, 2006.
- [93] "Material Safety Data Sheet Intergard 251", International Paint, Azko Nobel, 2005.
- [94] NACE Standard, Joint Surface Preparation Standard, 2000.
- [95] "Chartek 7", International Paint, Azko Nobel, 2003.
- [96] ASTM B117:1997, "Standard Practice for Operating Salt Spray (Fog) Apparatus", ASTM International, 1997.
- [97] ASTM D3163:2008, "Standard Test Method for Determining Strength of Adhesively Bonded Rigid Plastic Lap-Shear Joints in Shear by Tension Loading", ASTM International 2008.
- [98] Lab Report XRD S8, "Quantitative Analysis of Geological Sample : Combined XRD/XRF analysis", Bruker Advanced X-Ray solution, 2006.
- [99] "Material Hardness", Calce and the University of Maryland, 2001.  
url : [http://www.calce.umd.edu/general/Facilities/Hardness\\_ad\\_.htm](http://www.calce.umd.edu/general/Facilities/Hardness_ad_.htm).
- [100] ASTM E119 - 08a. "Standard Test Methods for Fire Tests of Building Construction and Materials", ASTM International vol. 04.07, 2009.
- [101] N. Wenzel, *Ind. Eng. Chem*, vol. 28, pp. 988, 1936.
- [102] Key to metals websites, "Low carbon steel", 2009.  
url : <http://steel.keytometals.com/Articles/Art15.htm>.
- [103] J. K. Kim and Y.W. Mai, "Engineered Interfaces In Fiber Reinforced Composites", *Elsevier*, 1998.
- [104] M. Kutz, "Heat Transfer Calculation", McGraw Hill, 2006
- [105] S. D. Gardener, C. U. Pittman, and R. M. Hackett, "Residual thermal stresses in filamentary polymer matrix composite materials incorporating an elastomeric interphase: A Mathematical assessment", *Journal of composite science Technology*, vol. 46, pp. 307-318, 1993a.
- [106] J.K. Kim and Y. W.Mai, "High Strength, High Fracture Toughness Fiber Composites

- With Interface Control - A Review", *Composites Science Technology*, vol. 41, pp. 333-378, 1991a.
- [107] G. Giunchi and S. Ceresara, "Article based on a metal alloy of nickel, chromium and metalloid elements including microcrystalline precipitates, metal alloy and preparation method", vol. US Patent 6461744 United States, 2002.
- [108] L. Bin, *Journal of Polymer Degradation Stabilization*, vol. 68, pp. 197, 2000.
- [109] L. Bin, *Journal of Polymer Degradation Stabilization*, vol. 74, pp. 195, 2001.
- [110] H. Joseph W, M. Marlborough, B. David C, and N. H. Nashua, "Low Density, Light weight, Intumescent coating", vol. US Patent 6096812 United States, 2000.
- [111] "Corrosion of Iron and Steel", *Technical Data Sheet*, vol. 1, Wattyl Australia Pty Ltd., 2008. url: [www.wattyl.co.nz/i-06%20corrosion%20of%20iron%20&%20steel.pdf](http://www.wattyl.co.nz/i-06%20corrosion%20of%20iron%20&%20steel.pdf)
- [112] Z. Z. Lazarevic, "Determination of the protective properties of electrodeposited organic epoxy coatings on aluminium and modified aluminium surfaces", *Corrosion Science*, vol. 47, pp. 823-834, 2005.
- [113] K. L. Reifsnider, "Modeling of the Interphase in Polymer-Matrix Composite Material Systems", *Composites*, vol. 25, pp. 461, 1994.
- [114] Z. Qiwu, M. Hiroki, S. Fumio, and M. Baron, "Debromination of hexabromobenzene by its co-grinding with CaO", *Chemosphere*, vol. 48, pp. 787-793, 2002.
- [115] A. V. Pocius, "Adhesion and Adhesives Technology - An Introduction 2nd edition", Hanser, 2002.
- [116] R. L. Patrick, "Treatise on Adhesion and Adhesives", vol. 6, 1988.
- [117] G. Jun-wei, Z. Guang-cheng, D. Shan-lai, Z. Qiu-yu, and J. Kong, "Study On Preparation And Fire-Retardant Mechanism Analysis Of Intumescent Flame-Retardant Coatings", *Surface and Coating Technology*, vol. 201, pp. 7835-7841, 2007.
- [118] S. Duquesne, S. Magnet, C. Jama, and R. Delobel, "Intumescent paint : fire protective coating for metallic substrates", *Journal Surface and Technology*, vol. 180-181, 2004.
- [119] G. Jun-Wei, Z. Guang –cheng, D. Shai-Lai, *Paint Coating Ind*, vol. 35, pp. 26, 2005.
- [120] M.S.Robert and *et. al*, "Spectrometric Identification of Organic Compounds : 7th edition", Wiley, 2005.
- [121] I. Toshiaki, K. Hiroyoshi, N. Akira, N. Takafumi, and M. Kakimoto, "Calcium borate flame retardation system for epoxy molding compounds", *Polymer Engineering and Science*, 2006.



- [122] Z. Qiwu, M. Hiroki, S. Fumio, and M. Baron, "Debromination of hexabromobenzene by its co-grinding with CaO", *Chemosphere*, vol. 48, pp. 787-793, 2002.
- [123] W. Zhen-Yu, En Hou, and K. Wei, *Progress Organic Coating*, vol. 53, pp. 29, 2005.
- [124] L. Guoxin, Y. Junfen, H. Tingshu, W. Yonghua, and G. Liang, "An Investigation of the thermal degradation of the intumescent coating containing MoO<sub>3</sub> and Fe<sub>2</sub>O<sub>3</sub>", *Journal Surface and Technology*, vol. 202, pp. 3121-3128, 2008.
- [125] S. Makoto, I. Kazuhiko, and M. Iji, "Flame-Retardant Resin Composition", *US Patent 7247666*, 2007.
- [126] "Ceramic Properties Tables", *Ferro-Ceramic Grinding Inc*, 2009.  
url : [http://www.ferroceramic.com/alumina\\_nitride\\_table.htm](http://www.ferroceramic.com/alumina_nitride_table.htm)
- [127] G. A. Skinner, "Smoke-the hazard, the measurement and the remedy", *Journal of Chemical Technology and Biotechnology*, vol. 31, pp. 445-452, 1981.
- [128] "Chlorine: Effects on Health and the Environment", The Chlorine Institute, 1999.  
url : [www.chlorineinstitute.org/files/PDFs/ChlorineEffectsOnHealth.pdf](http://www.chlorineinstitute.org/files/PDFs/ChlorineEffectsOnHealth.pdf)
- [129] S. Gee, *Surface Coatings International*, vol. 7, pp. 316-320, 1997.
- [130] J.J. Caprari, A.R. Di Sarli, and B. d. Amo, "Zinc phosphate as corrosion inhibitive pigment of waterborne epoxy paints used for steel protection", contributed paper, 2000.
- [131] MATWEB, Website Material Property Data, 2009.  
url: <http://www.matweb.com/search/MaterialGroupSearch.aspx>.
- [132] I. Toshiaki, K. Hiroyoshi, N. Akira, N. Takafumi, and M. Kakimoto, "Calcium borate flame retardation system for epoxy molding compounds", *Polymer Engineering and Science*, 2006.